

3 PTV

**3D-PTV Construction Based on Genetic Algorithm and Its Application
to the Wake Characteristics Near Circular Cylinder**

2001 2

本 論文 白泰實 工學博士 學位論文 認 准 .

委員長 工學博士 南 青 都 印

委 員 工學博士 孫 景 浩 印

委 員 工學博士 金 義 珩 印

委 員 工學博士 李 英 浩 印

委 員 工學博士 都 德 熙 印

2000年 12月 15日

韓國海洋大學校 大學院

List of Figures	i
------------------------	-------	---

List of Tables	
-----------------------	-------	--

Abstract	v
-----------------	-------	---

.....	vii
-------	-----

1	1
----------	-------	---

1.1	1
-----	-------	---

1.2	4
-----	-------	---

2 3 PTV	6
----------------	-------	---

2.1 가	6
-------	-------	---

2.2	8
-----	-------	---

2.3 3	13
-------	-------	----

2.4	17
-----	-------	----

2.4.1	17
-------	-------	----

2.4.2	18
-------	-------	----

2.4.3 (Centroid calculation)	19
------------------------------	-------	----

3 3	21
------------	-------	----

3.1	21
-----	-------	----

3.2 PTV	22
---------	-------	----

3.2.1	22
-------	-------	----

3.2.2	22
-------	-------	----

3.2.3	23
-------	-------	----

3.2.4	25
-------	-------	----

3.3	29
-----	-------	----

3.4	31
3.5 가	가	34
3.5.1 가	34
3.5.2 가	44
4	50
4.1	50
4.2	52
5	54
5.1 3	54
5.2	64
5.3	100
5.4	112
6	148
	150

List of Figures

2.1	Experimental arrangement for 3D velocity measurement·····	7
2.2	Procedure of 3D-PTV measurement·····	10
2.3	Picture of camera calibrator for GA-3D-PTV measurement·····	11
2.4	Coordinate relation of camera·····	12
2.5	Raw images captured by the three cameras·····	15
2.6	Definition of 3D-particle's position·····	16
3.1	Definition of operators in GA-3D-PTV·····	27
3.2	Flow chart of GA-3D-PTV calculation process·····	28
3.3	Picture of calibrator for the generation of a set of virtual image·····	35
3.4	Camera position for the acquisition of images·····	37
3.5	Virtual image of the calibrator viewed by camera 1·····	38
3.6	Virtual image of the calibrator viewed by camera 2·····	39
3.7	Virtual image of the calibrator viewed by camera 3·····	40
3.8	Velocity distribution made by random using the jet data(LES)·····	46
3.9	Virtual images viewed by cameras on an impinging jet·····	47
3.10	Recovered vectors(IHIK case)·····	48
3.11	Recovered vectors(RHRK case) ·····	48
3.12	Recovery ratio using GA-3D-PTV(Jet flow)·····	49
3.13	Overlapping rate of particles in the virtual images·····	49

4.1	Experimental set up for 3D-PTV measurement.....	51
4.2	Inlet flow condition at $y/D = -5$	53
5.1	Raw images viewed by each camera.....	55
5.2	Instantaneous 3D velocity vectors obtained by GA-3D-PTV.....	56
5.3	Temporal evolution of velocity field (continued).....	57
5.4	Instantaneous velocity field of xy-plane.....	59
5.5	Instantaneous velocity field of xz-plane.....	60
5.6	Vortices' structures.....	62
5.7	Mean velocity field.....	63
5.8	Turbulence intensity distribution ($T_u = \sqrt{u'^2} / U_0$) (a) (i).....	65
5.9	Turbulence intensity distribution ($T_u = \sqrt{u'^2} / U_0$) (a) (j).....	68
5.10	Turbulence intensity distribution ($T_u = \sqrt{u'^2} / U_0$) (a) (l).....	72
5.11	Turbulence intensity distribution ($T_v = \sqrt{v'^2} / U_0$) (a) (i).....	77
5.12	Turbulence intensity distribution ($T_v = \sqrt{v'^2} / U_0$) (a) (j).....	80
5.13	Turbulence intensity distribution ($T_v = \sqrt{v'^2} / U_0$) (a) (l).....	84
5.14	Turbulence intensity distribution ($T_w = \sqrt{w'^2} / U_0$) (a) (i)....	89
5.15	Turbulence intensity distribution ($T_w = \sqrt{w'^2} / U_0$) (a) (j)....	92
5.16	Turbulence intensity distribution ($T_w = \sqrt{w'^2} / U_0$) (a) (l)....	96
5.17	Turbulence kinetic energy distribution ($TKE = \frac{1}{2} q^2 / U_0^2$) (a) (i).....	101

5.18	Turbulence kinetic energy distribution ($TKE = \frac{1}{2} q^2 / U_0^2$)	
(a)	(j).....	104
5.19	Turbulence kinetic energy distribution ($TKE = \frac{1}{2} q^2 / U_0^2$)	
(a)	(l).....	108
5.20	Reynolds shear stress distribution ($-\overline{u'v'} / U_0^2$)	(a) (i)..... 113
5.21	Reynolds shear stress distribution ($-\overline{u'v'} / U_0^2$)	(a) (j)..... 116
5.22	Reynolds shear stress distribution ($-\overline{u'v'} / U_0^2$)	(a) (l)..... 120
5.23	Reynolds shear stress distribution ($-\overline{v'w'} / U_0^2$)	(a) (i)..... 125
5.24	Reynolds shear stress distribution ($-\overline{v'w'} / U_0^2$)	(a) (j)..... 128
5.25	Reynolds shear stress distribution ($-\overline{v'w'} / U_0^2$)	(a) (l)..... 132
5.26	Reynolds shear stress distribution ($-\overline{w'u'} / U_0^2$)	(a) (i)..... 137
5.27	Reynolds shear stress distribution ($-\overline{w'u'} / U_0^2$)	(a) (j)..... 140
5.28	Reynolds shear stress distribution ($-\overline{w'u'} / U_0^2$)	(a) (l)..... 144

List of Table

3.1	Definition of chromosomes of GA.....	22
3.2	Errors of three-dimensional geometrical measurement.....	33
3.3	Absolute coordinate of the calibrator used for the generation of virtual images[mm].....	36
3.4	Camera calibration by the use of a virtual image of the calibrator.....	42
3.5	Camera calibration by the use of actual image of the calibrator.....	43

3D-PTV Construction Based on Genetic Algorithm and Its Application to the Wake Characteristics Near Circular Cylinder

by

Baek Tae-Sil

**Department of Mechanical Engineering
Graduate School, Korea Maritime University**

Abstract

A GA(Genetic Algorithm) based 3D-PTV technique has been developed for the measurement of the wake of a circular cylinder. The measurement system consists of three CCD cameras, Ar-ion laser, an image grabber and a host computer. The fundamental of the developed technique was based on that one-to-one correspondence is found between two tracer particles selected at two different image frames taking advantage of combinatorial optimization of the genetic algorithm. The fitness function controlling reproductive success in the genetic algorithm was expressed by a kind of continuum theory on the sparsely distributed particles in space.

In order to verify the capability of the constructed measurement system, a performance test was made using a set of virtual images on a impinging jet. After confirming the performances of the constructed system, the system was applied to the measurement of flow characteristics of the wake of a circular cylinder.

The belows are the summary of the thesis.

GA based 3D-PTV system for the measurement of complex flow structure are constructed in the first half of the thesis.

The performances test on the constructed system is made using the sets of virtual images generated by a LES data set on a impinging jet flow. Through this test it is verified that the vector recovery ratio becomes higher three times than those of other studies. It is shown that about 1,100 three-dimensional instantaneous velocity vectors is obtained in an actual experiment, which implies that the recovery ratio is more than over about 65%. This percentage is most highest among other three-dimensional PTV techniques.

The constructed system having the above performances is applied to the measurement of the flow field near the wake of a circular cylinder and turbulent characteristics of the flow such as turbulent intensity, Reynolds stresses, turbulent kinetic energy are measured by the constructed system. Good qualitative and quantitative results on the turbulent properties are shown.

Lastly, it is shown that the constructed 3D-GA-PTV system will be able to be used for the investigation of the turbulent characteristics of complex flows since the number of 3D velocity vectors obtained by the system is big enough than the limits, 700, for probing the turbulences of complex flows.

$3DE$	fitness for Genetic Algorithm
$a_{\bar{j}}$	rotation matrix
c	plane distance from lens center
C	fitness for Genetic Algorithm
D	diameter of cylinder
Di	divergence of velocity
DM	threshold of Di
d_p	radius of particle
k_1, k_2	lens coefficient
I	intensity of particle
I_o	maximum intensity of particle
RES	Reynolds shear stress
R_{uv}	Reynolds shear stress ($R_{uv} = - \overline{u'v'} / U_0^2$)
R_{uw}	Reynolds shear stress ($R_{uw} = - \overline{u'w'} / U_0^2$)
R_{vw}	Reynolds shear stress ($R_{vw} = - \overline{v'w'} / U_0^2$)
t_1, t_2, t_3	variables used for calculation of 3-D particle position
T_u	streamwise turbulence intensity ($T_u = \sqrt{\overline{u'^2}} / U_0$)
T_v	transverse turbulence intensity ($T_v = \sqrt{\overline{v'^2}} / U_0$)
T_w	spanwise turbulence intensity ($T_w = \sqrt{\overline{w'^2}} / U_0$)
U_o	free stream velocity
TKE	turbulence kinetic energy ($TKE = \frac{1}{2} \overline{q^2} / U_0^2$)
u'	streamwise fluctuating component
v'	transverse fluctuating component
w'	spanwise fluctuating component
x_o, y_o	deviation of the principal point from the center of image

x_i, y_i	photographic coordinate system
x, y	coordinates on photograph
\bar{x}, \bar{y}	center point of Area moment
\tilde{x}, \tilde{y}	distance from the principal point
X_p, Y_p	projected particle to image plane
X, Y, Z	absolute coordinate system
X_o, Y_o, Z_o	center of projection
t	time interval between obtained field image
u, v, w	velocity of x, y, z direction
x, y	lens distortion

Greek characters

ω	tilted angle for X axis
ϕ	tilted angle for Y axis
κ	tilted angle for Z axis
σ_l	radius of cylindrical light
$\sigma_x, \sigma_y, \sigma_z$	standard deviation of X, Y, Z
ϕ_e	error ratio
ϕ_r	recovery ratio

1

1.1

가 가 .

Roshko¹⁾ 가

가 .

, ,

가 . 가

(hot-wire)

, 가

²⁾ .

Williamson³⁾ Review

, 190 1000 (wake

transition) 2

가 가 3 가

190 A , 260

B , 2 (secondary vortex)

.

. ,

(LDV)

.

PIV()

가 . Chyu Rockwell⁴⁾

, Wu⁵⁾ .
 , Lourenco
 6) PIV .
 Whittaker
 7)
 .
 2 x-y
 3 8)
 Cinematic PIV x-y z-x
 2 가 z-x z
 , z (vorticity correlation) z
 2 3
 . , 2
 가 3
 가 . ,
 .
 Chang Tattersoon⁹⁾, Chang¹⁰⁾ Bolex Stereoscopic lens
 16mm
 3
 가 .
 Yamakawa Iwashige¹¹⁾, Racca Dewey¹²⁾, Adamczyk
 Rimai¹³⁾, Kobayashi¹⁴⁾
 .
 ,
 ,
 Kasagi¹⁵⁾, Nishino¹⁶⁾, Papanroniou Dracos¹⁷⁾

. Kent Trigui¹⁸⁾ 3 PTV

. Kasagi¹⁹⁾ 3 2
400 , Mass²⁰⁾ 3
1000

. Malik²¹⁾ 4
850 .²²⁾ (Ballard
and Brown, 1982) 3 PTV (backward step)
400

. ,
. Nishino

() 700 3 가

.

3 가 700

.

3 PTV

가 . Kobayashi 2
2 2

3²³⁾(-),
100 3 .

8 (eight consecutive time)

.²⁴⁾ .

AOM(Acousto-Optical Modulator)²⁵⁾
3 가
400 3 . Okamoto²⁶⁾

400 3

가
(survival of the fittest)
(reproduction), (crossover),
(mutation)

Yamada ²⁷⁾

, Ohyama ²⁸⁾

가 가

2

3

가 . Kimura ²⁹⁾

2

()

³⁰⁾

2

100% 가

1.2

가

2

.
 30) ()
 , 3 PTV ()
 , 2) .
 2 3 PTV , 3
 , ,
 , 3 3 PTV
 ,
 3 PTV (3D-GA-PTV)
 VSJ(Visualization Society of Japan, <http://www.vsj.or.jp/piv>)
 LES 가
 가 가
 , 가
 .
 4 3D-GA-PTV 2
 , ,
 .
 5 2
 , , ,
 6 3D-GA-PTV가

2 3 PTV

2.1 가

Fig. 2.1

. 3 CCD (768 × 494 pixels),
 (512 × 512 pixels, 256 gray levels), (500mW), 3
 , 32bit .
 3 (Ditect
 64) 256gray levels(512 × 512)
 .
 . 64 Mega bytes RAM
 , R(), G(), B()
 64 . 3
 .
 .
 3 , .
 3

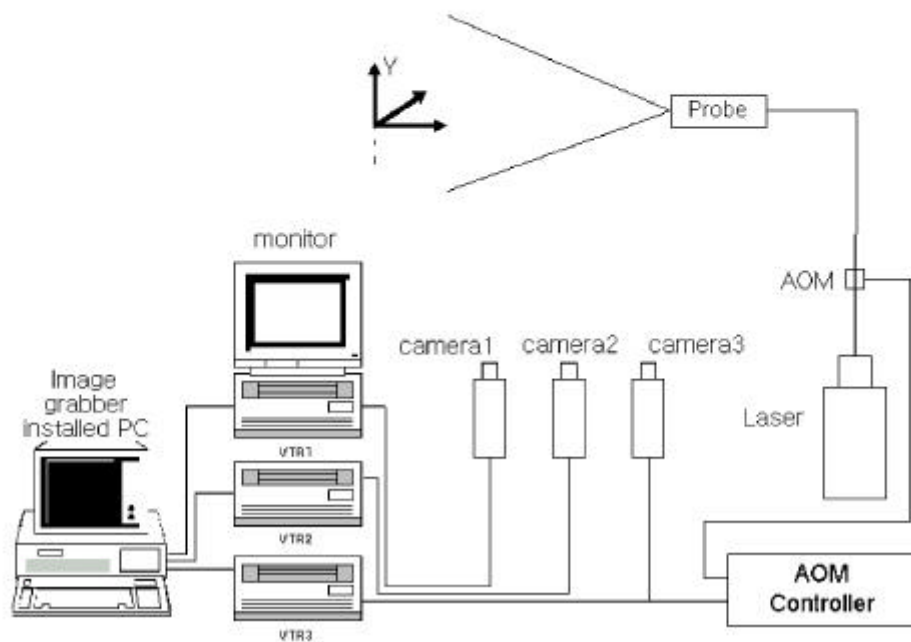


Fig. 2.1 Experimental arrangement for 3D velocity measurement

2.2

Fig. 2.2 3

3
 , , ,
 (標定)
 . 2 3
 3
 , 3
 3D-PTV 3
 Fig. 2.3 100mm
 1mm
 (가) × 70mm () × 60mm ()
 0.6mm 3
 . (Y) 5.0mm 60mm
 40 3
 1/ 1000 mm
 X, 가
 Y=2.500D, Z

(X=0, Y=0, Z=0) . X, Y, Z

Fig. 2.1

Fig. 2.3

Fig. 2.1

Y
 (X, Y, Z) (X₀, Y₀, Z₀)
 (x, y) Fig. 2.4 3

$$\begin{array}{ccc}
& \mathbf{P} & \mathbf{P}_i \\
\cdot & \mathbf{O}(\mathbf{X}_0, \mathbf{Y}_0, \mathbf{Z}_0), & \mathbf{P}_i(\mathbf{x}, \mathbf{y}) \quad \mathbf{P}(\mathbf{X}, \mathbf{Y}, \mathbf{Z}) \\
& (2.1) & \cdot
\end{array}$$

$$\begin{aligned}
x &= -c \frac{a_{11}(\mathbf{X} - \mathbf{X}_0) + a_{12}(\mathbf{Y} - \mathbf{Y}_0) + a_{13}(\mathbf{Z} - \mathbf{Z}_0)}{a_{31}(\mathbf{X} - \mathbf{X}_0) + a_{32}(\mathbf{Y} - \mathbf{Y}_0) + a_{33}(\mathbf{Z} - \mathbf{Z}_0)} + \Delta x \\
y &= -c \frac{a_{21}(\mathbf{X} - \mathbf{X}_0) + a_{22}(\mathbf{Y} - \mathbf{Y}_0) + a_{23}(\mathbf{Z} - \mathbf{Z}_0)}{a_{31}(\mathbf{X} - \mathbf{X}_0) + a_{32}(\mathbf{Y} - \mathbf{Y}_0) + a_{33}(\mathbf{Z} - \mathbf{Z}_0)} + \Delta y
\end{aligned} \tag{2.1}$$

$$a_{ij}, \quad \cdot$$

$$\begin{aligned}
a_{11} &= \cos \phi \cos \chi, \quad a_{12} = -\cos \phi \sin \chi, \\
a_{13} &= \sin \phi \\
a_{21} &= \cos \omega \sin \chi + \cos \omega \sin \phi \cos \chi, \\
a_{22} &= \cos \omega \cos \chi - \sin \omega \sin \phi \sin \chi, \\
a_{23} &= -\sin \omega \cos \phi \\
a_{31} &= \sin \omega \sin \chi - \cos \omega \sin \phi \cos \chi, \\
a_{32} &= \sin \omega \cos \chi + \cos \omega \sin \phi \sin \chi, \\
a_{33} &= \cos \omega \cos \phi
\end{aligned} \tag{2.2}$$

$$\mathbf{x}, \mathbf{y} \tag{2.3} \quad \cdot$$

$$\Delta \mathbf{x} = x_0 + \tilde{x}(k_1 r^2 + k_2 r^4) \tag{2.3}$$

$$\Delta \mathbf{y} = y_0 + \tilde{y}(k_1 r^2 + k_2 r^4)$$

$$r^2 = (\tilde{x}^2 + \tilde{y}^2)/c^2$$

$$\tilde{x} = x - x_0, \quad \tilde{y} = y - y_0$$

$$\begin{array}{ccc}
\cdot, & x_0 & y_0 \\
& & \cdot \\
& & (\mathbf{X}_0,
\end{array}$$

$Y_0, Z_0, \omega, \phi, \kappa)$

(c, x_0, y_0, k_1, k_2)

31)

40

3

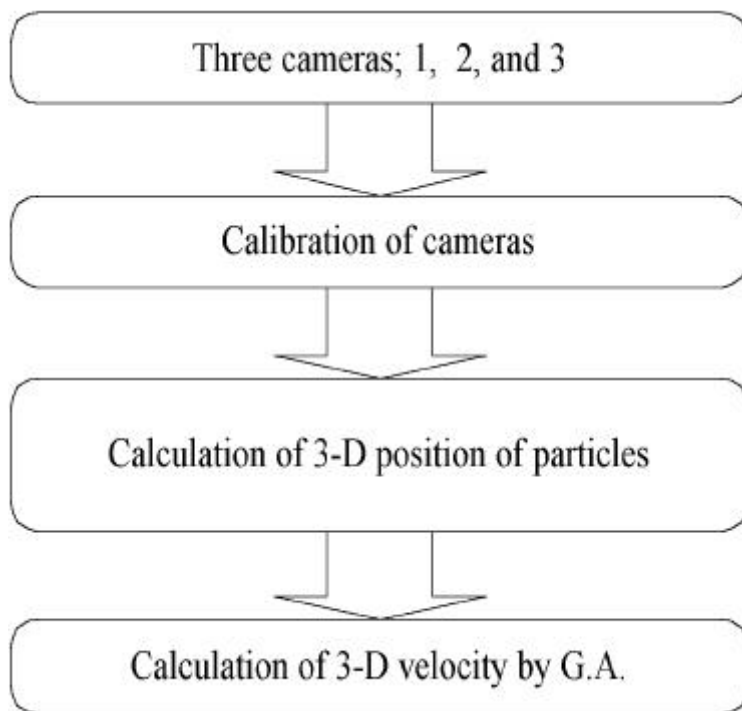


Fig. 2.2 Procedure of 3D-PTV measurement

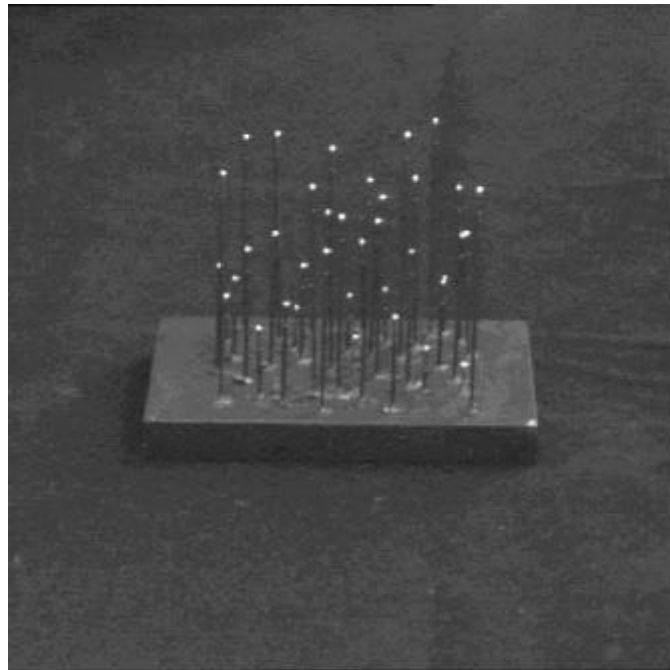


Fig. 2.3 Picture of camera calibrator for GA-3D-PTV measurement

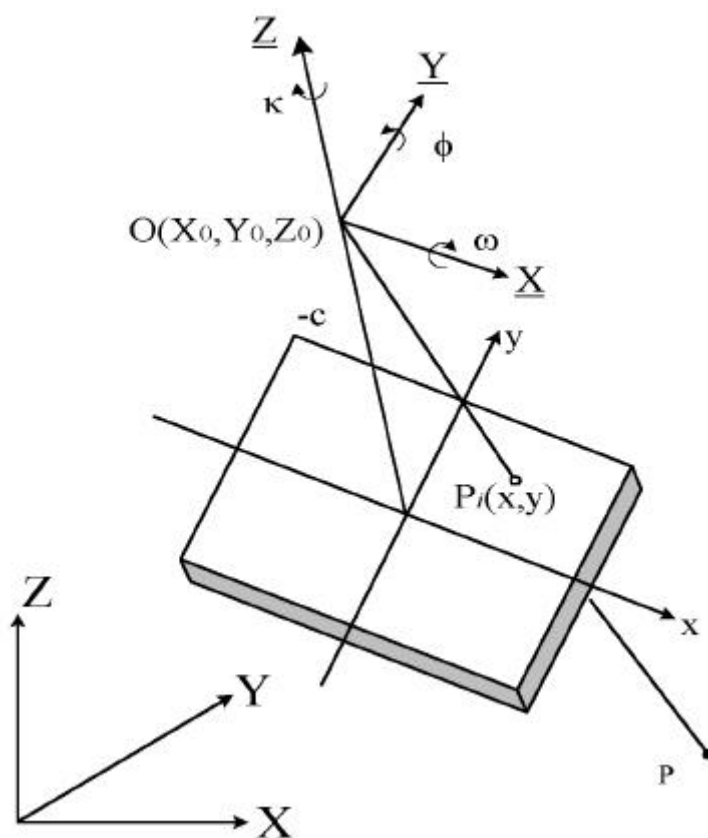


Fig. 2.4 Coordinate relation of camera

2.3 3

3

가

가

,

. Fig. 2.5

3

4 9

(gray level)가

(階調

値,gray level)

가

3

Fig. 2.6 3

3

Fig. 2.6

3

(colinear)

(2.4)

$$\begin{pmatrix} X \\ Y \\ Z \end{pmatrix} = \begin{pmatrix} a_{11} & a_{21} & a_{31} \\ a_{12} & a_{22} & a_{32} \\ a_{13} & a_{23} & a_{33} \end{pmatrix} \begin{pmatrix} x \\ y \\ -c \end{pmatrix} + \begin{pmatrix} X_0 \\ Y_0 \\ Z_0 \end{pmatrix} \quad (2.4)$$

, X,Y,Z x, y

3

14)

가

가

3

$$p_i(x_1, y_1),$$

$$p_i(x_2, y_2), \quad p_i(x_3, y_3) \tag{3}$$

.

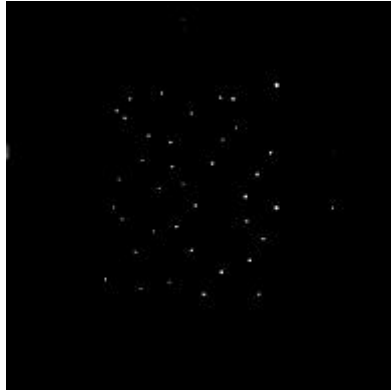
$$\begin{aligned} \begin{pmatrix} X \\ Y \\ Z \end{pmatrix} = \frac{1}{3} \left[\begin{pmatrix} X_{01} + X_{02} + X_{03} \\ Y_{01} + Y_{02} + Y_{03} \\ Z_{01} + Z_{02} + Z_{03} \end{pmatrix} + t_1 \begin{pmatrix} X_{p_1} - X_{01} \\ Y_{p_1} - Y_{01} \\ Z_{p_1} - Z_{01} \end{pmatrix} \right. \\ \left. + t_2 \begin{pmatrix} X_{p_2} - X_{02} \\ Y_{p_2} - Y_{02} \\ Z_{p_2} - Z_{02} \end{pmatrix} + t_3 \begin{pmatrix} X_{p_3} - X_{03} \\ Y_{p_3} - Y_{03} \\ Z_{p_3} - Z_{03} \end{pmatrix} \right] \tag{2.5} \end{aligned}$$

$$, \quad X_{0i}, \quad Y_{0i}, \quad Z_{0i} \qquad , \quad X_{p_i}, \quad Y_{p_i}, \quad Z_{p_i} \quad (i = 1, 2, 3)$$

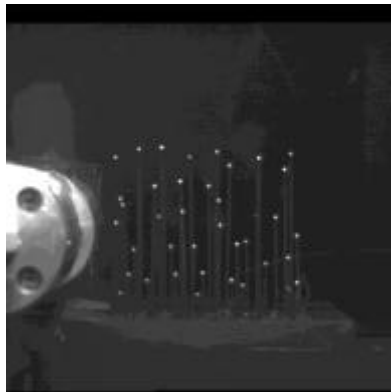
가 .

$$\text{가} \qquad t_1, \, t_2, \, t_3 \qquad \text{가}$$

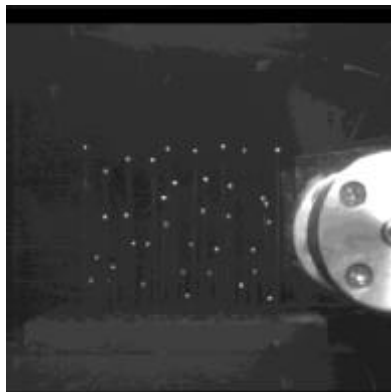
. .



(a) by camera 1



(b) by camera 2



(c) by camera 3

Fig. 2.5 Raw images captured by the three cameras

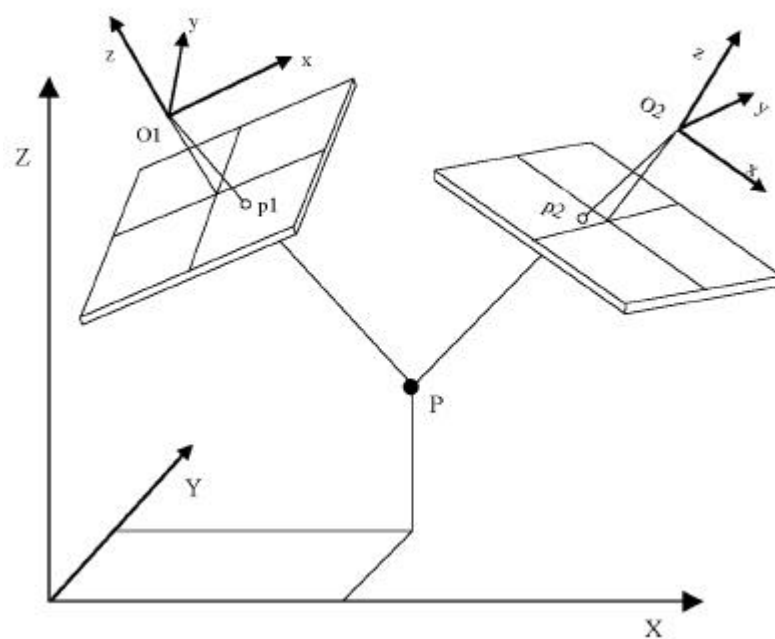


Fig. 2.6 Definition of 3D-particle's position

2.4

2.4.1

PIV PTV NTSC

. 1/30

1/60 가

.

.

가

. , PTV

.

가

-

. ,

가

가

가

가 가

.

1/30 64 2

128

2.4.2

가

. 가 .
() 가

. 2 A가 ,

$$A = \left[\begin{array}{ccc} a_{11} & a_{12} & a_{13} \\ a_{21} & a_{22} & a_{23} \\ a_{31} & a_{32} & 1 \end{array} \right] \tag{2.6}$$

Pixel A (x,y) 가 B (s_x,s_y) Pixel

.

$$x = \frac{a_{11} s_x + a_{12} s_y + a_{13}}{a_{31} s_x + a_{32} s_y + 1}, \quad y = \frac{a_{21} s_x + a_{22} s_y + a_{23}}{a_{31} s_x + a_{32} s_y + 1} \tag{2.7}$$

$$(\Delta x, \Delta y)$$

$$\begin{aligned} \Delta x &= \frac{x}{r} (k_1 r^2 + k_2 r^4) \\ \Delta y &= \frac{y}{r} (k_1 r^2 + k_2 r^4) \end{aligned} \tag{2.8}$$

.

$$\begin{aligned}
 F(x; a_{11}, a_{12}, a_{13}, \dots, k_2) &= \frac{a_{11}x + a_{12}y + a_{13}}{a_{31}x + a_{32} + 1} - sx \\
 &= \frac{a_{11}x + a_{12}y + a_{13}}{a_{31}x + a_{32} + 1} - \left(px + \frac{px}{r} (k_1 r^2 + k_2 r^4) \right)
 \end{aligned}
 \tag{2.9}$$

$$\begin{aligned}
 G(y; a_{11}, a_{12}, a_{13}, \dots, k_2) &= \frac{a_{21}x + a_{22}y + a_{23}}{a_{31}x + a_{32} + 1} - sy \\
 &= \frac{a_{21}x + a_{22}y + a_{23}}{a_{31}x + a_{32} + 1} - \left(py + \frac{py}{r} (k_1 r^2 + k_2 r^4) \right) \\
 r &= \sqrt{(px^2 + py^2)}
 \end{aligned}
 \tag{2.10}$$

Gauss-Newton

.

2.4.3

2 . 2
1, 0 가 .

(boundary trace) . (raster
scan) 가 0 1 가 1

가 .
8 3×3 .
1

가 .

.

$$(2.11) \quad \cdot \quad x_i, y_i$$

$$, A_i \quad .$$

$$\overline{x} = \frac{\sum_{i=1}^n A_i x_i}{\sum_{i=1}^n A_i} \quad , \quad \overline{y} = \frac{\sum_{i=1}^n A_i y_i}{\sum_{i=1}^n A_i} \quad (2.11)$$

3.1

GA

가 (gene) ,
 (chromosome) ,
 (population) (generation) . GA
 (individual) .
 가 (object function)
 (fitness function) ,
 .

, , 가 , , ,
 . GA 5가 가
 .
 가 가
 가 가
 , “ ” 가 가

가

(,)

3.2 PTV

3.2.1

PTV 3 , , .
 3 2 2 가 .

Table 3.1 Definition of chromosomes of GA

Camera 1		Camera 2		Fitness	
Start	End	Start	End	3DE	C

,

$$D = \sqrt{(X_B - X_A)^2 + (Y_B - Y_A)^2 + (Z_B - Z_A)^2}$$

$$3DE = [DS + DE] \tag{3.1}$$

D , $3DE$.

3.2.2

2 가

2 3
3 3DE 가
가

3.2.3

가

PIV

$$\begin{aligned}\left[\frac{\partial u}{\partial x}\right]_f &= \frac{-3u(i,j) + 4u(i+1,j) - u(i+2,j)}{2\Delta x} \\ \left[\frac{\partial v}{\partial y}\right]_f &= \frac{-3v(i,j) + 4v(i,j+1) - v(i,j+2)}{2\Delta y} \\ \left[\frac{\partial u}{\partial x}\right]_b &= \frac{u(i-2,j) - 4u(i-1,j) + 3u(i,j)}{2\Delta x} \\ \left[\frac{\partial v}{\partial y}\right]_b &= \frac{v(i,j-2) - 4v(i,j-1) + 3v(i,j)}{2\Delta y}\end{aligned}$$

$$4 \quad (D_1, D_4) \quad 4$$

$$\begin{aligned}D_1 &= \left| \left[\frac{\partial u}{\partial x}\right]_f + \left[\frac{\partial v}{\partial y}\right]_f \right| & D_2 &= \left| \left[\frac{\partial u}{\partial x}\right]_f - \left[\frac{\partial v}{\partial y}\right]_f \right| \\ D_3 &= \left| \left[\frac{\partial u}{\partial x}\right]_b + \left[\frac{\partial v}{\partial y}\right]_b \right| & D_4 &= \left| \left[\frac{\partial u}{\partial x}\right]_b - \left[\frac{\partial v}{\partial y}\right]_f \right| \quad (3.2)\end{aligned}$$

$$2 \quad (D_1, D_3) \quad (D_2, D_4)$$

DM

가 가

가 4

$$D(i,j) = \left| \left[\frac{\partial u}{\partial x} \right]_{\min} + \left[\frac{\partial v}{\partial y} \right]_{\min} \right| \quad (3.3)$$

$$, \left[\frac{\partial u}{\partial x} \right]_{\min} = Min \left\{ \left[\frac{\partial u}{\partial x} \right]_f, \left[\frac{\partial u}{\partial x} \right]_b \right\}, \left[\frac{\partial v}{\partial y} \right]_{\min} = Min \left\{ \left[\frac{\partial v}{\partial y} \right]_f, \left[\frac{\partial v}{\partial y} \right]_b \right\}$$

$D(i,j)$ 가 DM

3 ,

$$D(i,j,k) = \left| \left[\frac{\partial u}{\partial x} \right]_{\min} + \left[\frac{\partial v}{\partial y} \right]_{\min} + \left[\frac{\partial w}{\partial z} \right]_{\min} \right| \quad (3.4)$$

, PTV 가

, 가 가

가 .

가

.

,

, 10

.

PTV

1 .

C

$$C = \left| \frac{\partial u}{\partial x} \right|_{\min} + \left| \frac{\partial v}{\partial y} \right|_{\min} + \left| \frac{\partial w}{\partial z} \right|_{\min} \quad (3.5)$$

, (C)

가 가 .
 $3DE$ C 가 가 .

가 .

3.2.4

(isolation), (migration), (crossover)
 (reproduction) . Fig. 3.1 ,

Fig. 3.2

4 가
 $3DE$ 가 . $3DE$
 (isolation) .
 3 C
 . C
 (reproduction) .
 .
 (crossover) .
 2 $3DE$
 . $3DE$ 가

.
 (migration) . $3DE$
 0.5, 10% , 10 15 (
) .
 ,
 .

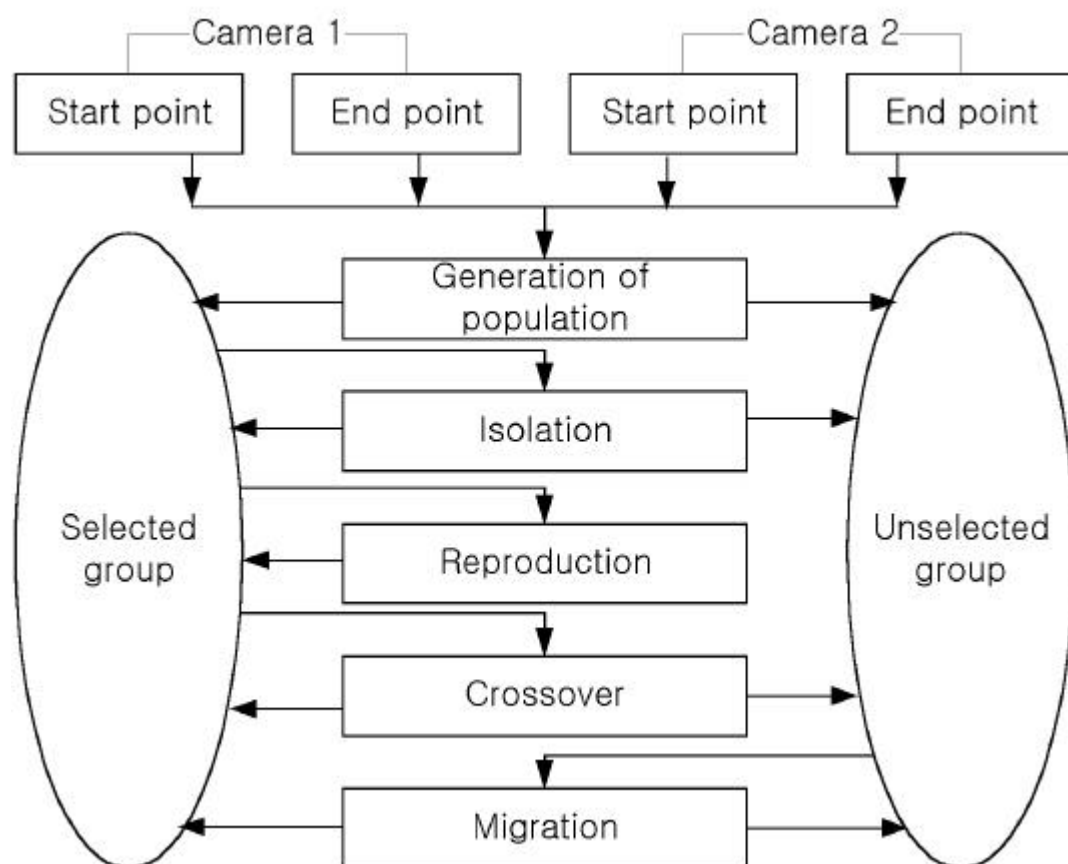


Fig. 3.1 Definition of operators in GA-3D-PTV

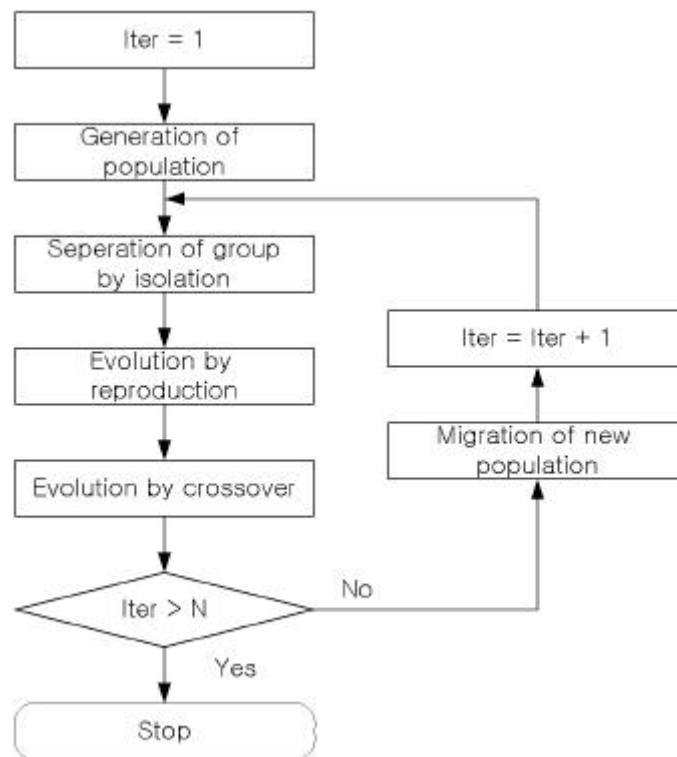


Fig. 3.2 Flow chart of GA-3D-PTV calculation process

3.3

가 , , 가 .

PIV

³²⁾ P , D DM P .

$$D(i,j) \; = \; \left| \left[\frac{\partial u}{\partial x} \right]_{\min} \right| + \left| \left[\frac{\partial v}{\partial y} \right]_{\min} \right| \tag{3.6}$$

$$X \qquad \left[\frac{\partial u}{\partial x} \right]_{\min} = Min \left\{ \left[\frac{\partial u}{\partial x} \right]_f, \left[\frac{\partial u}{\partial x} \right]_b \right\}$$

$$Y \qquad \left[\frac{\partial v}{\partial y} \right]_{\min} = Min \left\{ \left[\frac{\partial v}{\partial y} \right]_f, \left[\frac{\partial v}{\partial y} \right]_b \right\}$$

3

$$(3.7)$$

, Tomson's value, (異狀) ³³⁾ .

$$S = \left[\sum_{k=1}^N (X_k - \overline{X})^2 / (N - 1) \right]^{1/2} \tag{3.7}$$

$$\overline{X} = \sum_{k=1}^N X_k / N$$

S , N , \overline{X} X_k .
 X_k \overline{X}
 $(\sigma = |X_k - \overline{X}|)$ S “ $\sigma \geq \tau S$ ”
 X_k .

. PIV

. PTV ,
 가
 PIV PTV .

. Gaussian Window³⁴⁾

GA-3D-PTV
 3 1100 .
 가
 (3.8) Gaussian Window

.

$$\begin{aligned}
 u_i(x_i, y_i, z_i) &= \frac{\sum_{k=1}^{N_0} \gamma_k u_k}{\sum_{k=1}^{N_0} \gamma_k} \\
 v_i(x_i, y_i, z_i) &= \frac{\sum_{k=1}^{N_0} \gamma_k v_k}{\sum_{k=1}^{N_0} \gamma_k} \\
 w_i(x_i, y_i, z_i) &= \frac{\sum_{k=1}^{N_0} \gamma_k w_k}{\sum_{k=1}^{N_0} \gamma_k}
 \end{aligned} \tag{3.8}$$

$$, \quad \gamma_k = \exp \left(- \frac{(x_i - x_k)^2 + (y_i - y_k)^2 + (z_i - z_k)^2}{h^2} \right)$$

가 γ_k 1 , h=3mm .

3.4

가

3

,

3

,

3

가

.

3

가

.

, 3

40

가

. , Table 3.2

(X_{ref} , Y_{ref} , Z_{ref} :

, X_{calc} , Y_{calc} , Z_{calc} :

)

, S_x , S_y , S_z

X , Y , Z

3

. 3

，
， 3
。
0.21mm 。

$$U_{RSS} = [(2S_x)^2 + (2S_y)^2 + (2S_z)^2]^{1/2} \quad (3.9)$$

X(-40 40mm), Y(-50 50mm), Z(0 60mm)

1%

。

Table 3.2 Errors of three-dimensional geometrical measurement

NO	X _{calc} - X _{ref}	Y _{calc} - Y _{ref}	Z _{calc} - Z _{ref}	dx	dy	dz
1	-7.74 - -7.75	0.21 - 0.20	6.63 - 6.52	0.01	0.01	0.11
2	-3.81 - -3.84	7.36 - 7.34	13.11 - 13.08	0.03	0.02	0.03
3	4.89 - 4.89	7.19 - 7.18	17.14 - 17.03	0.00	0.01	0.11
4	8.76 - 8.75	0.57 - 0.58	39.68 - 39.70	0.00	0.01	0.02
5	4.16 - 4.16	-6.56 - -6.54	16.07 - 15.91	0.00	0.02	0.16
6	-3.26 - -3.26	-6.31 - -6.31	24.54 - 24.52	0.01	0.00	0.02
7	-17.72 - -17.75	0.83 - 0.84	29.10 - 29.07	0.02	0.01	0.03
8	-8.91 - -8.92	16.99 - 16.94	43.25 - 43.12	0.02	0.04	0.13
9	0.67 - 0.66	19.43 - 19.40	27.94 - 27.90	0.01	0.03	0.04
10	9.07 - 9.08	16.54 - 16.53	32.37 - 32.36	0.01	0.01	0.01
11	16.43 - 16.43	9.59 - 9.58	12.14 - 12.02	0.00	0.01	0.12
12	18.88 - 18.92	1.60 - 1.55	51.59 - 51.58	0.03	0.05	0.01
13	16.66 - 16.70	-8.50 - -8.47	23.02 - 22.98	0.04	0.03	0.04
14	9.63 - 9.64	-15.48 - -15.47	40.29 - 40.23	0.02	0.01	0.06
15	0.42 - 0.41	-18.17 - -18.19	8.99 - 8.92	0.01	0.02	0.07
16	-8.51 - -8.54	-15.11 - -15.10	31.51 - 31.53	0.03	0.02	0.02
17	-15.62 - -15.61	-8.59 - -8.59	14.01 - 13.87	0.01	0.00	0.15
18	-32.69 - -32.77	0.61 - 0.61	43.40 - 43.42	0.08	0.00	0.02
19	-26.63 - -26.73	17.14 - 17.14	52.47 - 52.54	0.10	0.00	0.07
20	-15.83 - -15.89	28.22 - 28.20	37.86 - 37.90	0.06	0.03	0.04
21	0.66 - 0.60	33.35 - 33.32	5.09 - 4.98	0.06	0.03	0.11
22	16.89 - 16.92	28.96 - 28.93	46.54 - 46.47	0.03	0.03	0.06
23	28.52 - 28.67	16.86 - 16.85	17.58 - 17.47	0.15	0.01	0.10
24	33.14 - 33.22	1.02 - 1.05	34.22 - 34.18	0.08	0.03	0.04
25	28.86 - 28.88	-16.41 - -16.40	6.77 - 6.64	0.02	0.01	0.14
26	16.83 - 16.87	-28.17 - -28.14	20.97 - 20.82	0.05	0.03	0.15
27	0.26 - 0.29	-32.61 - -32.60	50.45 - 50.45	0.03	0.01	0.00
28	-16.31 - -16.33	-28.09 - -28.12	10.37 - 10.19	0.02	0.03	0.18
29	-28.29 - -28.33	-15.09 - -15.13	33.28 - 33.23	0.03	0.04	0.05
30	-49.94 - -50.03	0.20 - 0.27	38.23 - 38.20	0.09	0.07	0.02
31	-42.73 - -42.79	26.29 - 26.42	30.31 - 30.16	0.06	0.13	0.15
32	-24.36 - -24.41	43.83 - 43.83	8.52 - 8.32	0.05	0.00	0.20
33	0.04 - 0.01	49.48 - 49.46	49.37 - 49.47	0.03	0.02	0.10
34	25.25 - 25.31	43.64 - 43.65	36.06 - 36.06	0.06	0.01	0.00
35	49.84 - 49.95	-0.34 - -0.32	24.98 - 24.92	0.11	0.02	0.06
36	43.75 - 43.83	-23.82 - -23.81	45.80 - 45.75	0.09	0.00	0.05
37	25.28 - 25.34	-42.68 - -42.71	42.07 - 42.03	0.06	0.03	0.04
38	-0.02 - 0.02	-49.58 - -49.59	47.70 - 47.82	0.04	0.01	0.12
39	-24.93 - -24.92	-42.05 - -42.03	25.88 - 25.87	0.01	0.02	0.01
40	-42.97 - -43.03	-24.08 - -24.12	19.29 - 19.16	0.06	0.04	0.12
Average error				0.04	0.02	0.07
Standard deviation				0.05	0.03	0.09

3.5 가 가

3.5.1 가

Willert Gharib³⁵⁾ DPIV(Digital PIV) 가 PIV 가
 (32X32 pixel) 11 가 8 pixel
 가 0.8 pixel), Okamoto³⁶⁾ 3
 PIV PIV (PIV-STD3D)

.

가 Okamoto 3

가 (virtual image)

가 .

512 x 512 pixel , pixel 256

(gray level, 8bit) .

.

$$I(X, Y) = I_0 \exp \left(\frac{(X - X_p)^2 + (Y - Y_p)^2}{(d_p/2)^2} \right) \quad (3.10)$$

$$I_0 = 240 \exp \left(- \frac{z_p^2 + x_p^2}{\sigma_l^2} \right)$$

0.3mm(3 pixels) ,

60mm ,²²⁾ 50

2000 .

, Fig. 3.3 (X, Y, Z가 -50 50, -50 50, 0 50 mm)

가 . Table 3.3

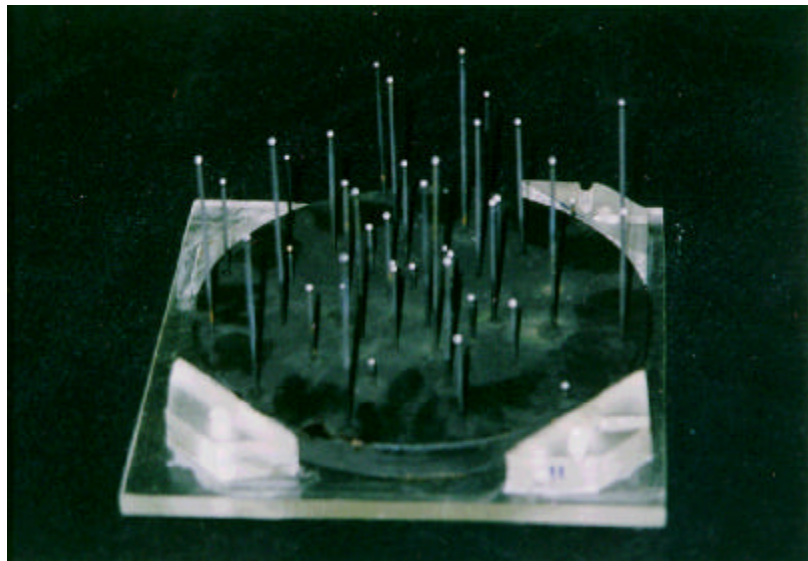


Fig. 3.3 Picture of calibrator for the generation of a set of virtual image

Table 3.3 Absolute coordinate of the calibrator used for the generation of virtual images[mm]

No.	X	Y	Z
1	0.2000	- 7.7516	6.5188
2	7.3386	- 3.8389	13.0829
3	7.1826	4.8918	17.0283
4	0.5809	8.7543	39.7021
5	- 6.5406	4.1629	15.9084
6	- 6.3076	- 3.2634	24.5248
7	0.8383	- 17.7463	29.0704
8	10.2142	- 15.4834	21.4611
9	16.9448	- 8.9227	43.1246
10	19.4009	0.6626	27.9001
11	16.5258	9.0808	32.3592
12	9.5821	16.4280	12.0234
13	1.5498	18.9168	51.5761
14	- 8.4680	16.7006	22.9841
15	- 15.4715	9.6417	40.2301
16	- 18.1874	0.4146	8.9176
17	- 15.0978	- 8.5400	31.5309
18	- 8.5938	- 15.6116	13.8650
19	0.6080	- 32.7680	43.4187
20	17.1421	- 26.7340	52.5382
21	28.1973	- 15.8846	37.8964
22	33.3205	0.5987	4.9782
23	28.9298	16.9216	46.4743
24	16.8530	28.6673	17.4736
25	1.0476	33.2205	34.1831
26	- 16.4029	28.8808	6.6368
27	- 28.1422	16.8719	20.8206
28	- 32.6023	0.2917	50.4479
29	- 28.1175	- 16.3255	10.1926
30	- 15.1312	- 28.3268	33.2271
31	0.2715	- 50.0334	38.2043
32	26.4238	- 42.7926	30.1636
33	43.8331	- 24.4106	8.3207
34	49.4580	0.0109	49.4652
35	43.6475	25.3076	36.0622
36	25.5517	44.0473	3.8494
37	- 0.3152	49.9450	24.9162
38	- 23.8146	43.8323	45.7507
39	- 42.7111	25.3380	42.0268
40	- 49.5878	0.0228	47.8234
41	- 42.0264	- 24.9213	25.8710
42	- 24.1197	- 43.0299	19.1620

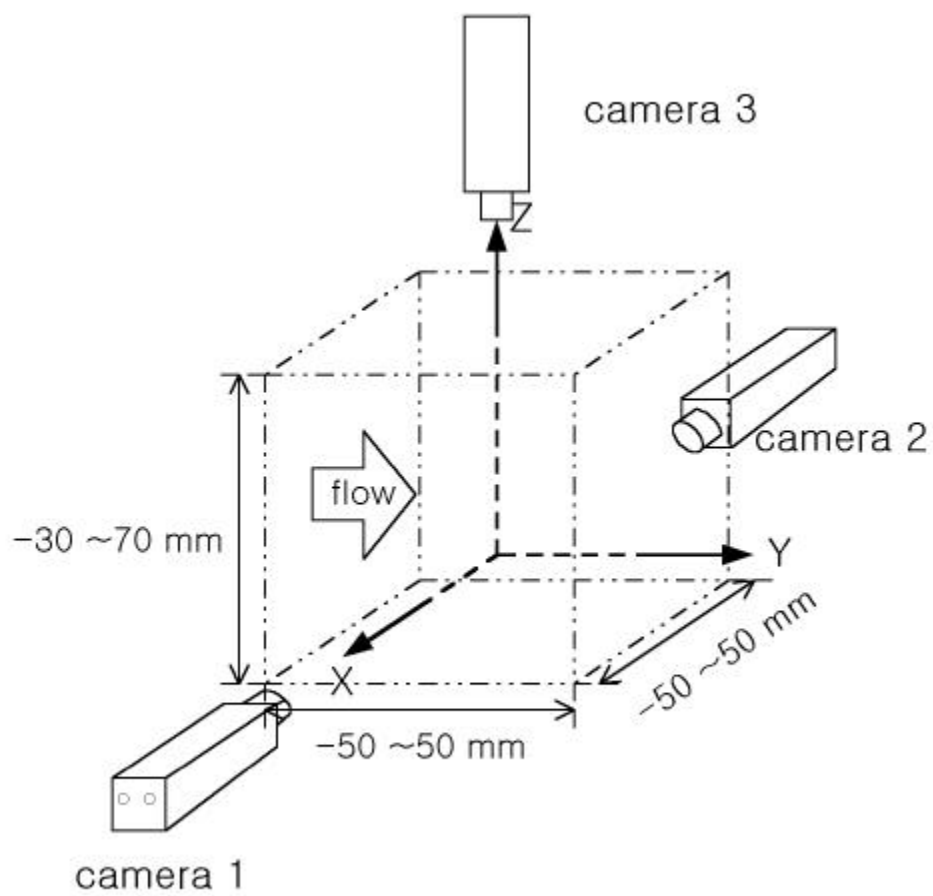


Fig. 3.4 Camera position for the acquisition of images

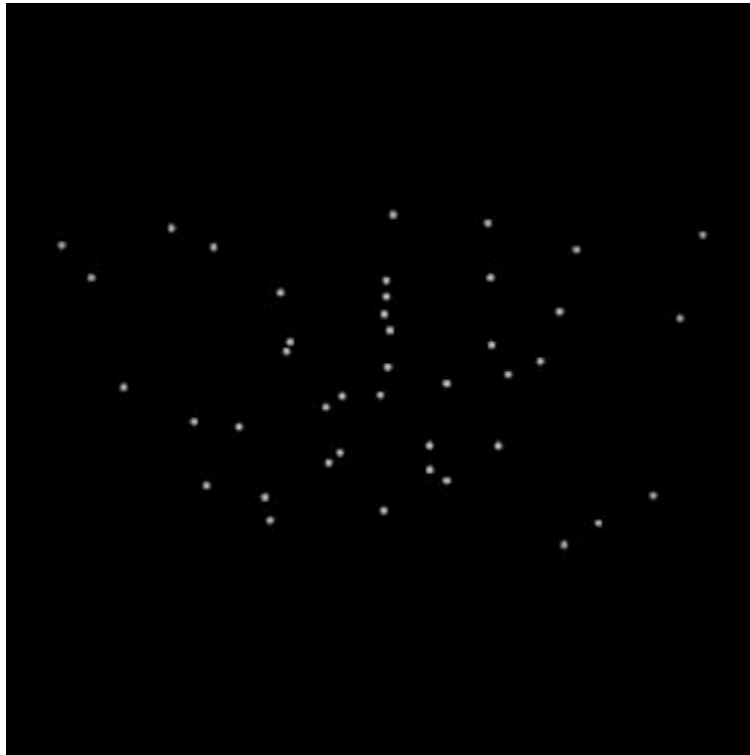


Fig. 3.5 Virtual image of the calibrator viewed by camera 1

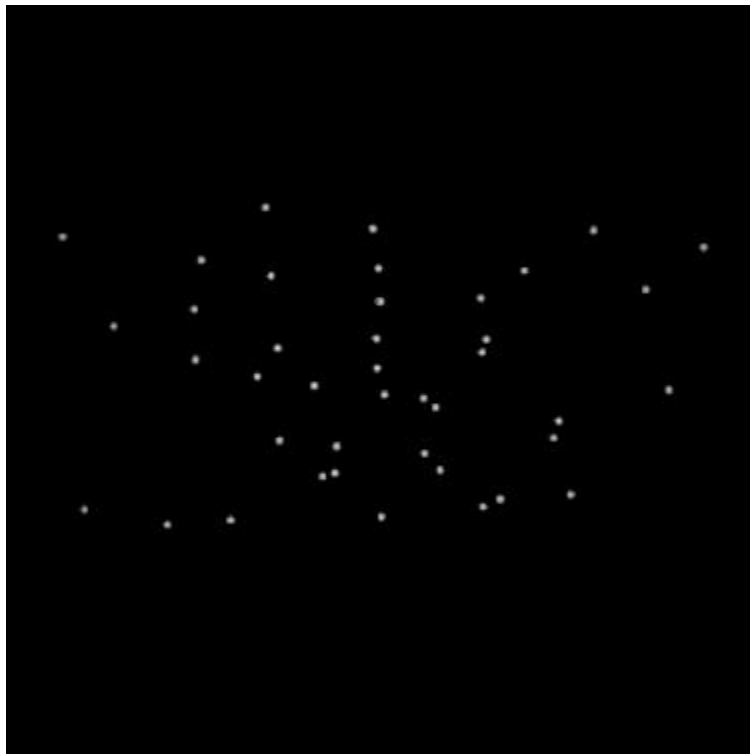


Fig. 3.6 Virtual image of the calibrator viewed by camera 2

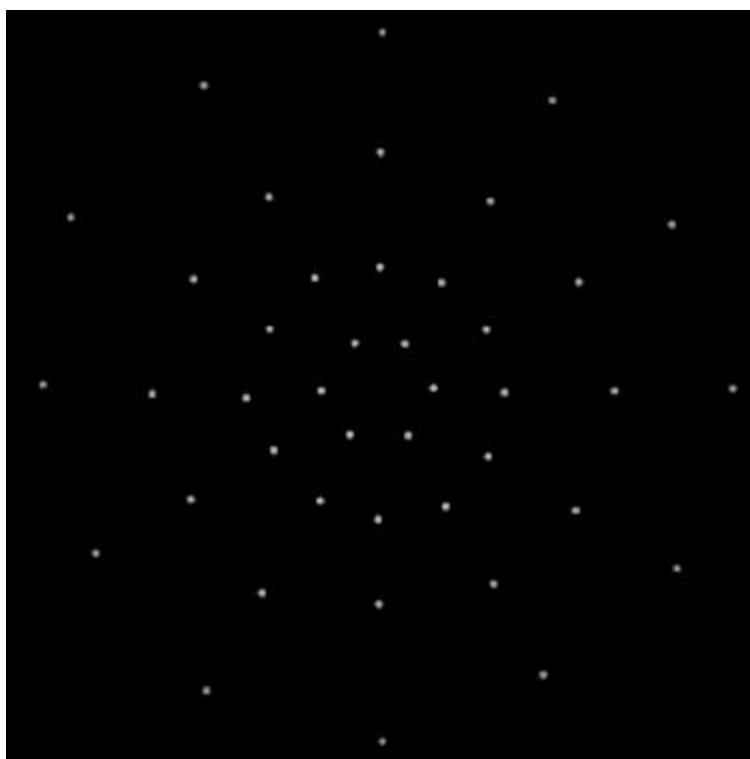


Fig. 3.7 Virtual image of the calibrator viewed by camera 3

Fig. 3.4 가

가 가

Fig. 3.5, Fig. 3.6 Fig. 3.7

가

3

Doh ²³⁾

2

(IH)

(RH)

Table 3.4 11

IH, RH

가

1 3

2 3

, Table 3.5

1

3

, 3

가

Table 3.4 Camera calibration by the use of a virtual image of
the calibrator

Parameter		IH (11 parameter)	RH (11 parameter)
$X_0(\text{mm})$		0.0000	0.0105
$Y_0(\text{mm})$		0.0000	0.0073
$Z_0(\text{mm})$		499.9997	500.0433
$\alpha(^{\circ})$		0.0000	-0.0082
$\beta(^{\circ})$		-0.0000	0.0095
$\kappa(^{\circ})$		0.0000	-0.0001
c(pixel)		-2199.9992	-2200.2813
Average Error	X	0.00	0.00
	Y	0.00	0.02
	Z	0.00	0.01
Standard deviation	X	0.00	0.00
	Y	0.00	0.03
	Z	0.00	0.01

Table 3.5 Camera calibration by the use of actual image of the calibrator

Parameter		(11 parameter)		
		Camera 1	Camera 2	Camera 3
X_0		298.2380	- 294.3097	212.176
Y_0		590.6079	- 636.8735	1.7067
Z_0		19.6709	28.7552	715.6505
α		83.8680	- 98.9806	9.4330
β		- 0.5757	0.1542	- 1.3937
κ		27.6702	24.3260	- 784.2893
c		- 2922.2584	3310.1608	2989.1971
		Camera 1, 3		Camera 2, 3
Average error	X	0.05		0.05
	Y	0.09		0.07
	Z	0.34		0.04
Standard deviation	X	0.07		0.06
	Y	0.12		0.11
	Z	1.27		0.05

3.5.2 가

Visualization Society of Japan(<http://www.vsj.or.jp/piv>) Okamoto³⁶⁾

가
(- 50 50, - 50 50, - 30 70)mm
50 2000 10 pixel

PTV 3
2
(IK)
(RK) IHIK, RHRK

Fig. 3.8 CFD 3
. Fig. 3.9 가

GA-3D-PTV
3 . Fig. 3.10 Fig. 3.11 IHIK RHRK

IHIK
가
, RHRK 가

$$R_r = 100 \frac{V_r}{V_g} \quad (3.11)$$

R_r : (%)

V_g :

V_r : 가 0.1mm

Fig. 3.12 3 Jet Flow 가

. GA 3 PTV

IK RK 3
2

가 . Fig. 3.13

15%, 300

가 . 3

가 2000

가 2

2

3

1000 1500

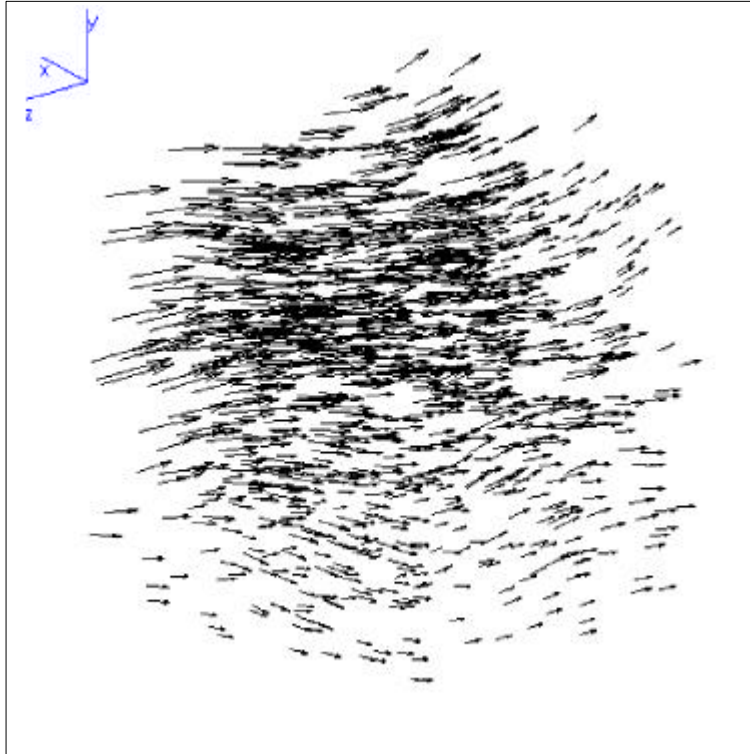


Fig. 3.8 Velocity distribution made by random using the jet data(LES)

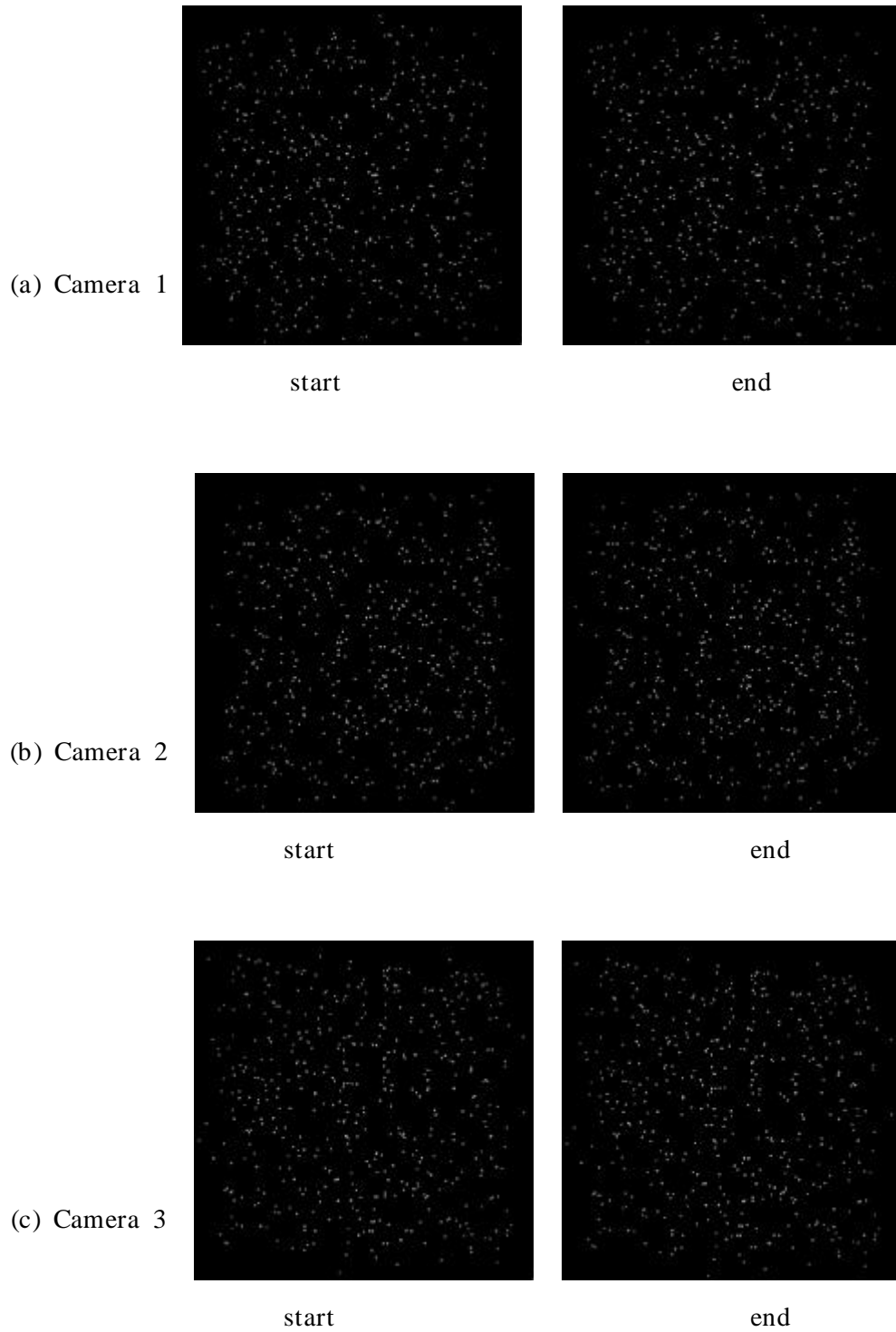


Fig. 3.9 Virtual images viewed by cameras on an impinging jet

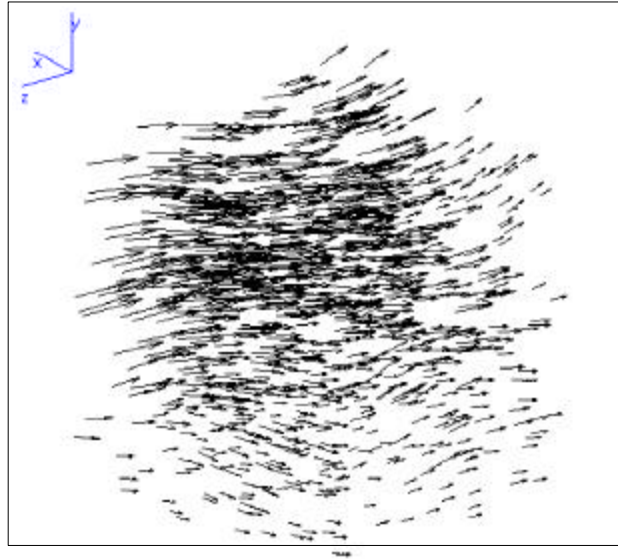


Fig. 3.10 Recovered vectors(IHIK case)

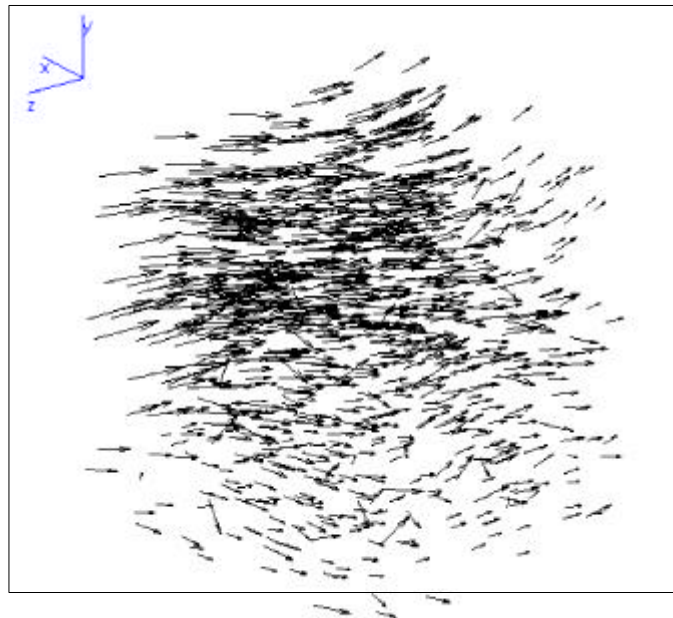


Fig. 3.11 Recovered vectors(RHRK case)

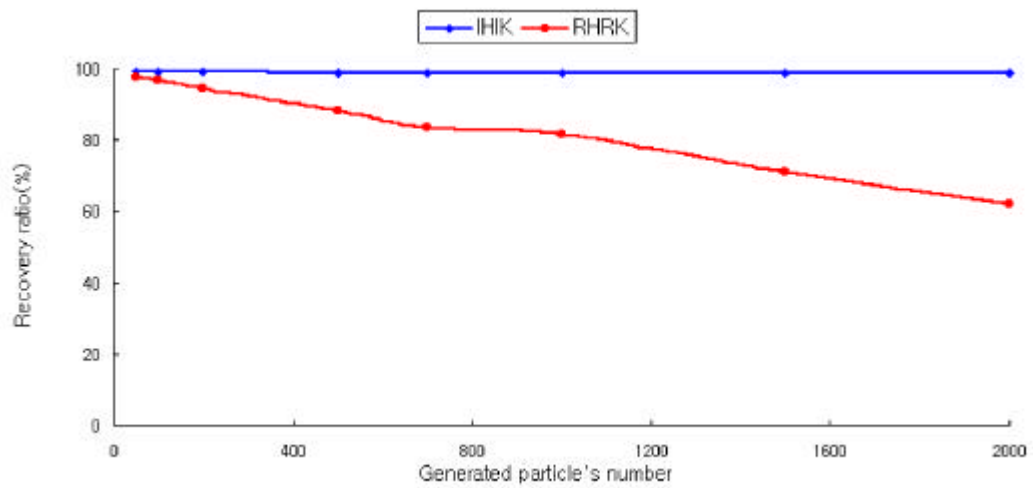


Fig. 3.12 Recovery ratio using GA-3D-PTV(Jet flow)

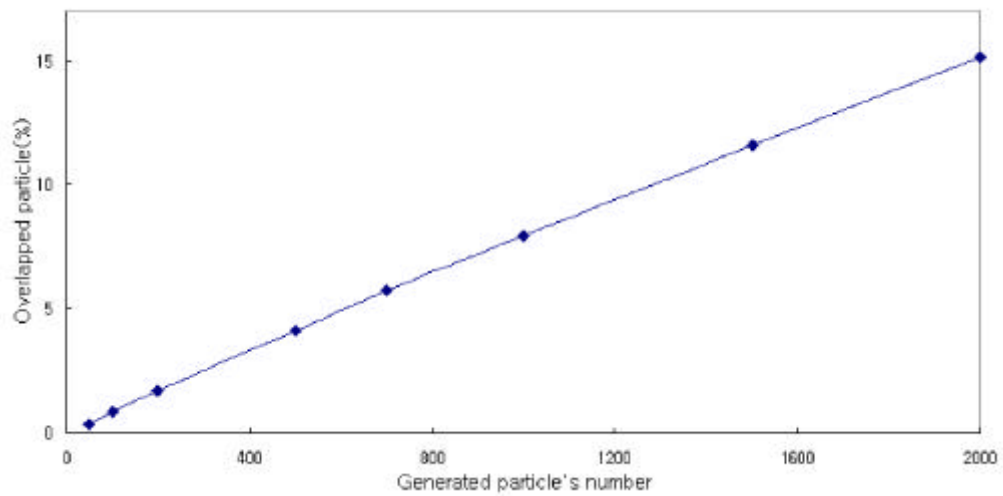


Fig. 3.13 Overlapping rate of particles in the virtual images

4

4.1

Fig. 4.1 $D=30\text{mm}$

3 PTV .

3 CCD (768 × 494 pixels), (

image grabber : 512 × 512 pixels, 256 gray levels), (500mW), AOM

, 3 , 32bit .

AOM(Acousto-Optical Modulator)

. AOM CCD

, 1 1/30 (1/60)

(1/60)

. 3 (Ditect 64)

256gray levels(512 × 512) .

64 M RAM , R, G, B

64 .

, ,

.

(boundary trace) (2.11)

.

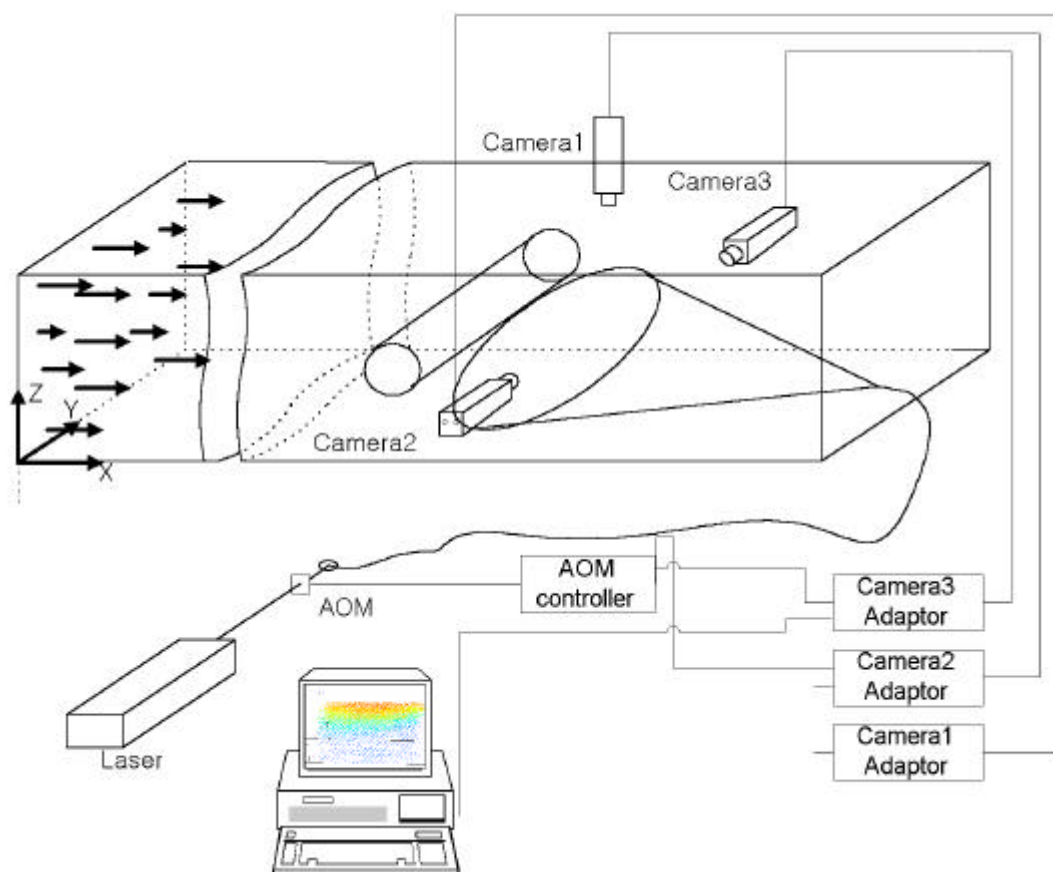


Fig. 4.1 Experimental set up for 3D-PTV measurement

4.2

$$250 \times 75 \times 2400 \text{mm}^3$$

1020mm

Fig. 2.3

0.33D 3.7D (X, Y, Z)
2.500D X(-40 40mm), Y(-50 50mm), Z(0 70mm)

(12, 1.02)

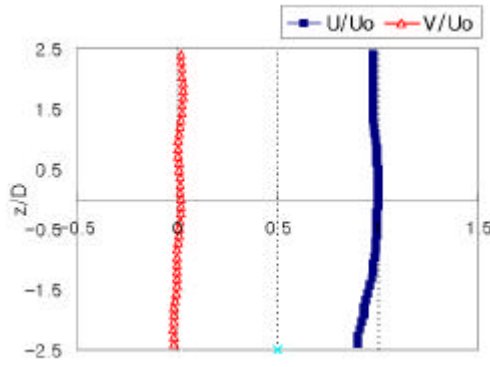
Ar-ion (500mW)

D 30mm ,

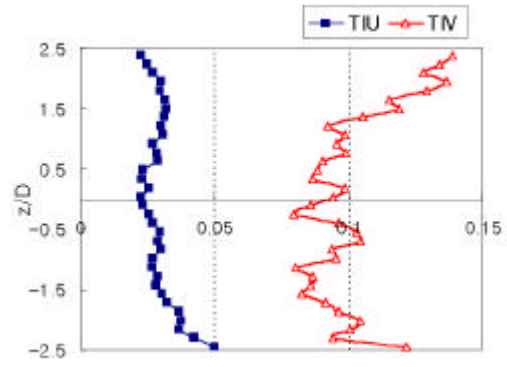
Re = 1050 .

Fig.4.2

y/D=-5D

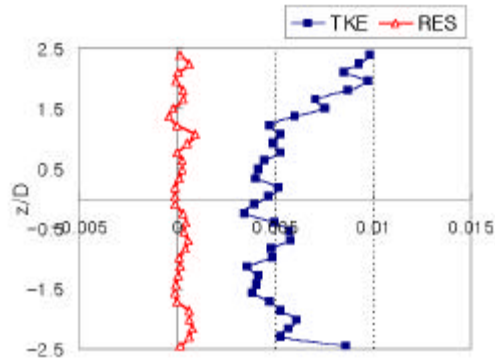


(a) Mean velocity profile



(b) Turbulence intensity (U and V)

$$(T_u = \sqrt{u'^2} / U_0, \quad T_v = \sqrt{v'^2} / U_0)$$



(c) Turbulence kinetic energy and Reynolds stress

$$(TKE = \frac{1}{2} q^2 / U_0^2, \quad RES = - \overline{u'v'} / U_0^2)$$

Fig. 4.2 Inlet flow condition at $y/D = -5$

5

5.1 3

Fig. 5.1 Fig. 4.1

. Fig. 5.2

3

3

, (1

Frame 1) 1100

Gaussian Window

Fig. 5.3 3

. Karman 가 가

. Karman 가

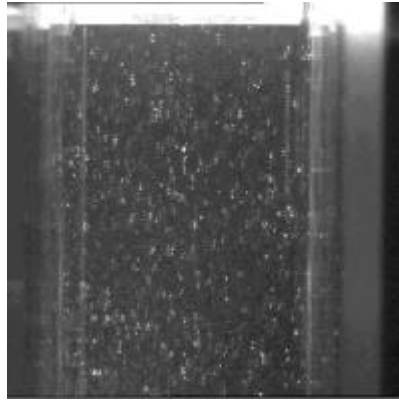
.

Fig. 5.4 Fig. 5.5

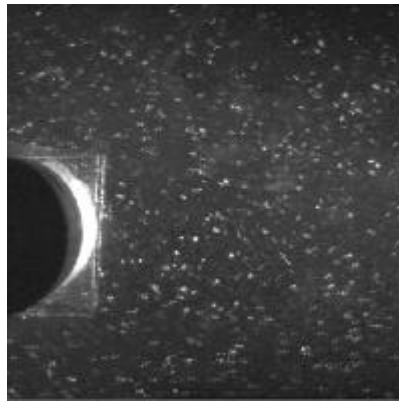
xy , xz

. Brede ³⁷⁾ 가 300

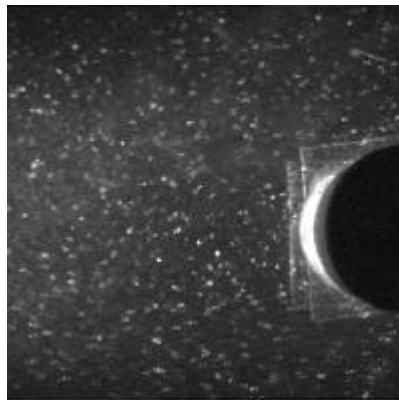
B (Fig. 5.6)가 .



(a) Camera 1



(b) Camera 2



(c) Camera 3

Fig. 5.1 Raw images viewed by each camera

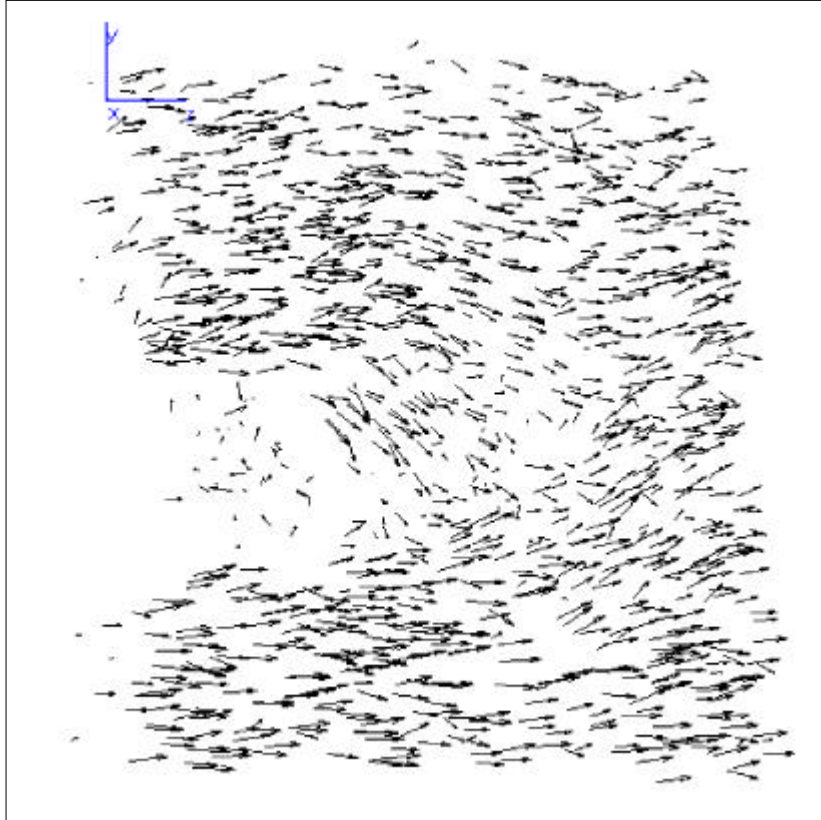
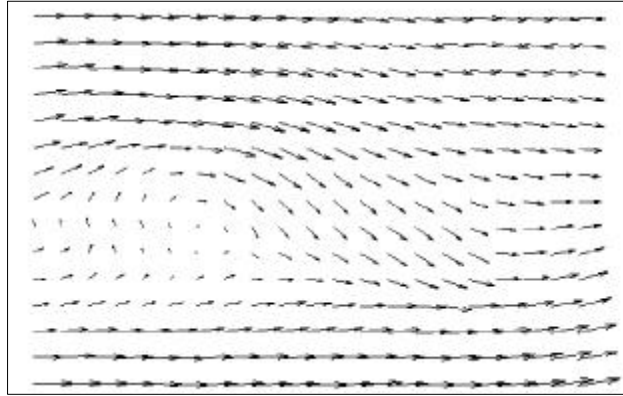
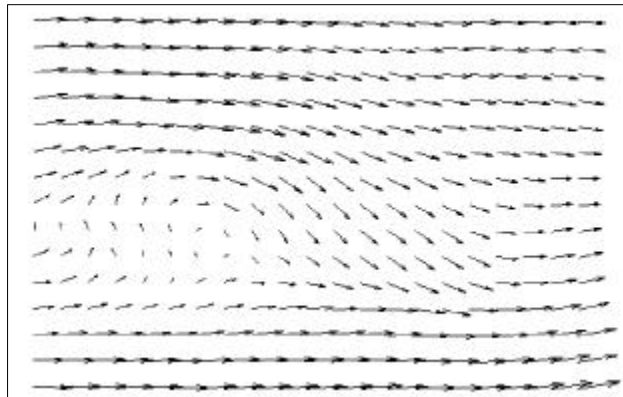


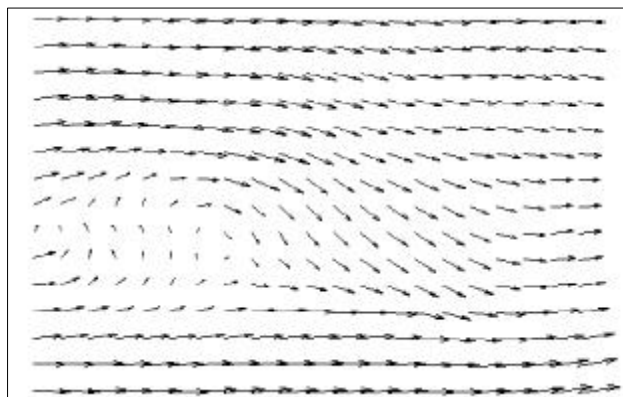
Fig. 5.2 Instantaneous 3D velocity vectors obtained by GA-3D-PTV



(a) $t=t_0$

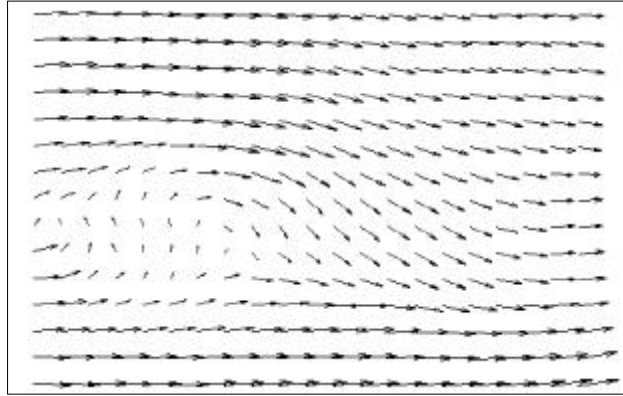


(b) $t=t_0 + 1/30$

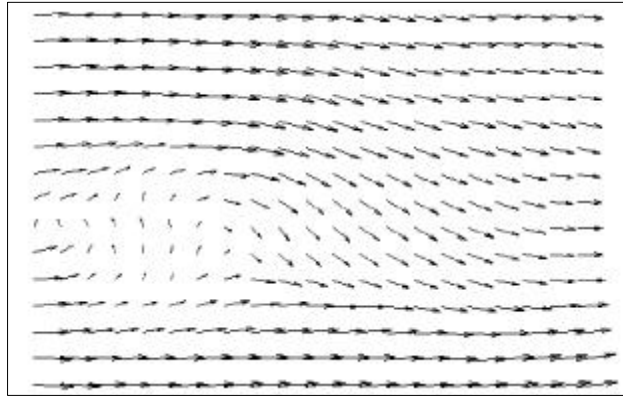


(c) $t=t_0 + 2/30$

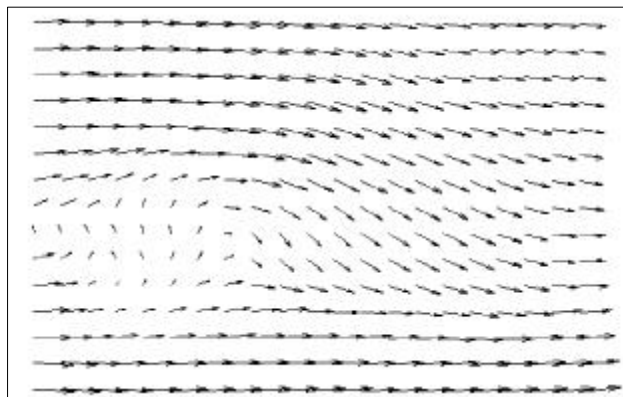
Fig. 5.3 Temporal evolution of velocity field (continued)



(d) $t = t_0 + 3/30$

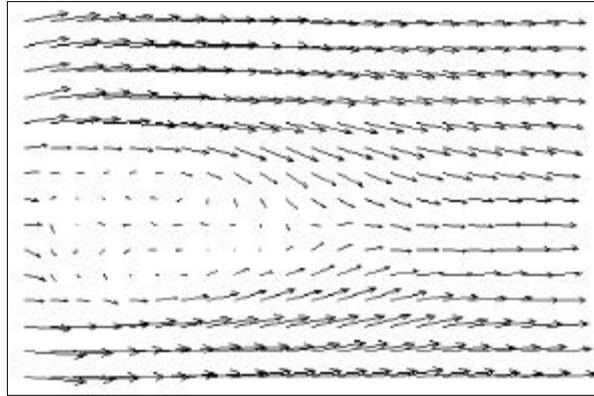


(e) $t = t_0 + 4/30$

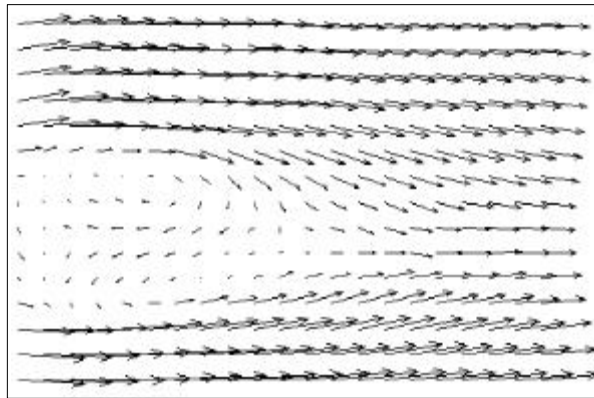


(f) $t = t_0 + 5/30$

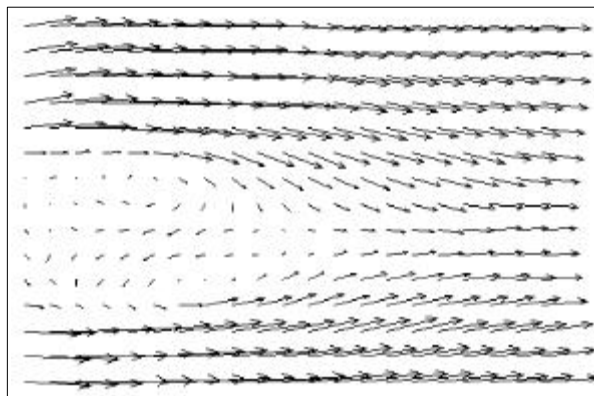
Fig. 5.3 Temporal evolution of velocity field



(a) $Z = 10\text{mm}$

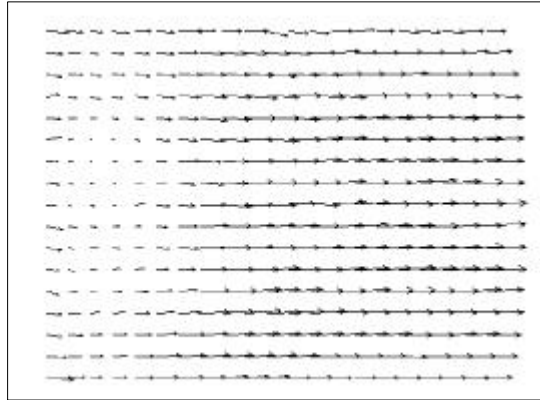


(b) $Z = 35\text{mm}$

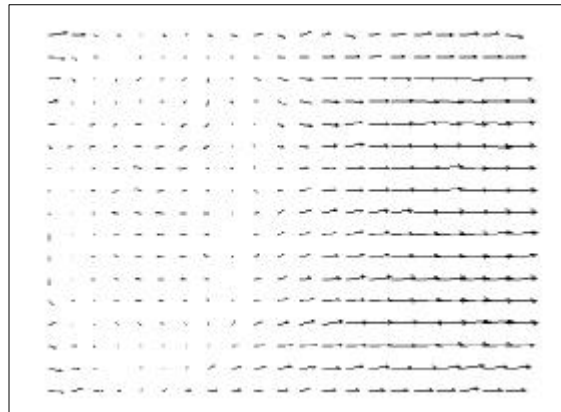


(c) $Z = 45 \text{ mm}$

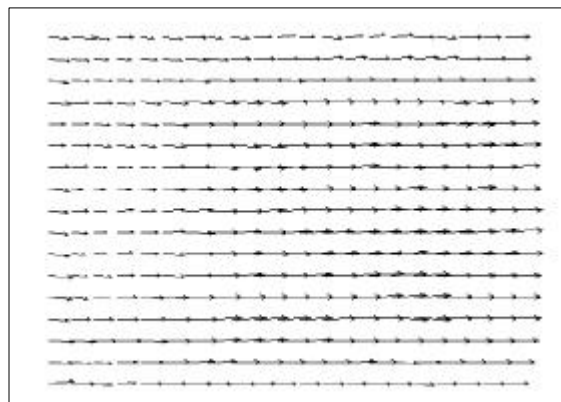
Fig. 5.4 Instantaneous velocity field of xy-plane



(a) $Y = 10 \text{ mm}$



(b) $Y = 35 \text{ mm}$



(c) $Y = 45 \text{ mm}$

Fig. 5.5 Instantaneous velocity field of xz-plane

Fig. 5.7 1,500,000 3 Gaussian Window
3 .



(a) A-mode



(b) B-mode

Fig. 5.6 Vortices' structures

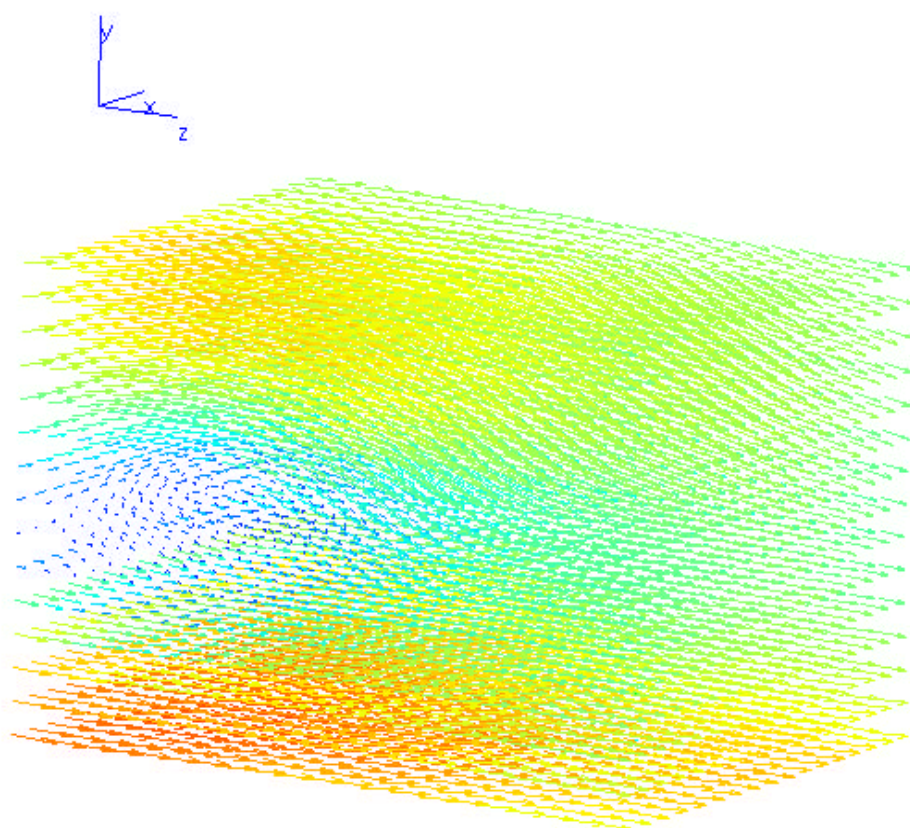


Fig. 5.7 Mean velocity field

5.2

Fig. 5.8 (a) (u)

Y=2.500D
D 2.500D X=0.000D, Z=0.000D

Fig. 5.8 (b) (i) X-Y plane Z 0.333D 가
(u) Z=-0.167D
Z=0.167D Y=2.500D 가
가 Y
X-Y

Fig. 5.9 Y-Z (u)

X=0.000D
X=-0.333D 가
Y=2.500D, Z=0.000D(), X=-0.333D

Y=2.500D X
B

Fig. 5.10 X-Z plane Y 0.333D 가

(u) Z=-0.167D

vortex trail 가

가

Y=2.500D

가

X-Y

Y=2.500D

가

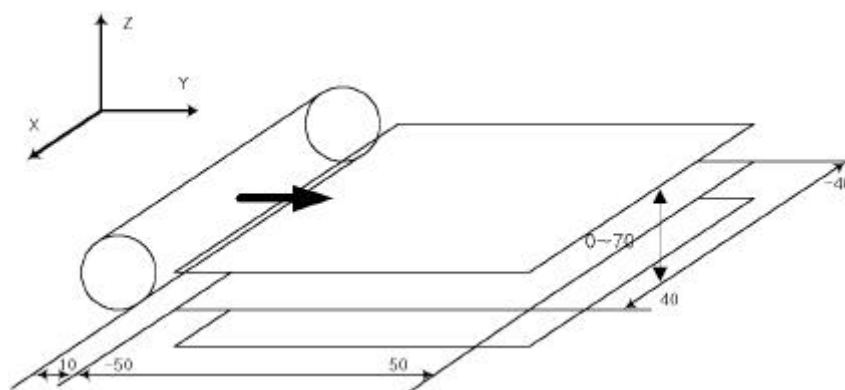
, Y=2.500D, Z=0.000D

vortex trail

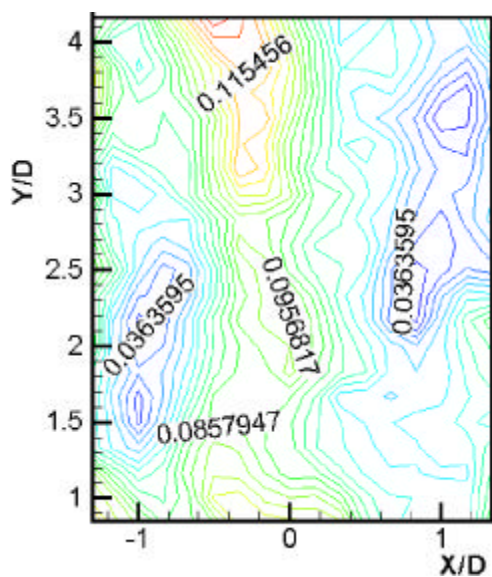
, Brede³⁷⁾

B

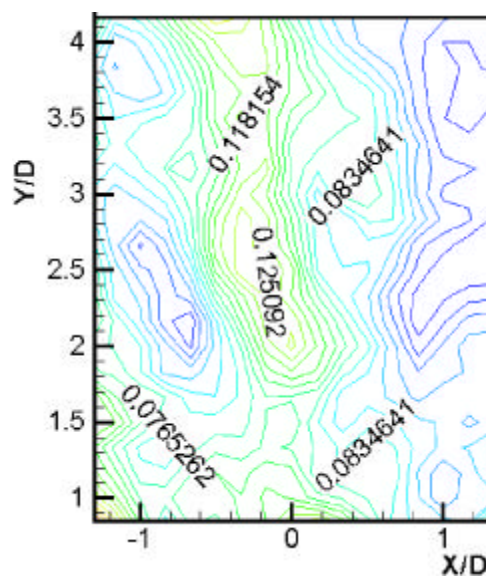
(Fig. 5.6)



(a) Measuring region

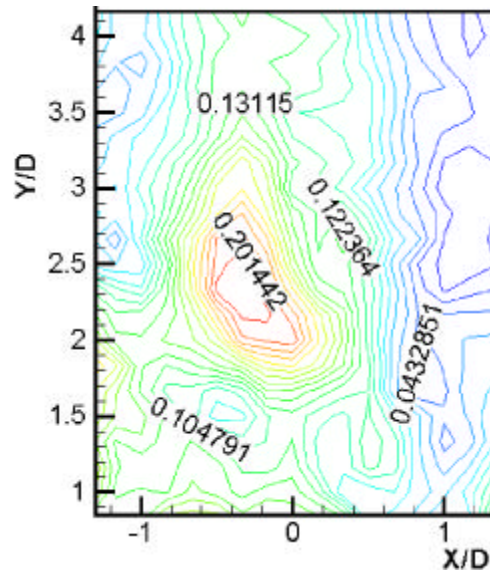


(b) $Z = -1.167D$

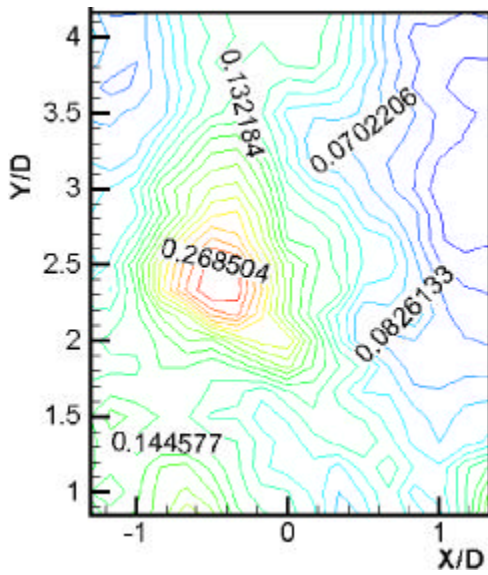


(c) $Z = -0.833D$

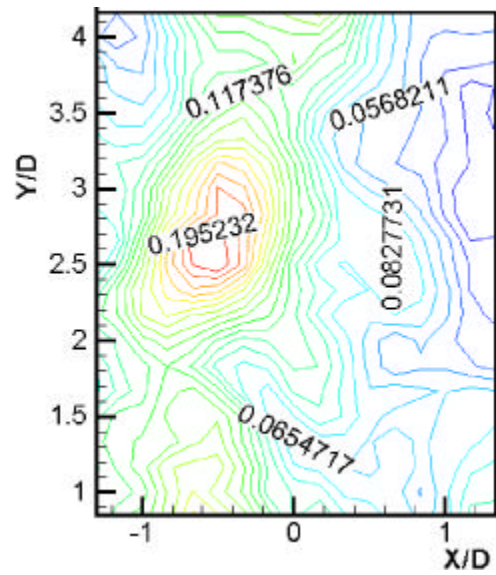
Fig. 5.8 Turbulence intensity distribution ($T_u = \sqrt{u'^2} / U_0$) (continued)



(d) $Z = -0.500D$

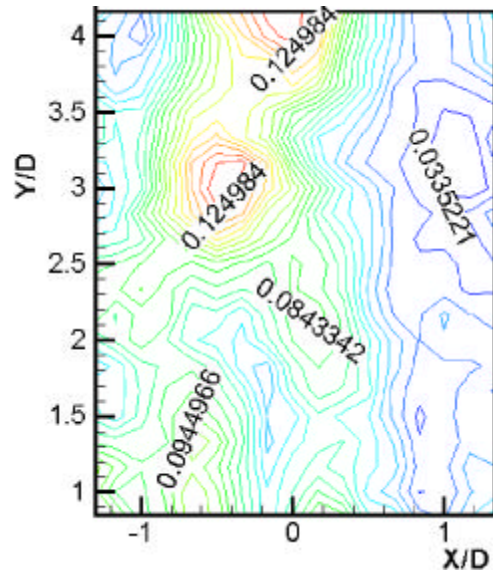


(e) $Z = -0.167D$

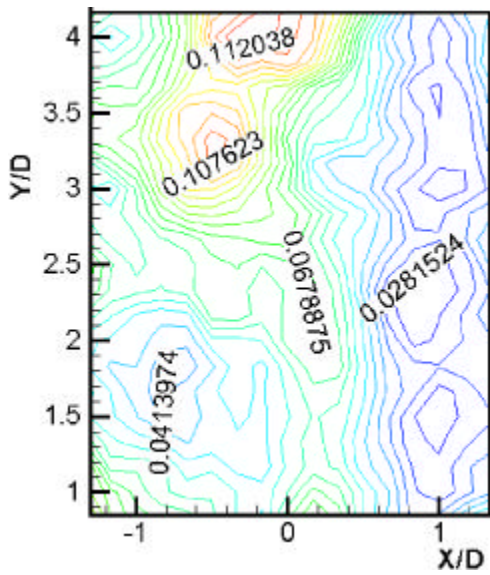


(f) $Z = 0.167D$

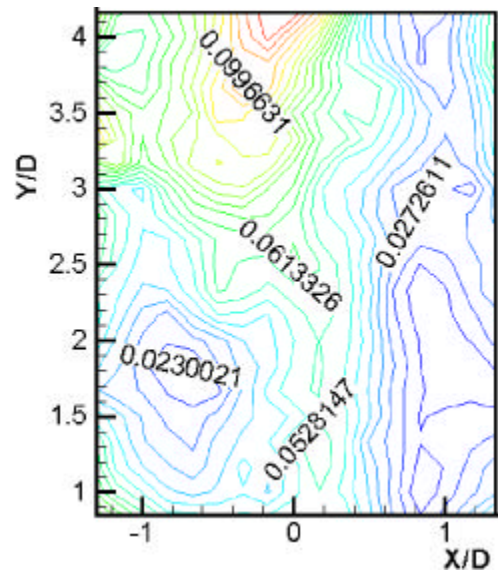
Fig. 5.8 Turbulence intensity distribution ($T_u = \sqrt{u'^2} / U_0$) (continued)



(g) $Z = 0.500D$

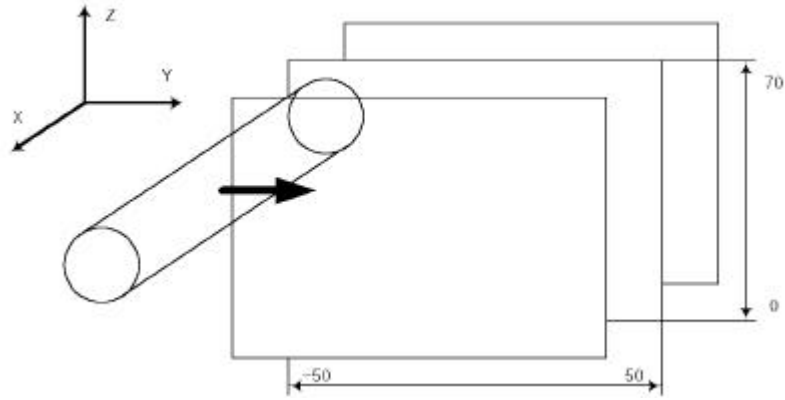


(h) $Z = 0.833D$

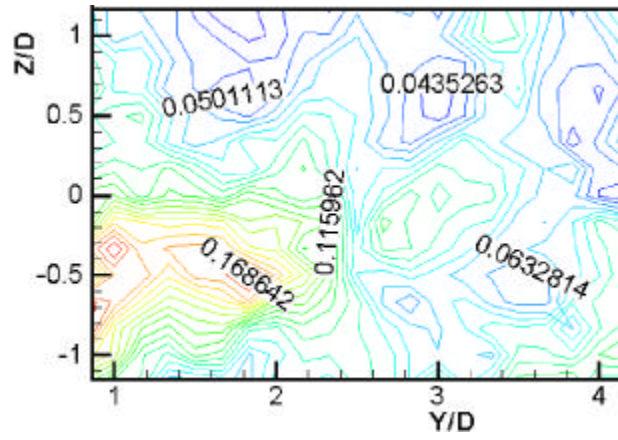


(i) $Z = 1.167D$

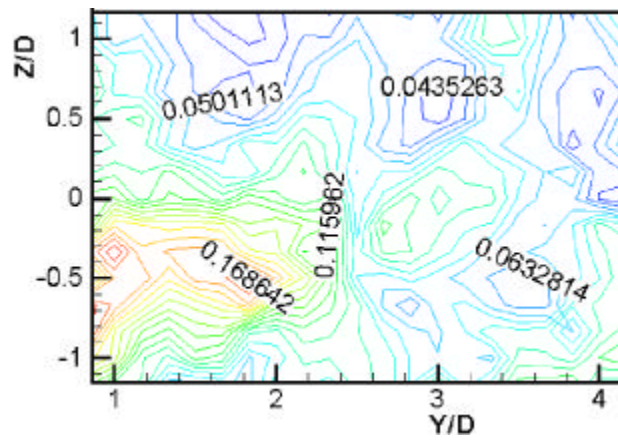
Fig. 5.8 Turbulence intensity distribution ($T_u = \sqrt{u'^2} / U_0$) (continued)



(a) Measuring region

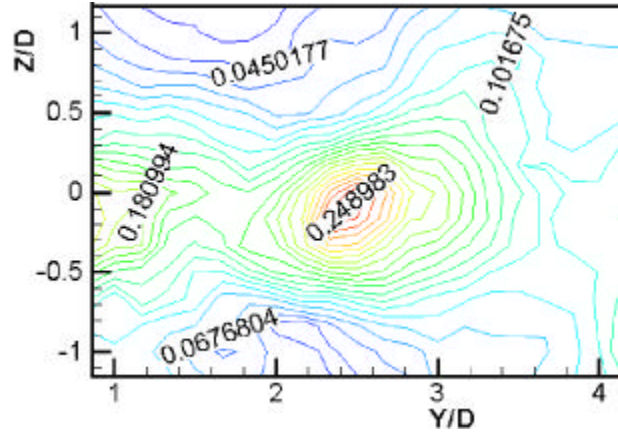


(b) $X = -1.333D$

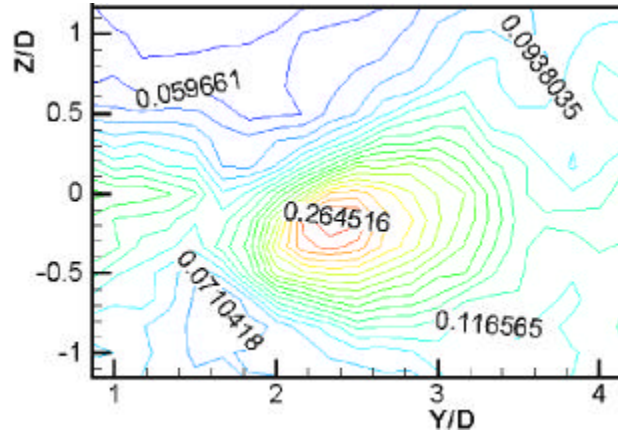


(c) $X = -1.000D$

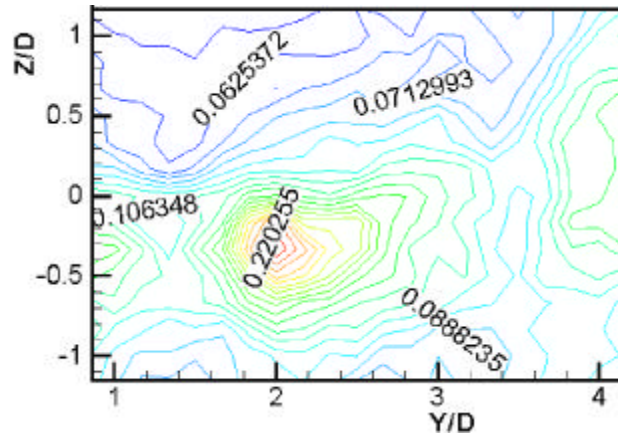
Fig. 5.9 Turbulence intensity distribution ($T_u = \sqrt{u'^2} / U_0$) (continued)



(d) $X = -0.667D$

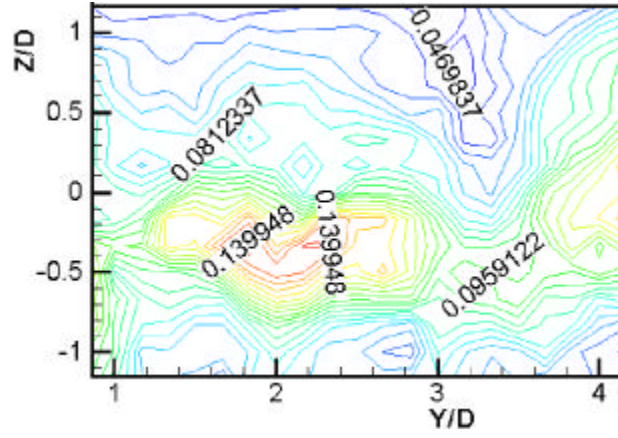


(e) $X = -0.333D$

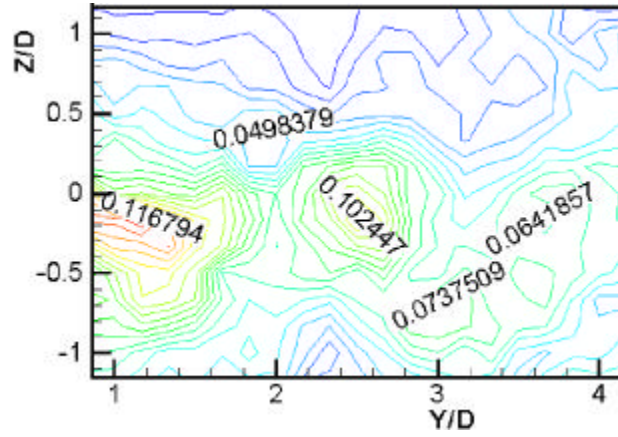


(f) $X = 0.000D$

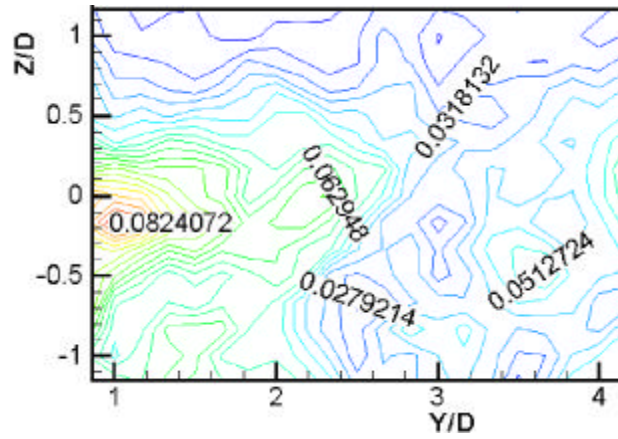
Fig. 5.9 Turbulence intensity distribution ($T_u = \sqrt{u'^2} / U_0$) (continued)



(g) $X = 0.333D$

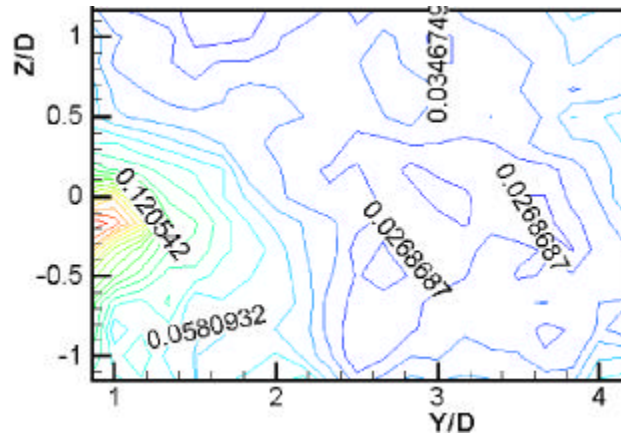


(h) $X = 0.667D$



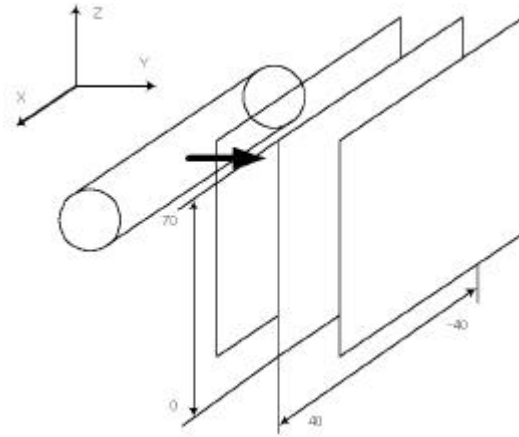
(i) $X = 1.000D$

Fig. 5.9 Turbulence intensity distribution ($T_u = \sqrt{u'^2} / U_0$) (continued)

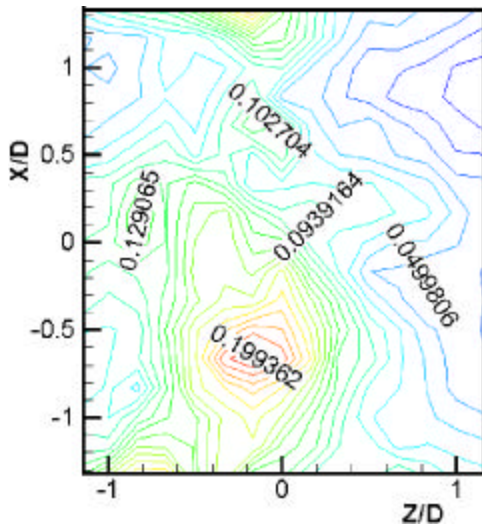


(j) $X = 1.333D$

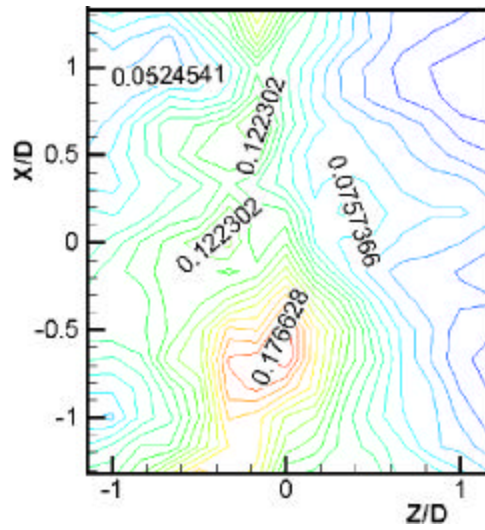
Fig. 5.9 Turbulence intensity distribution ($T_u = \sqrt{u'^2} / U_0$) (continued)



(a) Measuring region

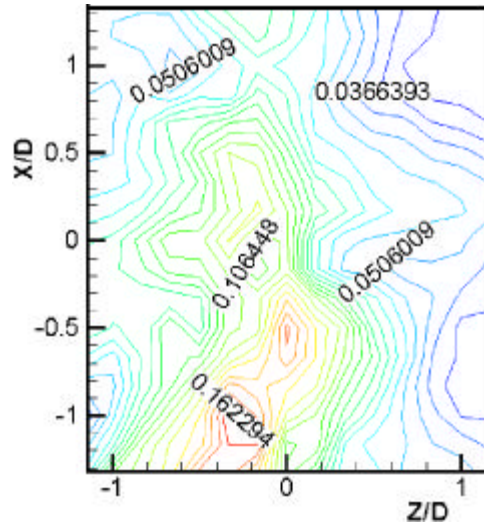


(b) $Y = 0.833D$

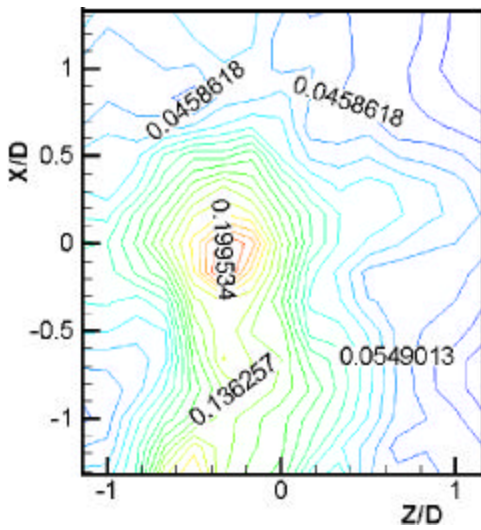


(c) $Y = 1.167D$

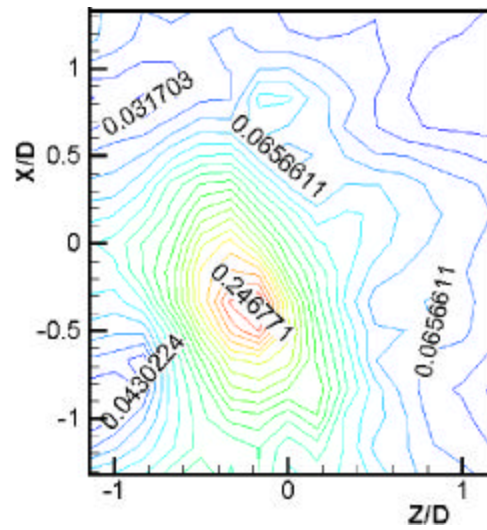
Fig. 5.10 Turbulence intensity distribution ($T_u = \sqrt{u'^2} / U_0$) (continued)



(d) $Y = 1.500D$

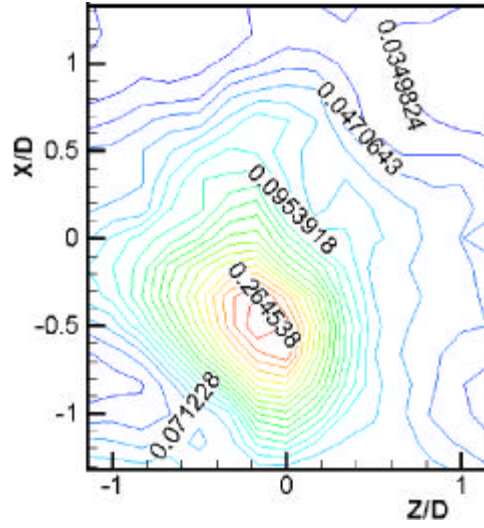


(e) $Y = 1.833D$

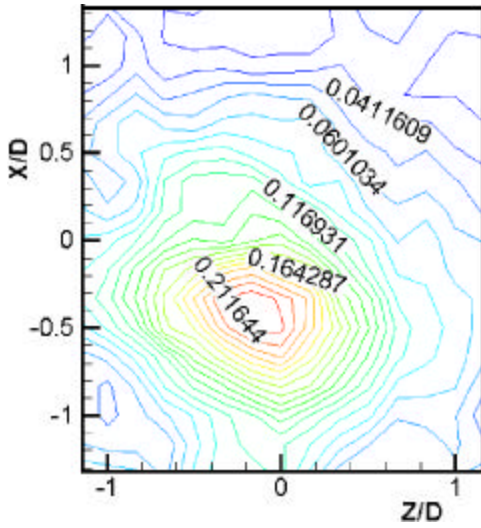


(f) $Y = 2.167D$

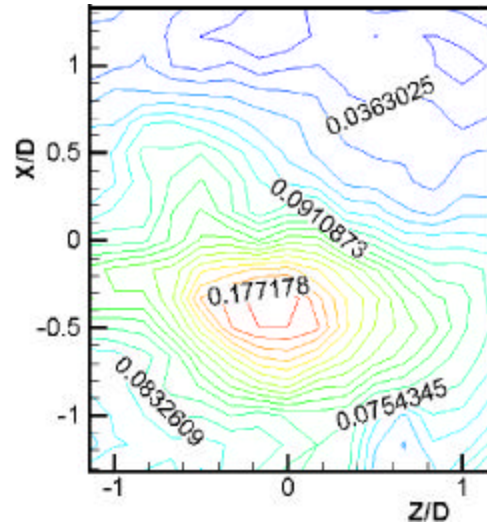
Fig. 5.10 Turbulence intensity distribution ($T_u = \sqrt{u'^2} / U_0$) (continued)



(g) $Y = 2.500D$

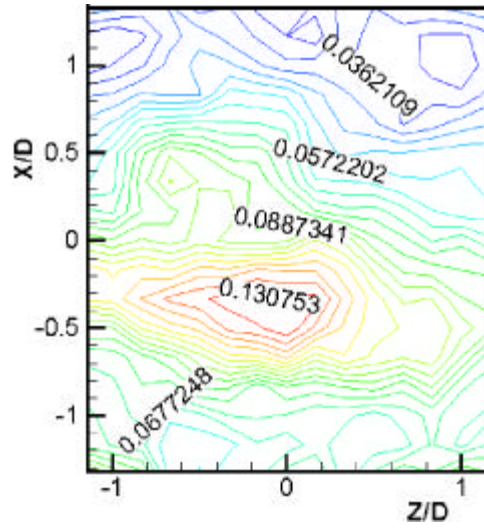


(h) $Y = 2.833D$

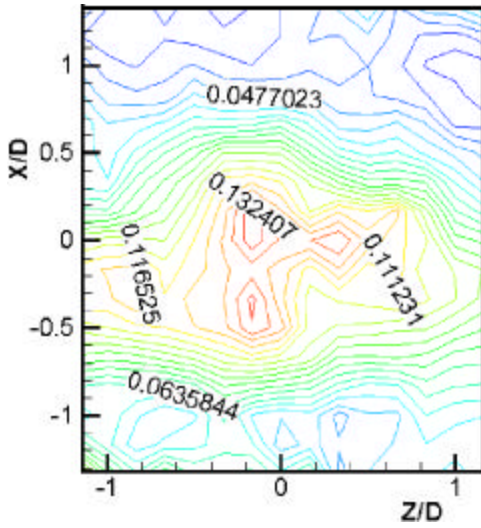


(i) $Y = 3.167D$

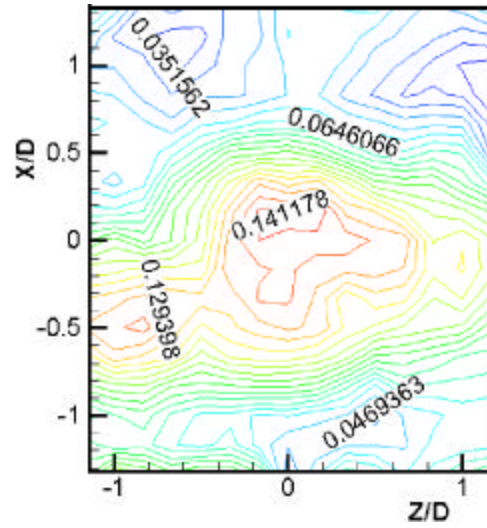
Fig. 5.10 Turbulence intensity distribution ($T_u = \sqrt{u'^2} / U_0$) (continued)



(j) $Y = 3.500D$



(k) $Y = 3.833D$



(l) $Y = 4.167D$

Fig. 5.10 Turbulence intensity distribution ($T_u = \sqrt{u'^2} / U_0$)

Fig. 5.11 (a) (v)

Y=2.500D
D 2.5D X=0.000D, Z=0.000D

Fig. 5.11 (b) (i) X- Y plane Z 0.333D 가

(v) Z=0.000D(
) Y=1.667D (0.245907) 가
가 Z
X- Y

Fig. 5.12 Y- Z (v)

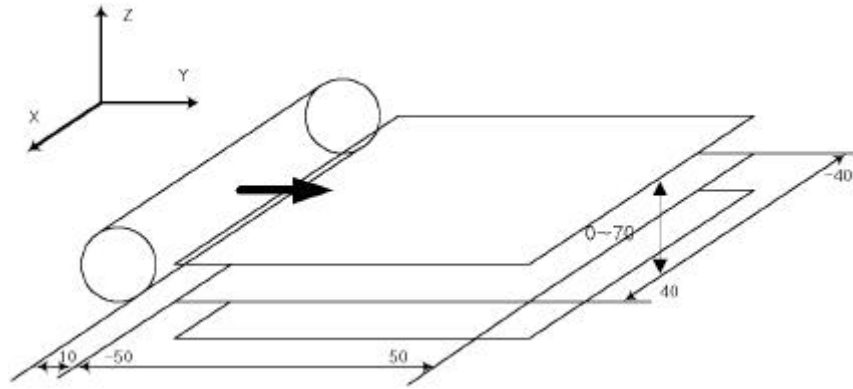
X=0.000D
X=- 1.333D 가 X=0.000D
v 가

spanwise w 가

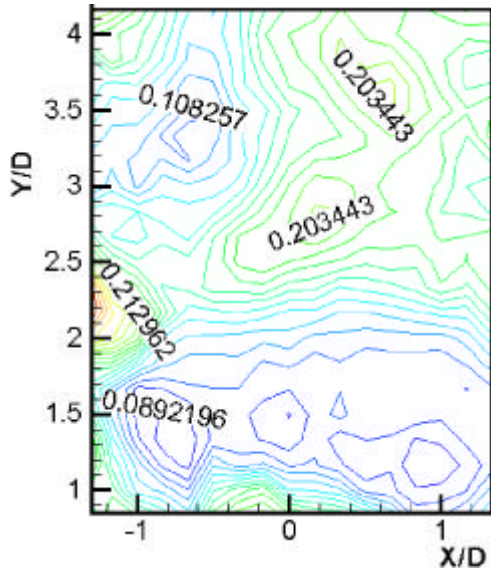
Fig. 5.14 w

Fig. 5.13 X- Z plane Y 0.333D 가

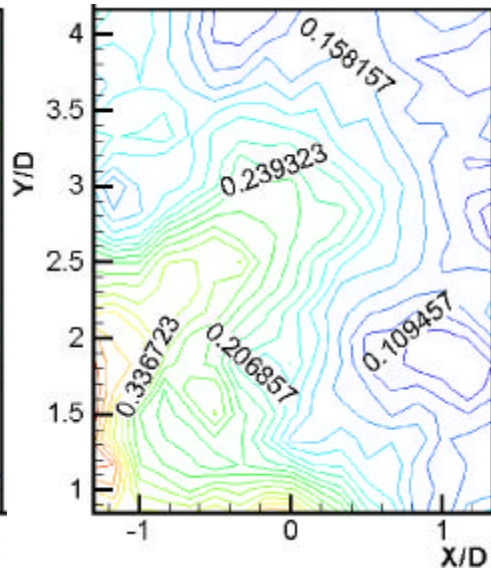
(v) X=- 0.667D, Y=4.000D,
Z=- 0.167D ,
vortex trail (Z=0.000D) 가
Z=0.000D(
가



(a) Measuring region

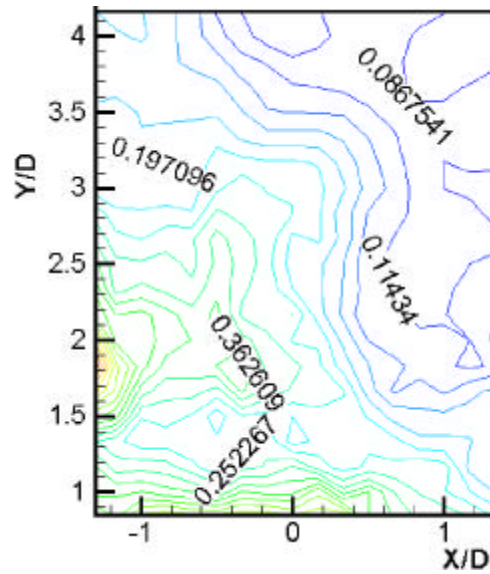


(b) $Z = -1.167D$

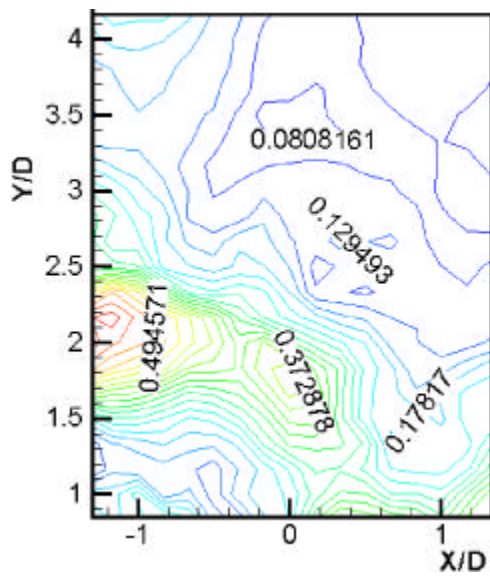


(c) $Z = -0.833D$

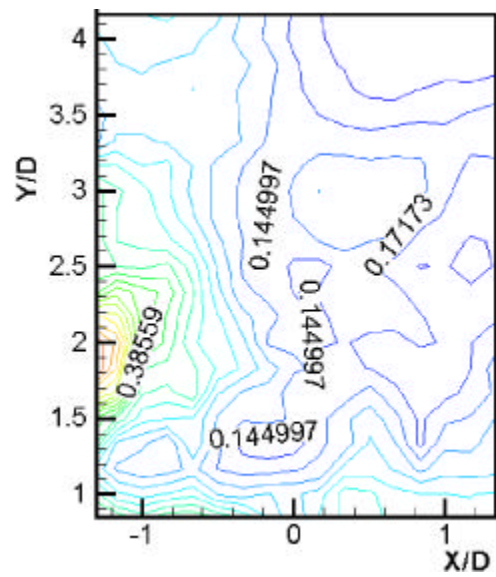
Fig. 5.11 Turbulence intensity distribution ($T_v = \sqrt{v'^2} / U_0$) (continued)



(d) $Z = -0.500D$

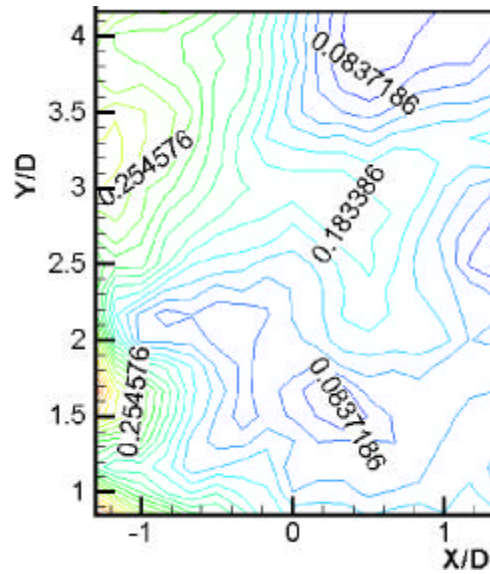


(e) $Z = -0.167D$

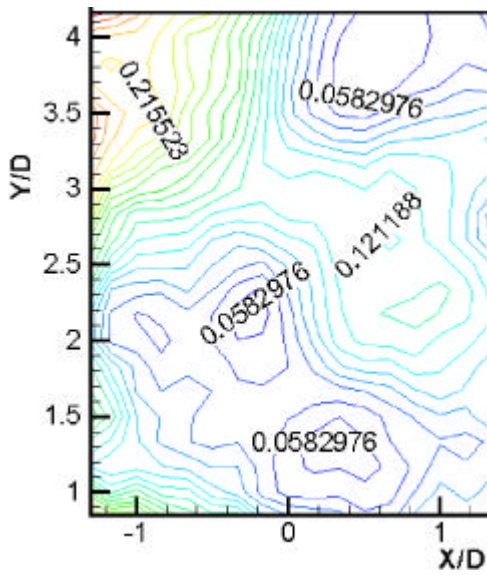


(f) $Z = 0.167D$

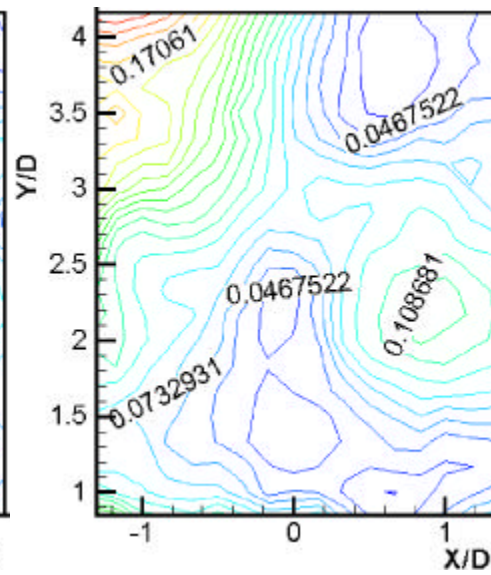
Fig. 5.11 Turbulence intensity distribution ($T_v = \sqrt{v'^2} / U_0$) (continued)



(g) $Z = 0.500D$

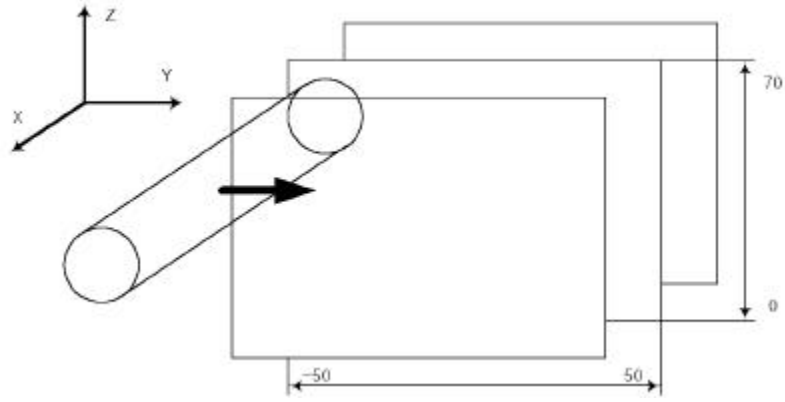


(h) $Z = 0.833D$

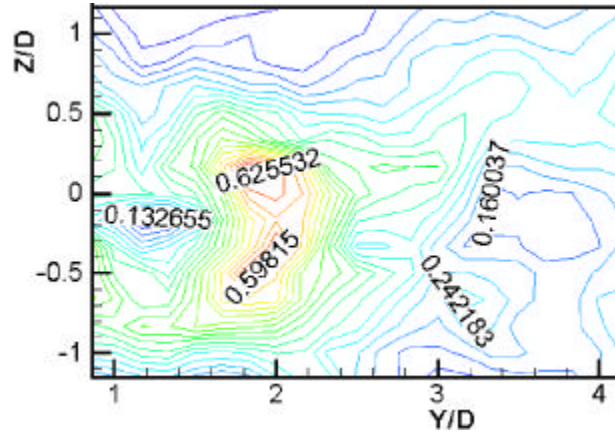


(i) $Z = 1.167D$

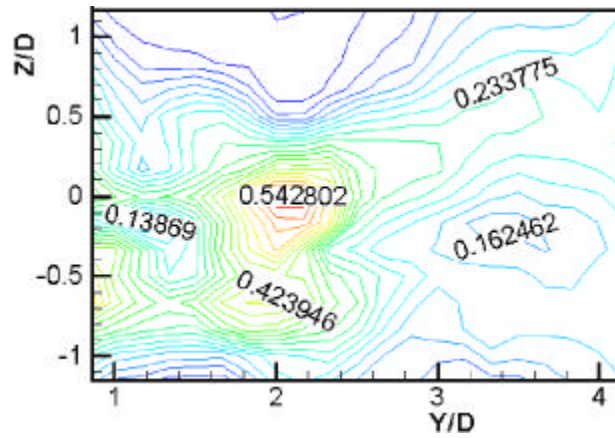
Fig. 5.11 Turbulence intensity distribution ($T_v = \sqrt{v'^2} / U_0$) (continued)



(a) Measuring region

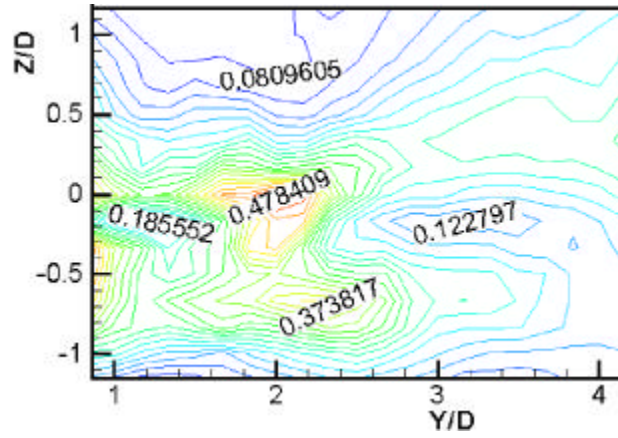


(b) $X = -1.333D$

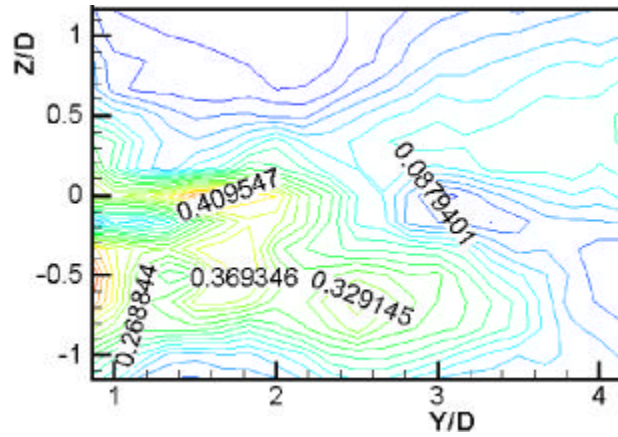


(c) $X = -1.000D$

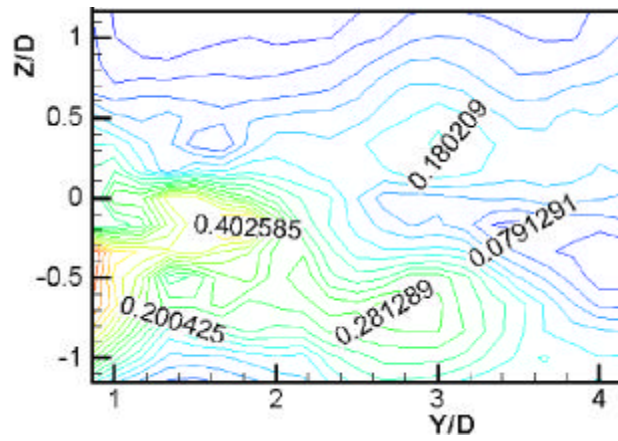
Fig. 5.12 Turbulence intensity distribution ($T_v = \sqrt{v'^2} / U_0$) (continued)



(d) $X = -0.667D$

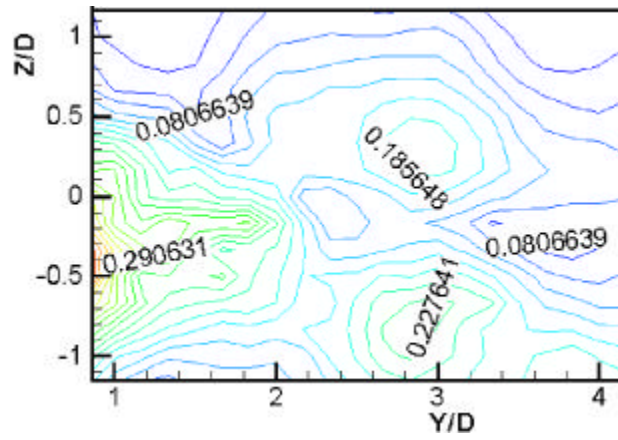


(e) $X = -0.333D$

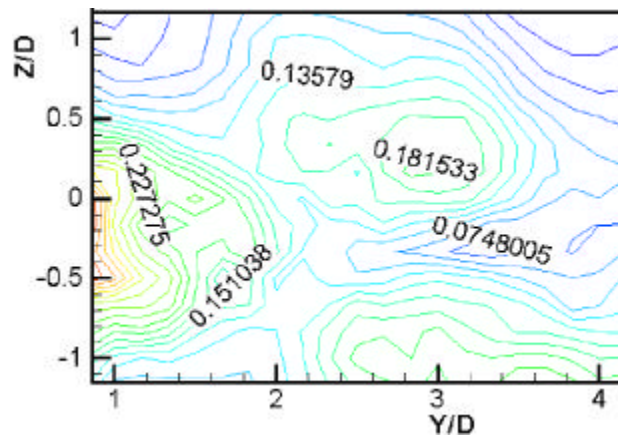


(f) $X = 0.000D$

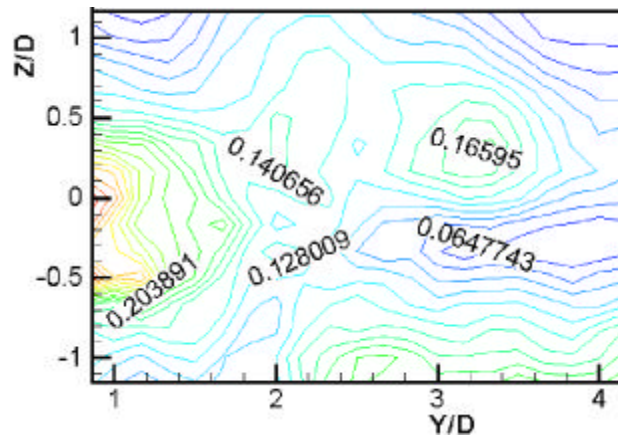
Fig. 5.12 Turbulence intensity distribution ($T_v = \sqrt{v'^2} / U_0$) (continued)



(g) $X = 0.333D$

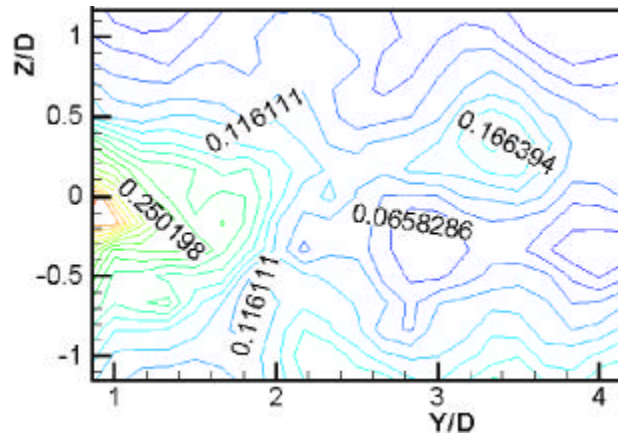


(h) $X = 0.667D$



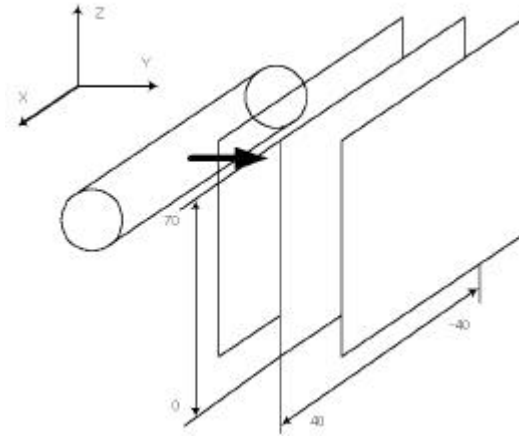
(i) $X = 1.000D$

Fig. 5.12 Turbulence intensity distribution ($T_v = \sqrt{v'^2} / U_0$) (continued)

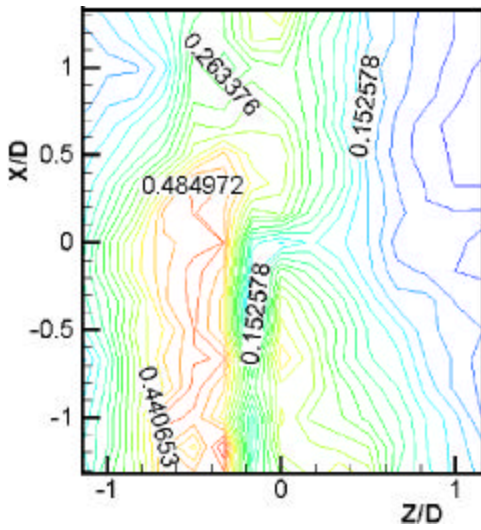


(j) $X = 1.333D$

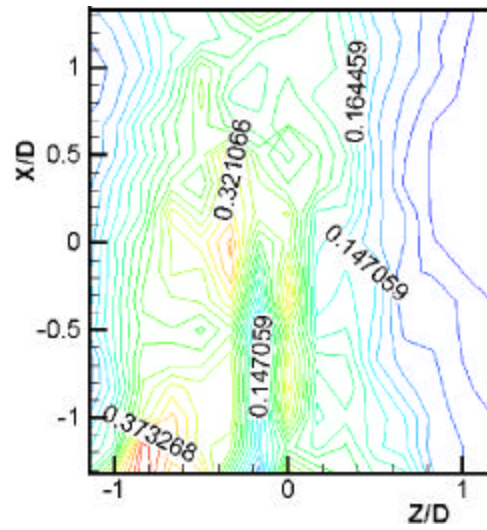
Fig. 5.12 Turbulence intensity distribution ($T_v = \sqrt{v'^2} / U_0$) (continued)



(a) Measuring region

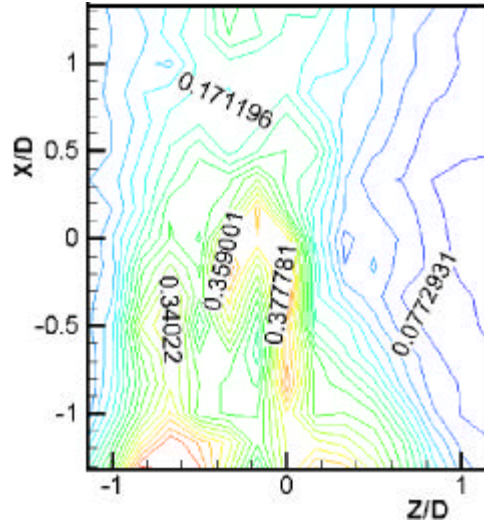


(b) $Y = 0.833D$

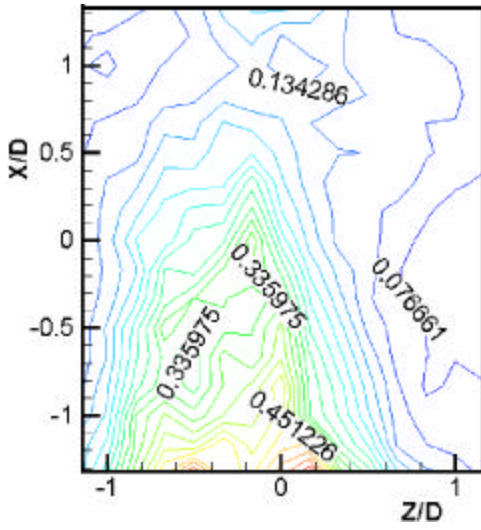


(c) $Y = 1.167D$

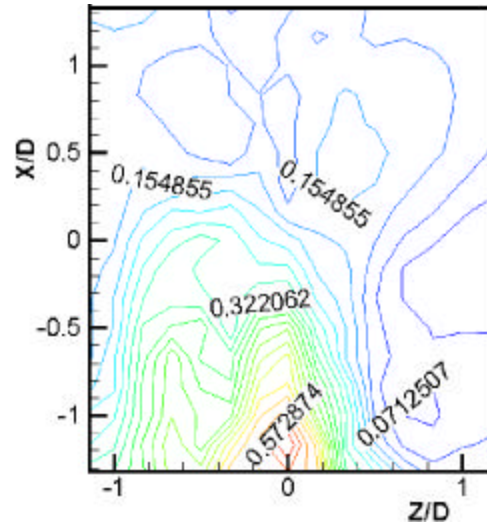
Fig. 5.13 Turbulence intensity distribution ($T_v = \sqrt{v'^2} / U_0$) (continued)



(d) $Y = 1.500D$

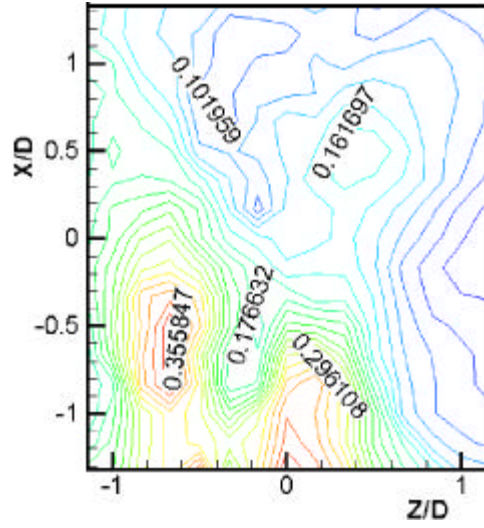


(e) $Y = 1.833D$

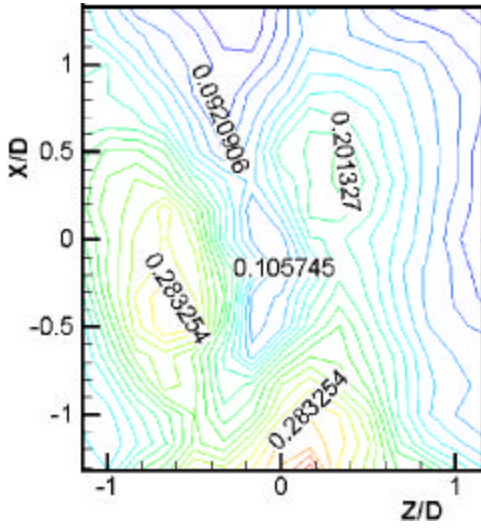


(f) $Y = 2.167D$

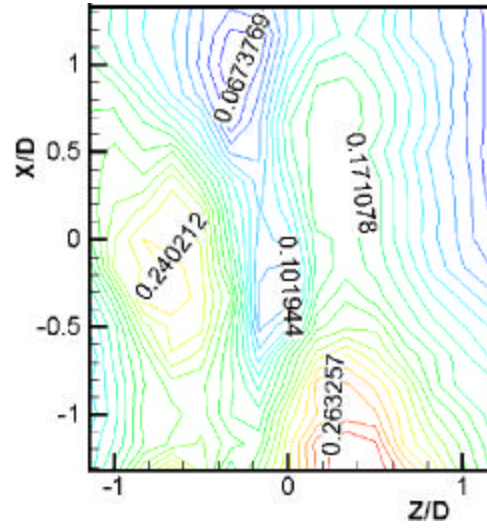
Fig. 5.13 Turbulence intensity distribution ($T_v = \sqrt{v'^2} / U_0$) (continued)



(g) $Y = 2.500D$

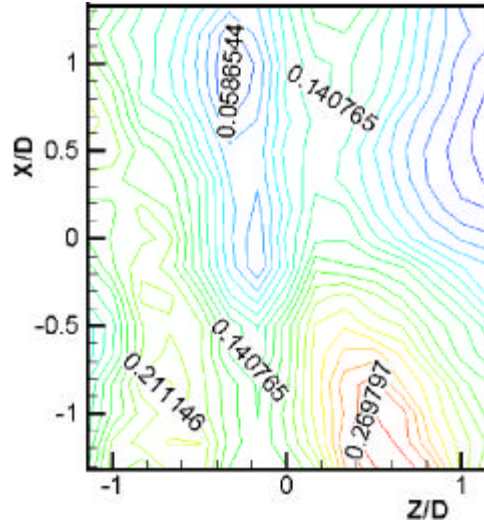


(h) $Y = 2.833D$

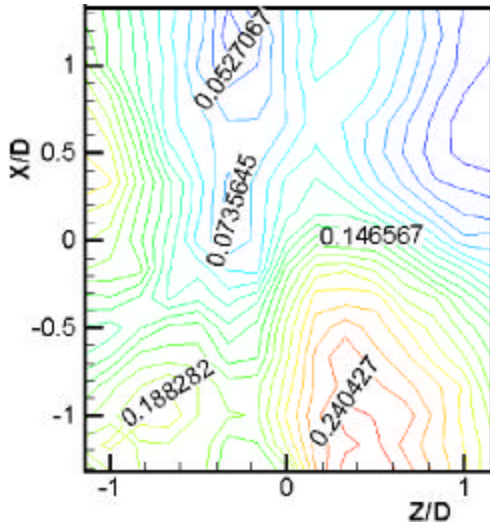


(i) $Y = 3.167D$

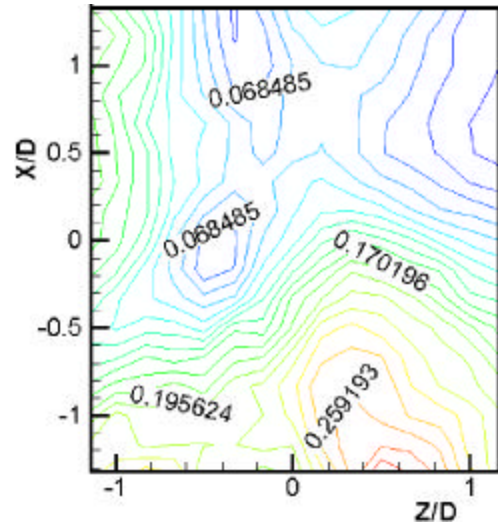
Fig. 5.13 Turbulence intensity distribution ($T_v = \sqrt{v'^2} / U_0$) (continued)



(j) $Y = 3.500D$



(k) $Y = 3.833D$



(l) $Y = 4.167D$

Fig. 5.13 Turbulence intensity distribution ($T_v = \sqrt{\overline{v'^2}} / U_0$) (continued)

Fig. 5.14 (a) (w)

$Y=2.500D$
 $D \quad 2.500D \quad X=0.000D, Z=0.000D$

Fig. 5.14 (b) (i) X-Y plane Z 0.333D 가
(w) . Y=2.5D, Z=0.000D(

$), X=0.000D \quad w \quad Z$
 w

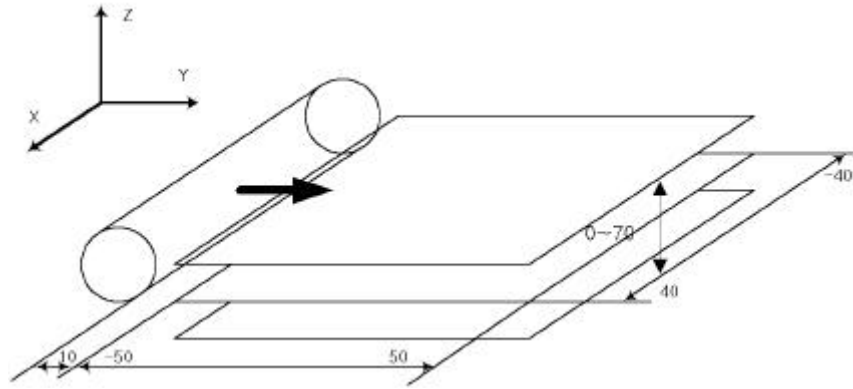
X
 dissipation , Z=0.000D

spanwise
 (homogeneous)

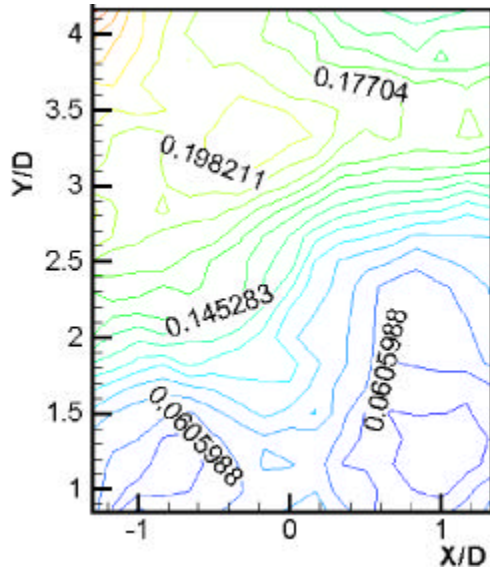
Fig. 5.15 Y-Z (w)
(w) 가
X
B (Fig. 5.6)

Fig. 5.16 X-Z plane Y 0.333D 가
(w) . X=- 0.500D, Y=3.500D,
Z=- 0.333D

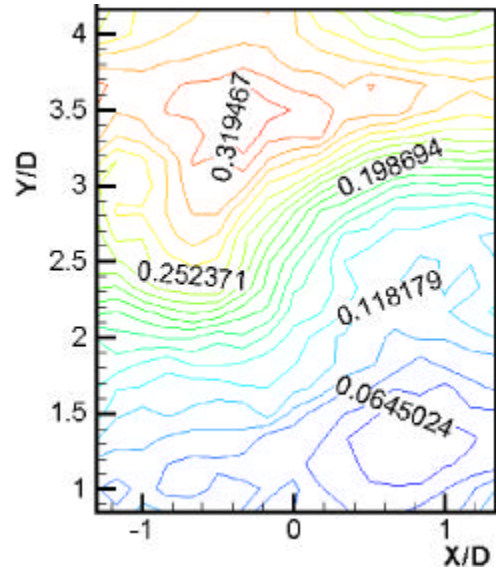
$Y=2.500D \quad Z=- 0.333D$
 가 Y=2.500D 가 가
 X
 가



(a) Measuring region

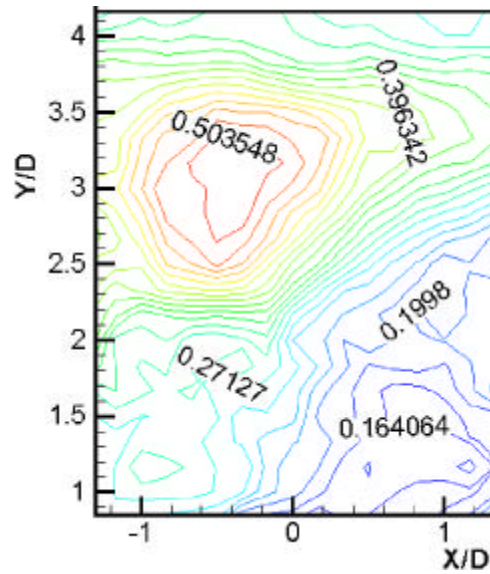


(b) $Z = -1.167D$

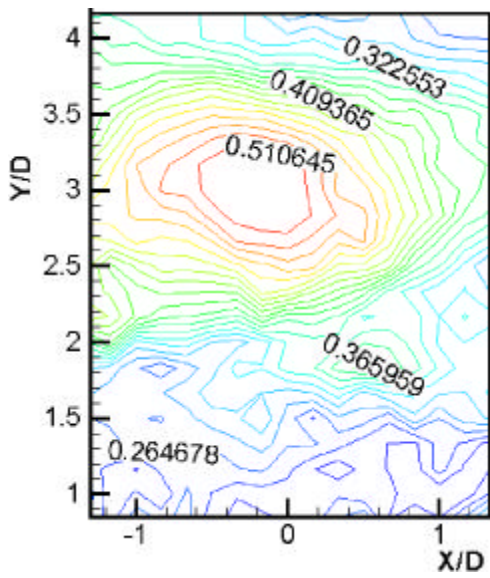


(c) $Z = -0.833D$

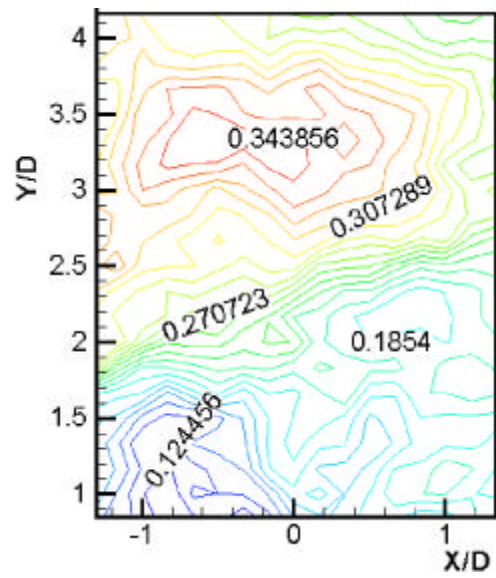
Fig. 5.14 Turbulence intensity distribution ($T_w = \sqrt{w'^2} / U_0$) (continued)



(d) $Z = -0.500D$

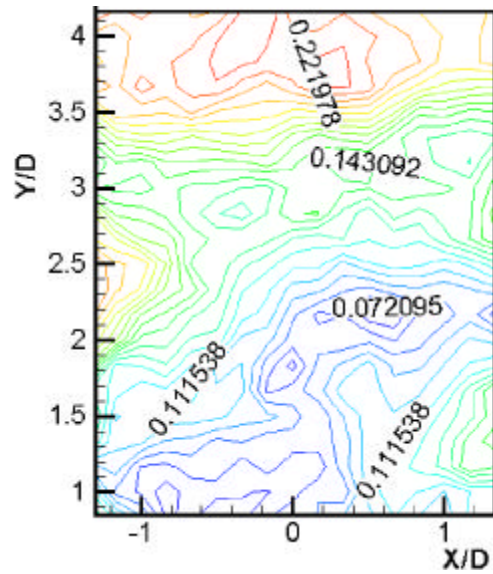


(e) $Z = -0.167D$

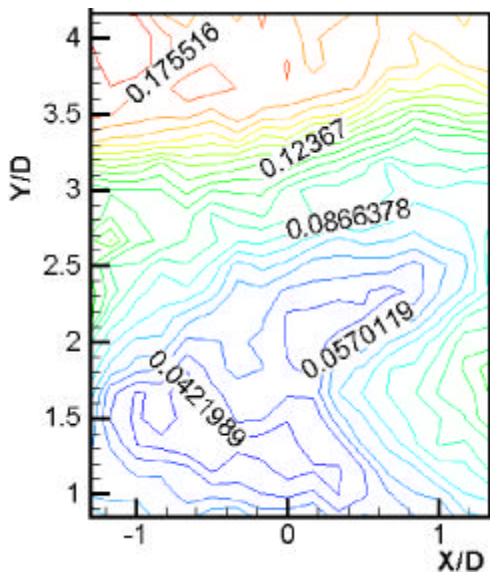


(f) $Z = 0.167D$

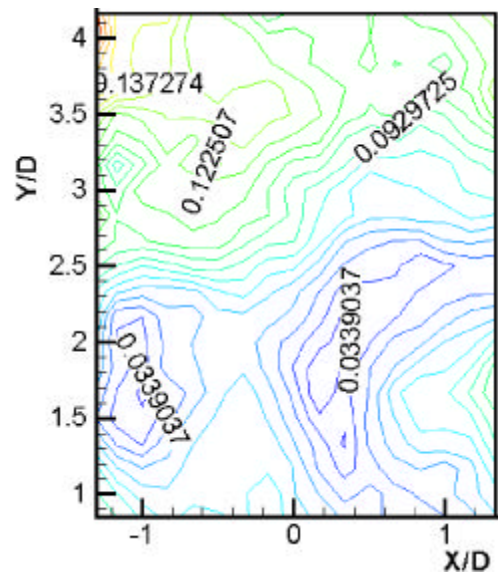
Fig. 5.14 Turbulence intensity distribution ($T_w = \sqrt{w'^2} / U_0$) (continued)



(g) $Z = 0.500D$

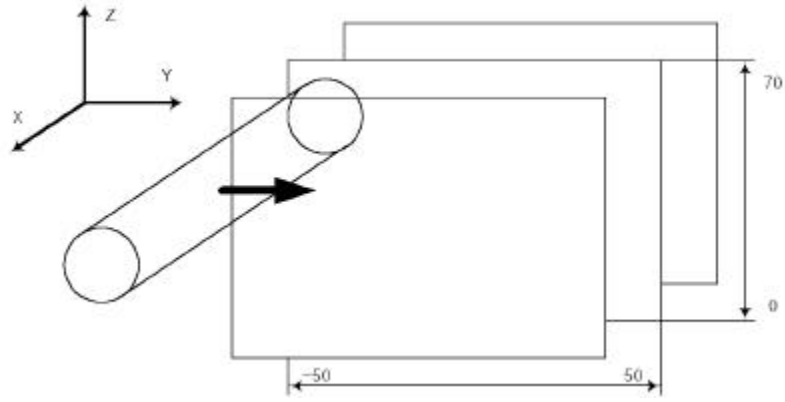


(h) $Z = 0.833D$

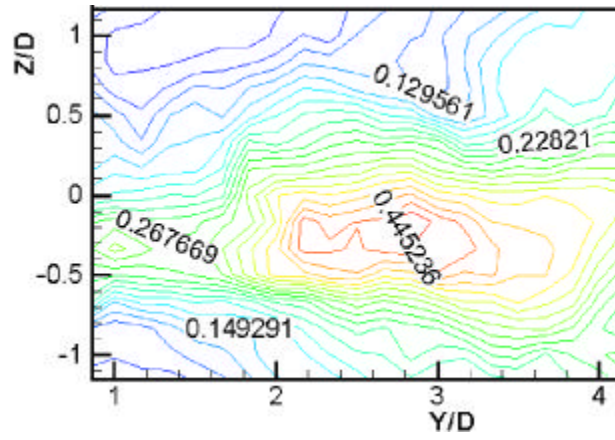


(i) $Z = 0.167D$

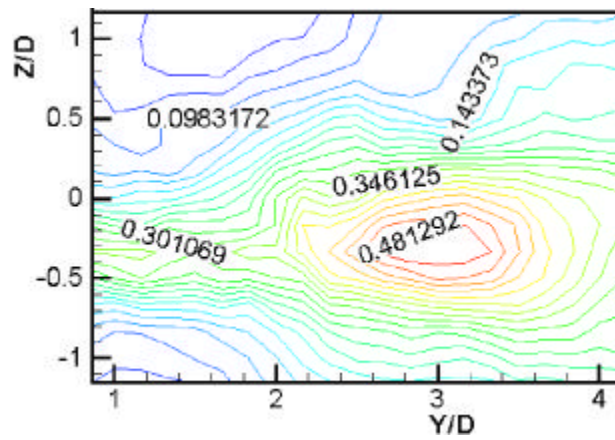
Fig. 5.14 Turbulence intensity distribution ($T_w = \sqrt{w'^2} / U_0$) (continued)



(a) Measuring region

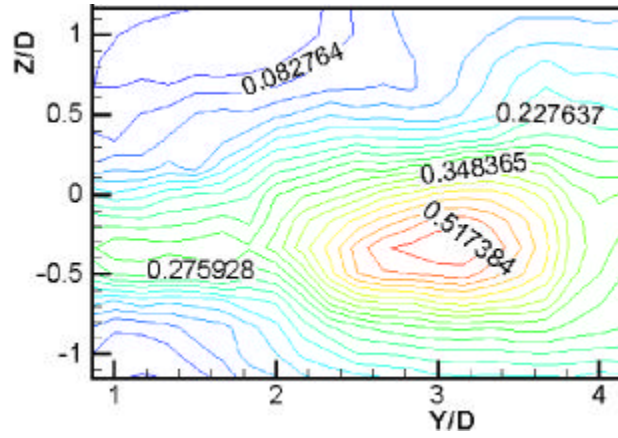


(b) $X = -1.333D$

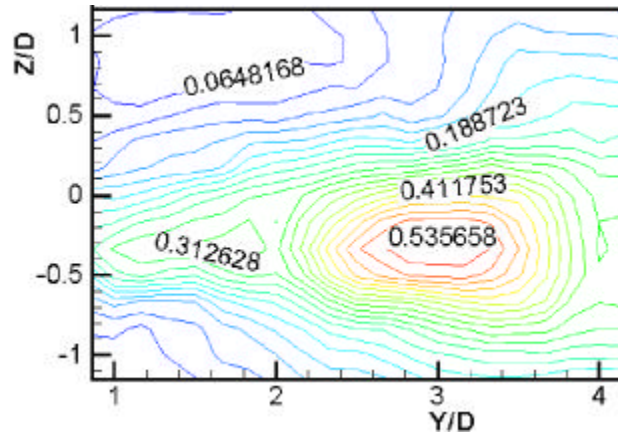


(c) $X = -1.000D$

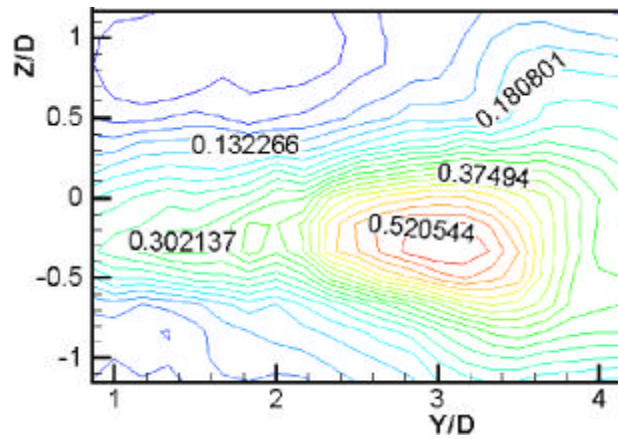
Fig. 5.15 Turbulence intensity distribution ($T_w = \sqrt{w'^2} / U_0$) (continued)



(d) $X = -0.667D$

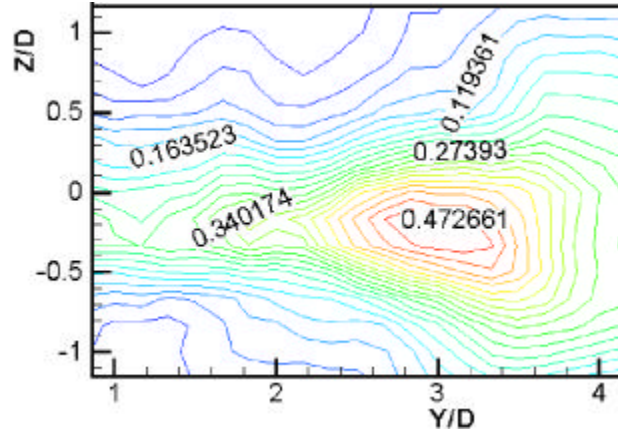


(e) $X = -0.333D$

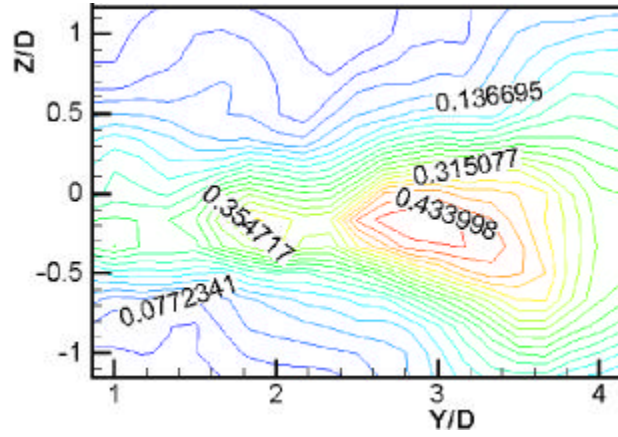


(f) $X = 0.000D$

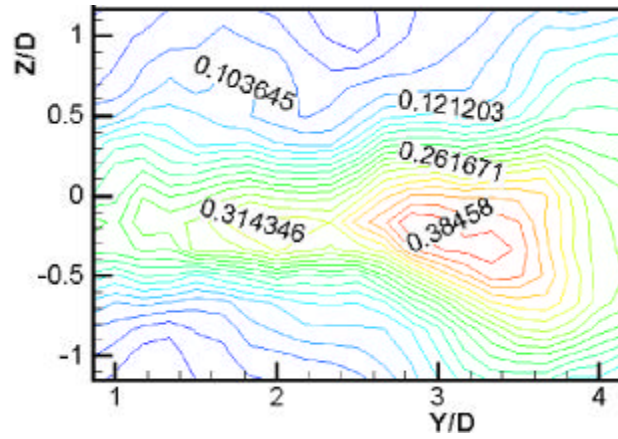
Fig. 5.15 Turbulence intensity distribution ($T_w = \sqrt{w'^2} / U_0$) (continued)



(g) $X = 0.333D$

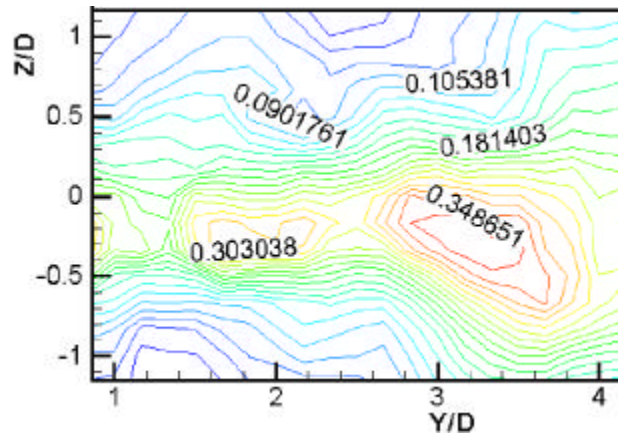


(h) $X = 0.667D$



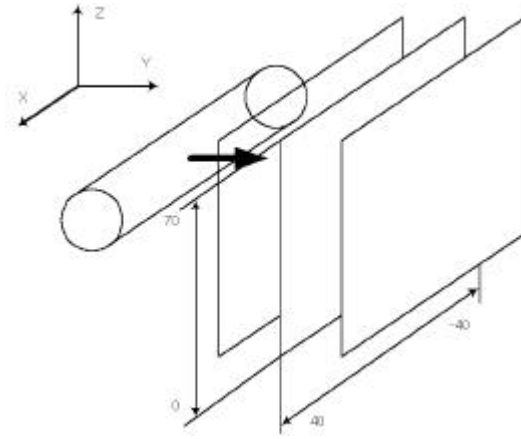
(i) $X = 1.000D$

Fig. 5.15 Turbulence intensity distribution ($T_w = \sqrt{w'^2} / U_0$) (continued)

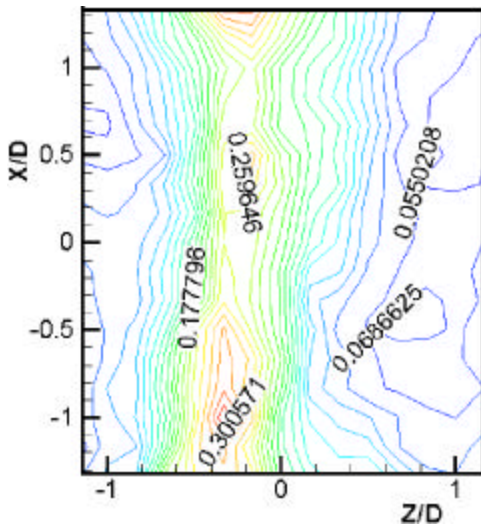


(j) $X = 1.333D$

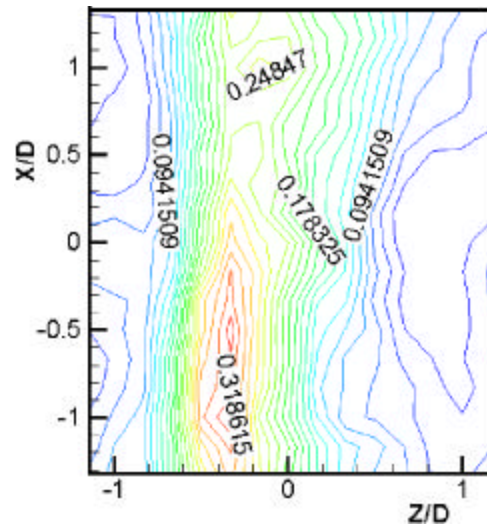
Fig. 5.15 Turbulence intensity distribution ($T_w = \sqrt{w'^2} / U_0$) (continued)



(a) Measuring region

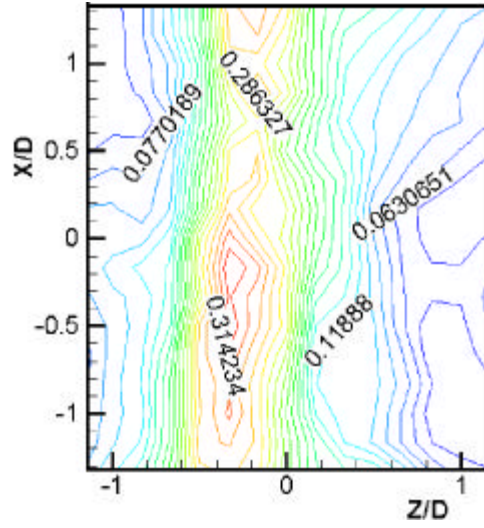


(b) $Y = 0.833D$

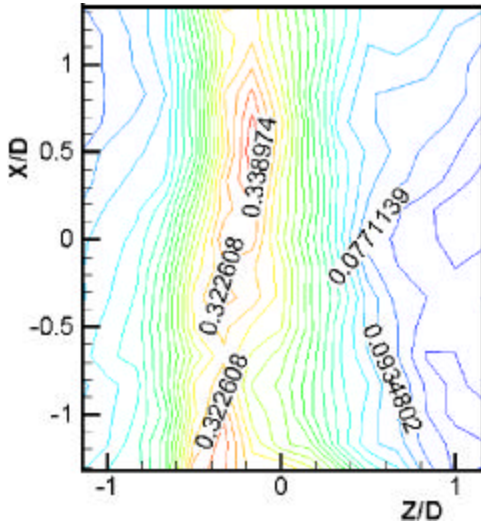


(c) $Y = 1.167D$

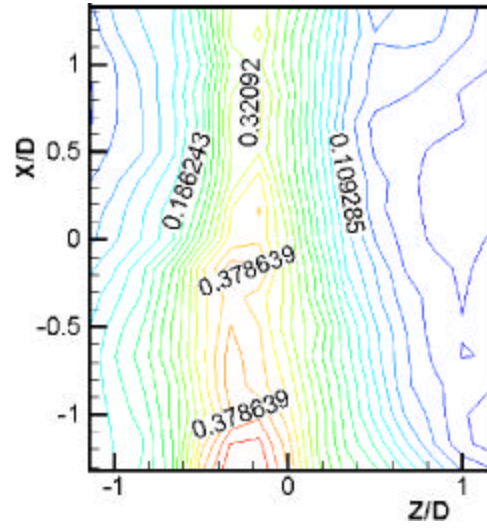
Fig. 5.16 Turbulence intensity distribution ($T_w = \sqrt{w'^2} / U_0$) (continued)



(d) $Y = 1.500D$

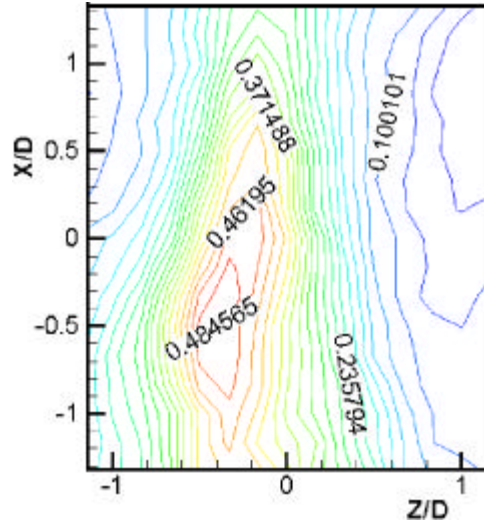


(e) $Y = 1.833D$

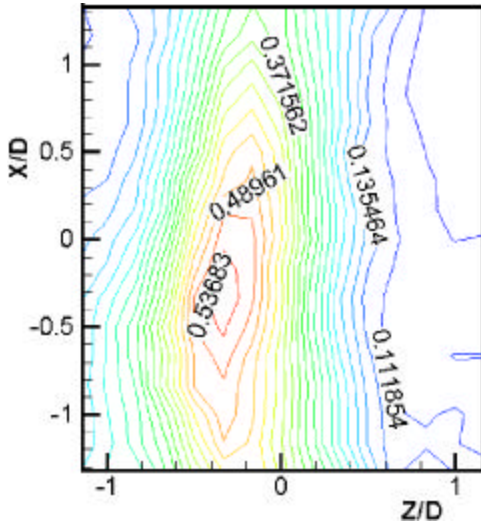


(f) $Y = 2.167D$

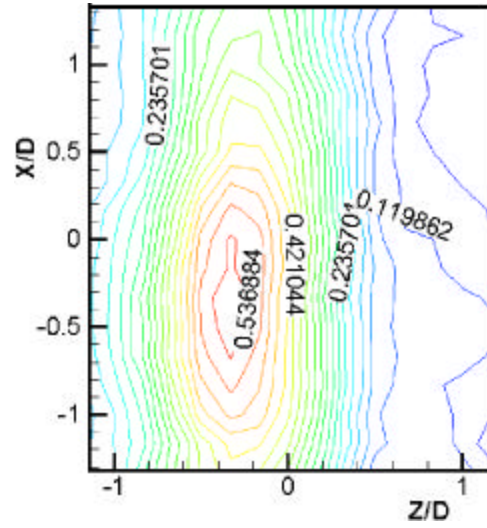
Fig. 5.16 Turbulence intensity distribution ($T_w = \sqrt{w'^2} / U_0$) (continued)



(g) $Y = 2.500D$

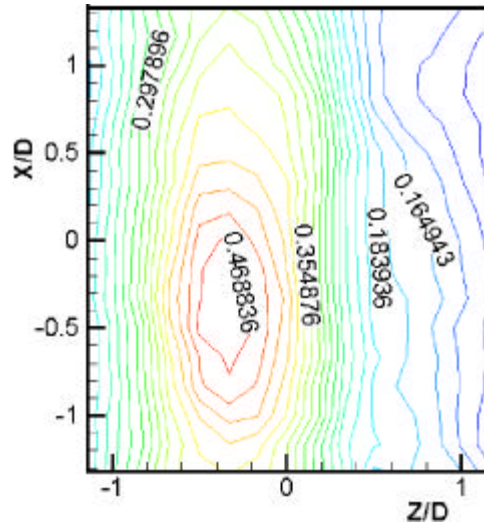


(h) $Y = 2.833D$

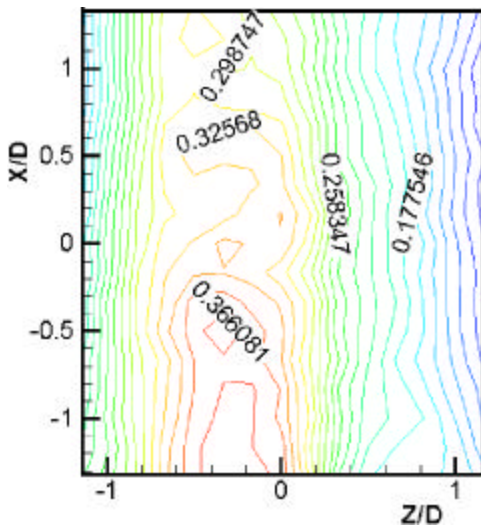


(i) $Y = 3.167D$

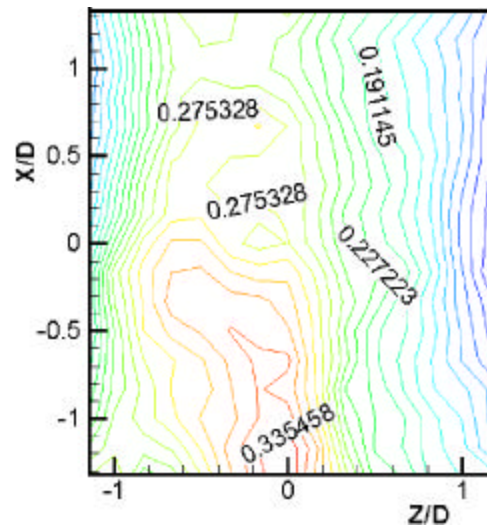
Fig. 5.16 Turbulence intensity distribution ($T_w = \sqrt{w'^2} / U_0$) (continued)



(j) $Y = 3.500D$



(k) $Y = 3.833D$



(l) $Y = 4.167D$

Fig. 5.16 Turbulence intensity distribution ($T_w = \sqrt{w'^2} / U_0$) (continued)

5.3

Fig. 5.17 (a)

. $Y=2.500D$
 D $2.500D$ $X=0.000D, Z=0.000D$

Fig. 5.17 (b) (i) X-Y plane Z $0.333D$ 가

Fig. 5.18 Y-Z

, $X=-0.333D, Y=2.500D, Z=-0.500D$

. 3 가
 . 가 가

island

. Fig. 5.18 (b) (j) Y-Z plane

, $X=-1.333D, Y=2.000D, Z=-0.333D$ & $Z=0.000D$

가 ,
 2 .

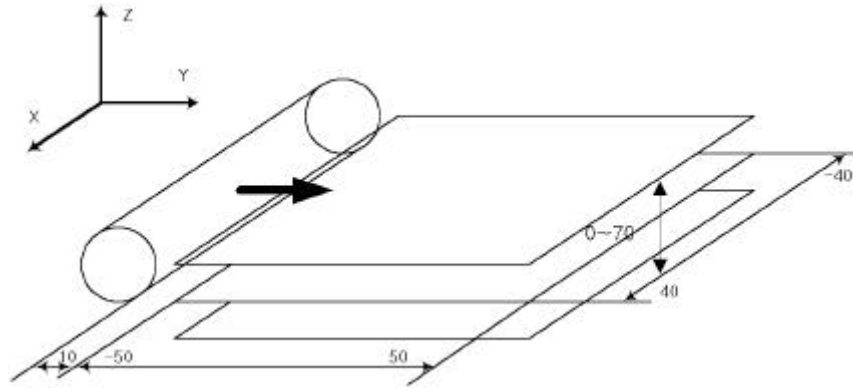
3

2

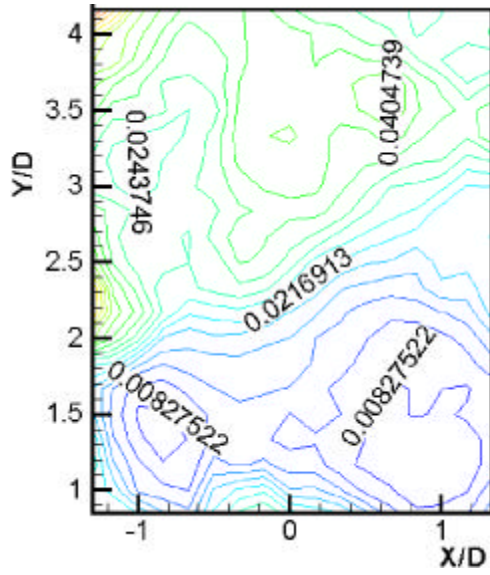
. ,

Fig. 5.19 X-Z plane

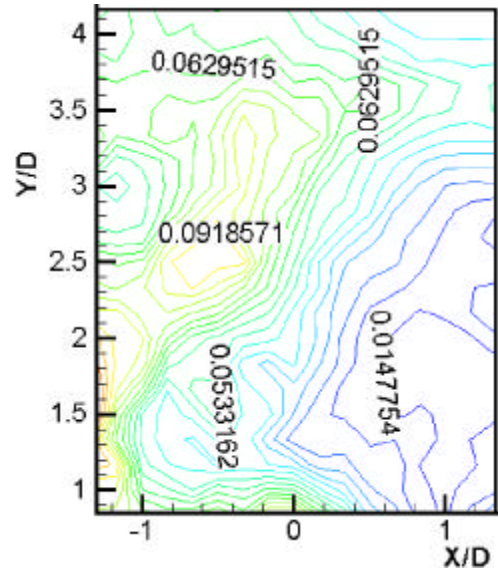
Y $0.333D$ 가



(a) Measuring region



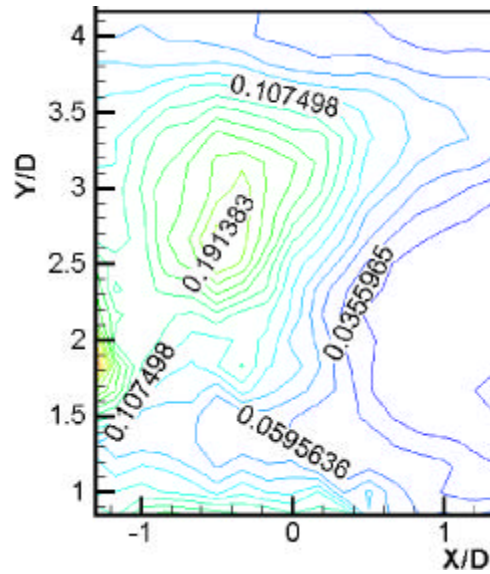
(b) $Z = -1.167D$



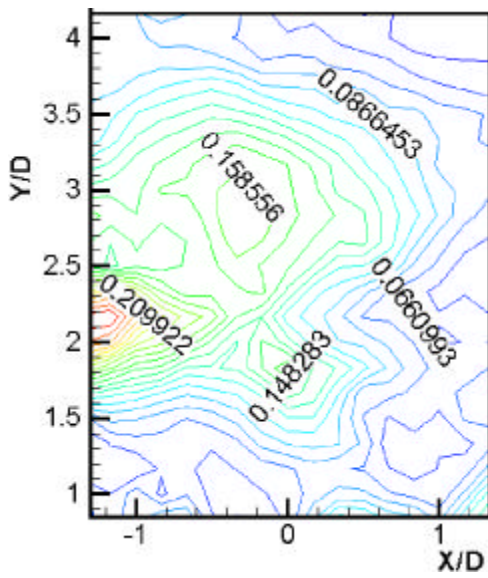
(c) $Z = -0.833D$

Fig. 5.17 Turbulence kinetic energy distribution ($TKE = \frac{1}{2} q^2 / U_0^2$)

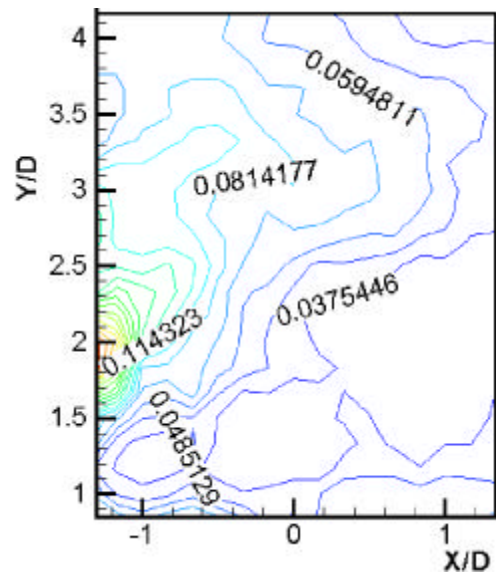
(continued)



(d) $Z = -0.500D$



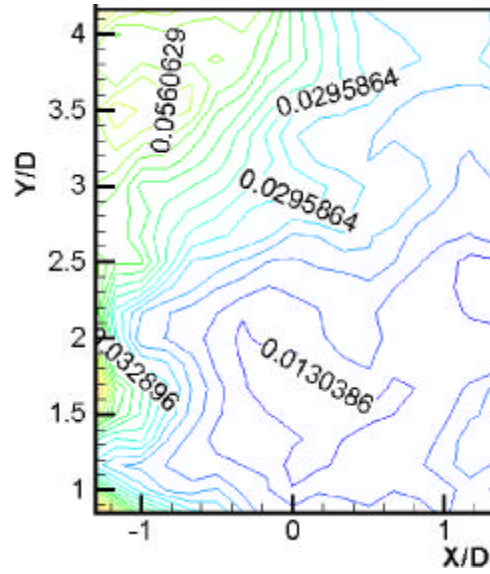
(e) $Z = -0.167D$



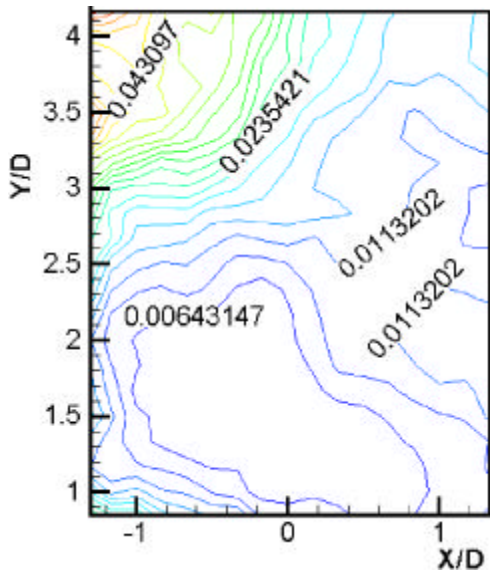
(f) $Z = 0.167D$

Fig. 5.17 Turbulence kinetic energy distribution ($TKE = \frac{1}{2} q^2 / U_0^2$)

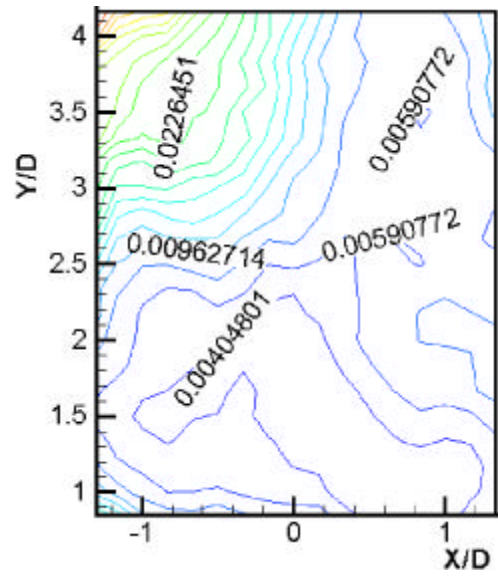
(continued)



(g) $Z = 0.500D$



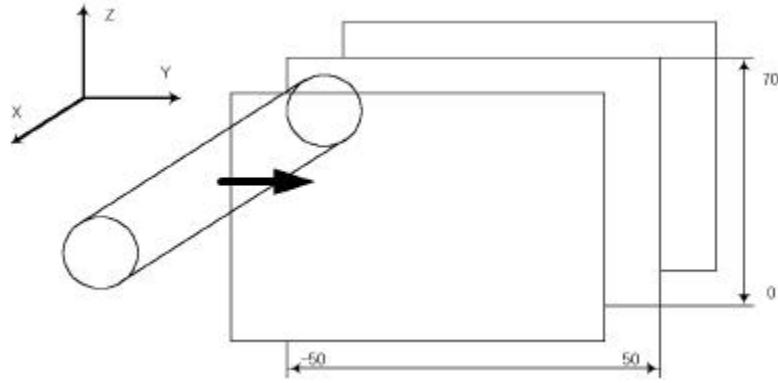
(h) $Z = 0.833D$



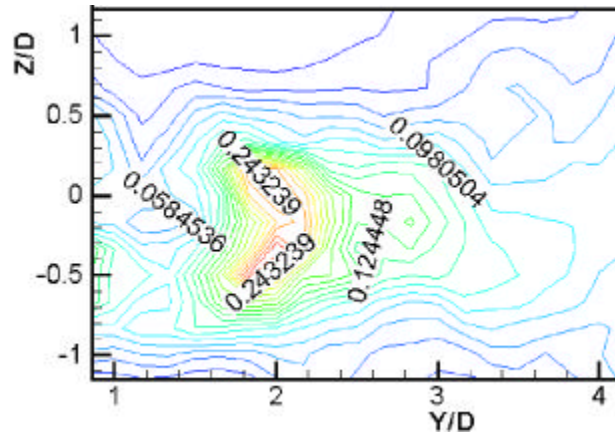
(i) $Z = 1.167D$

Fig. 5.17 Turbulence kinetic energy distribution ($TKE = \frac{1}{2} q^2 / U_0^2$)

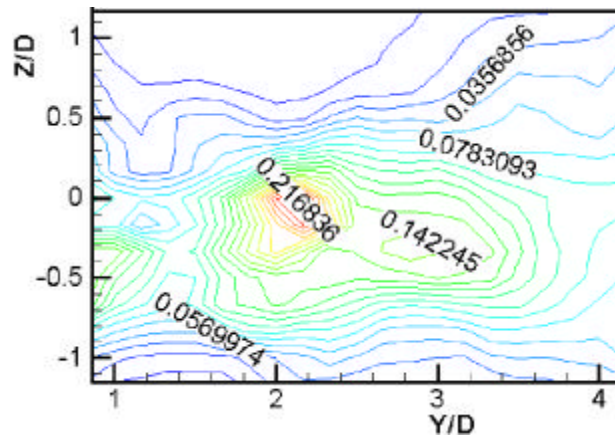
(continued)



(a) Measuring region



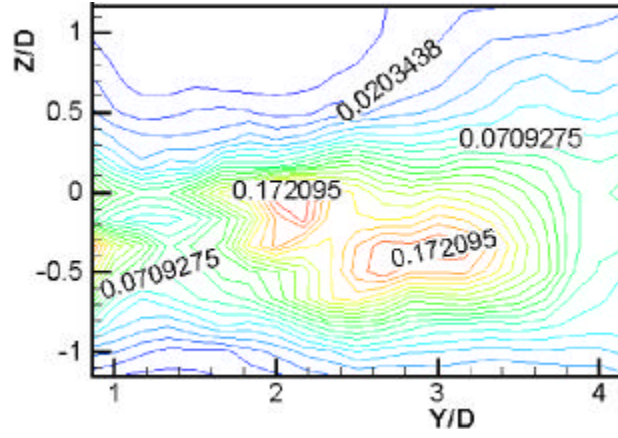
(b) $X = -1.333D$



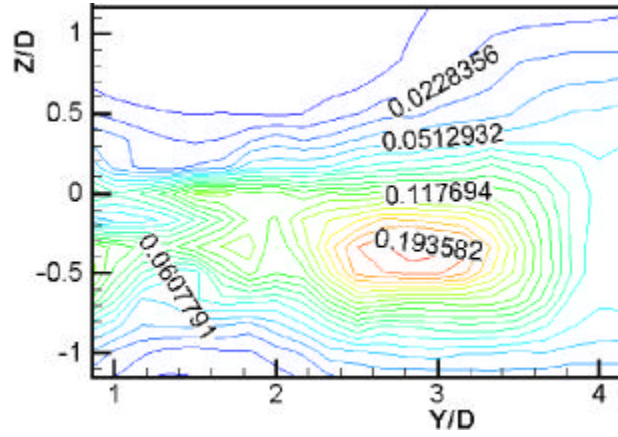
(c) $X = -1.000D$

Fig. 5.18 Turbulence kinetic energy distribution ($TKE = \frac{1}{2} \overline{q^2} / U_0^2$)

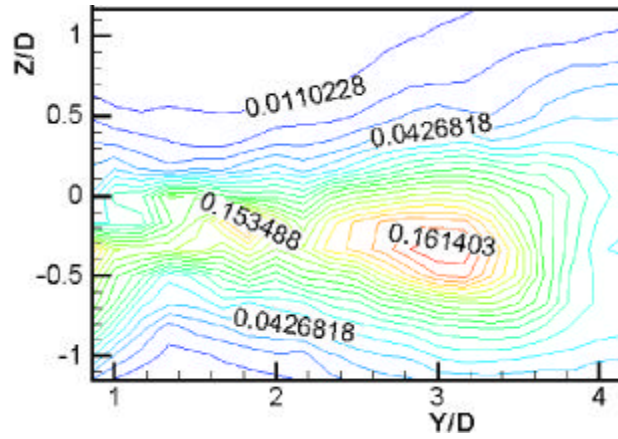
(continued)



(d) $X = -0.667D$

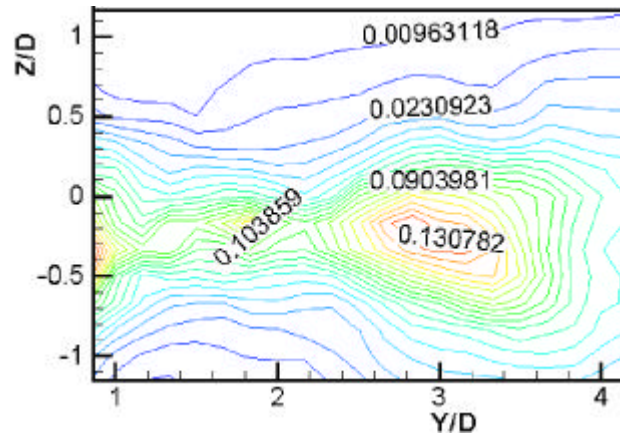


(e) $X = -0.333D$

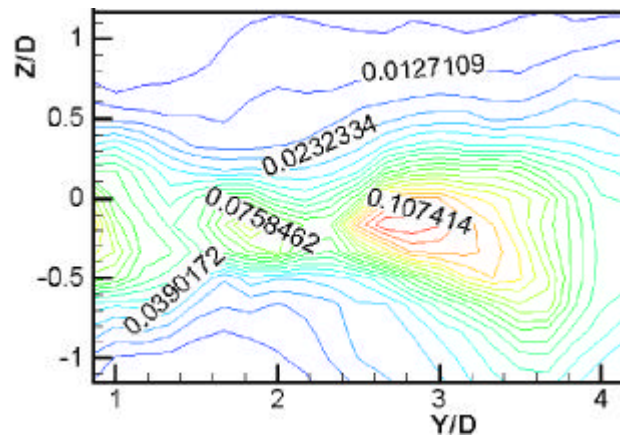


(f) $X = 0.000D$

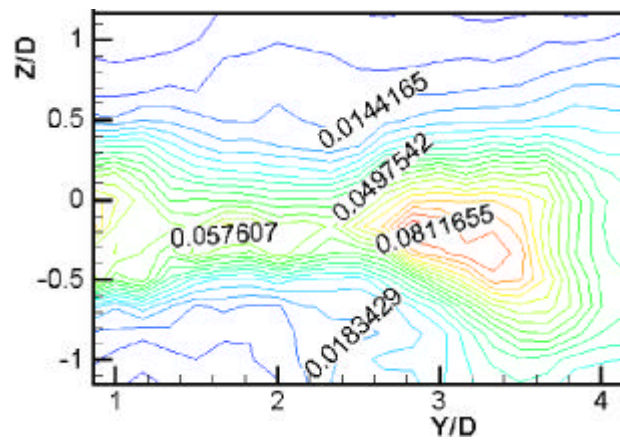
Fig. 5.18 Turbulence kinetic energy distribution ($TKE = \frac{1}{2} q^2 / U_0^2$)



(g) $X = 0.333D$

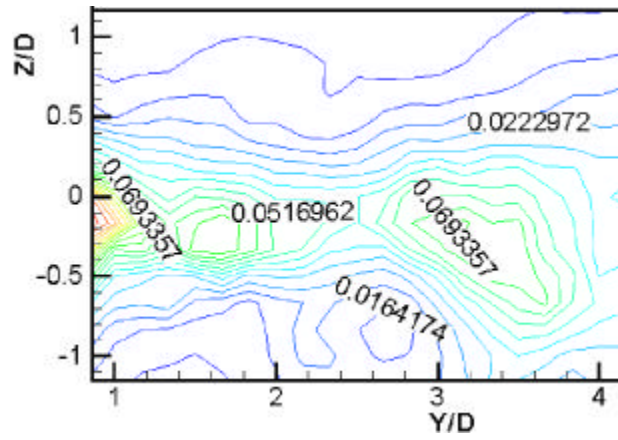


(h) $X = 0.667D$



(i) $X = 1.000D$

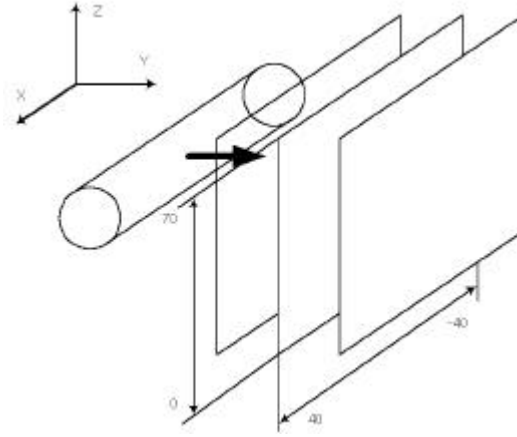
Fig. 5.18 Turbulence kinetic energy distribution ($TKE = \frac{1}{2} q^2 / U_0^2$)



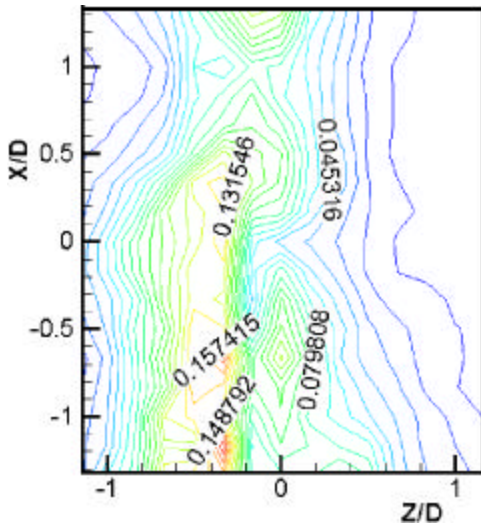
(j) $X = 1.333D$

Fig. 5.18 Turbulence kinetic energy distribution ($TKE = \frac{1}{2} q^2 / U_0^2$)

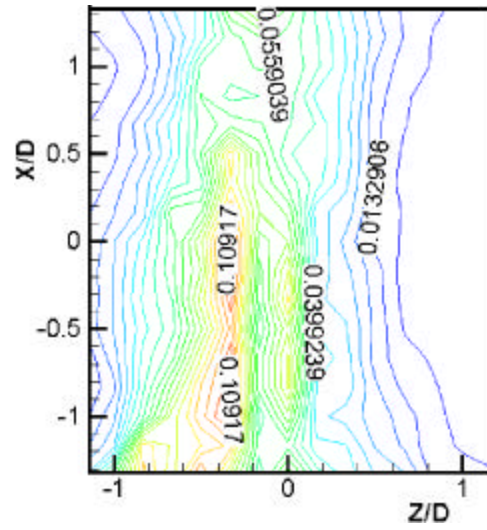
(continued)



(a) Measuring region



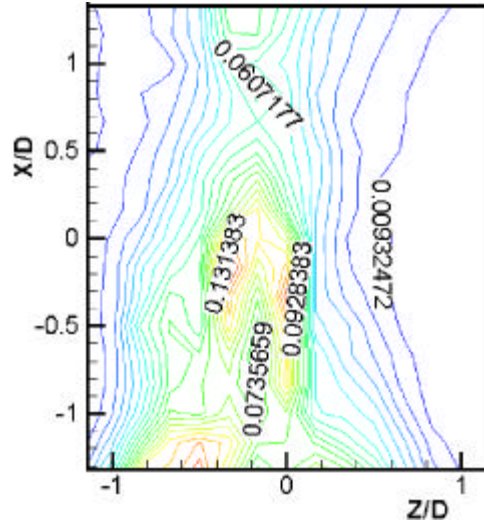
(b) $Y = 0.833D$



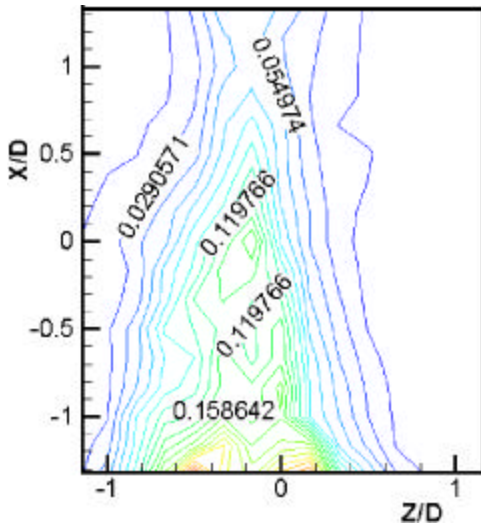
(c) $Y = 1.167D$

Fig. 5.19 Turbulence kinetic energy distribution ($TKE = \frac{1}{2} q^2 / U_0^2$)

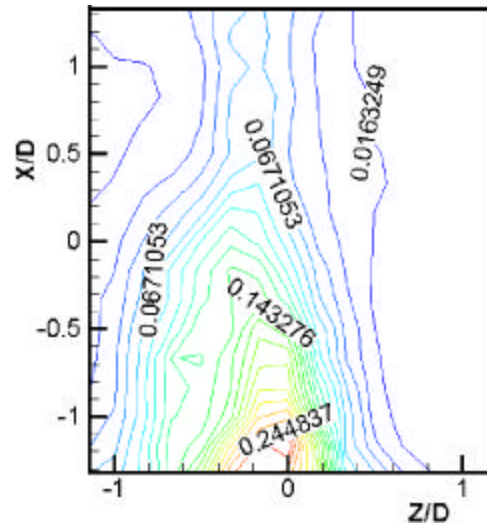
(continued)



(d) $Y = 1.500D$



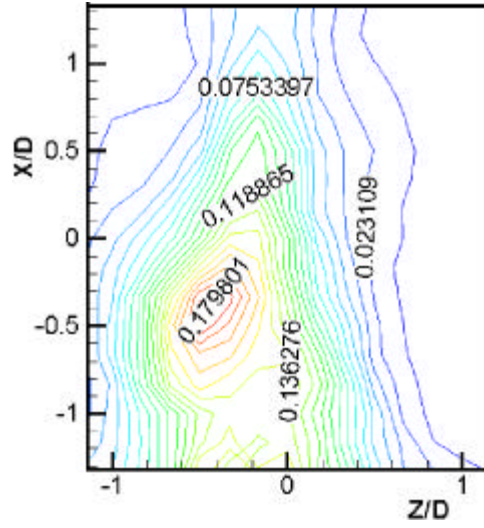
(e) $Y = 1.833D$



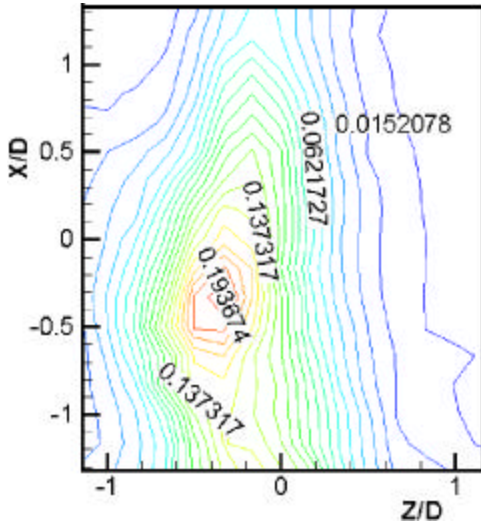
(f) $Y = 2.167D$

Fig. 5.19 Turbulence kinetic energy distribution ($TKE = \frac{1}{2} q^2 / U_0^2$)

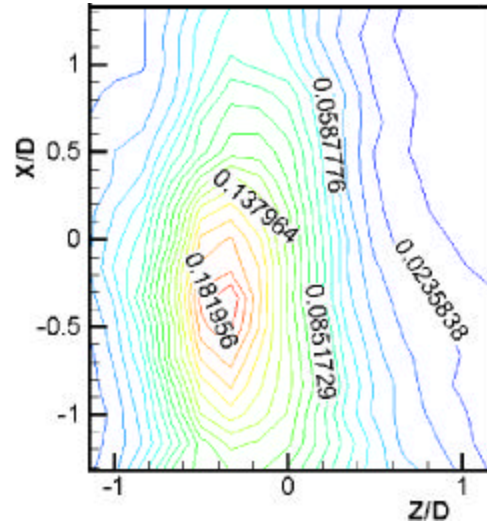
(continued)



(g) $Y = 2.500D$



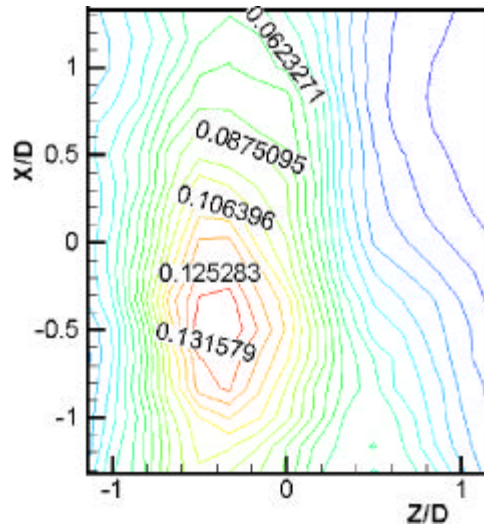
(h) $Y = 2.833D$



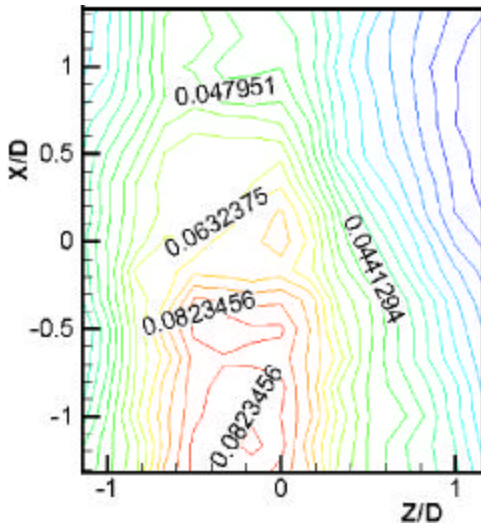
(i) $Y = 3.167D$

Fig. 5.19 Turbulence kinetic energy distribution ($TKE = \frac{1}{2} q^2 / U_0^2$)

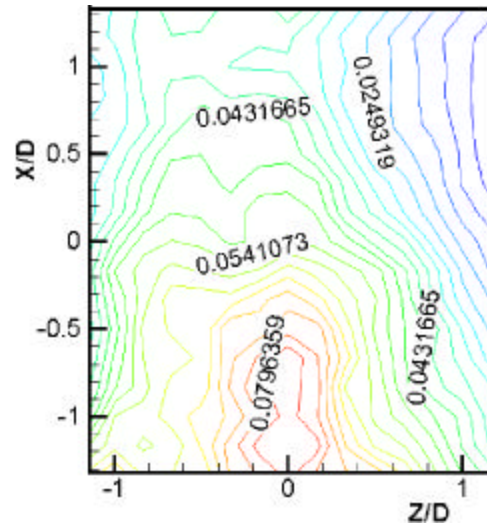
(continued)



(j) $Y = 3.500D$



(k) $Y = 3.833D$



(l) $Y = 4.167D$

Fig. 5.19 Turbulence kinetic energy distribution ($TKE = \frac{1}{2} q^2 / U_0^2$)

(continued)

5.4

Fig. 5.20 (a)

(u'v') . Y=2.500D
D 2.500D X=0.000D, Z=0.000D

Fig. 5.20 (b) (i) X-Y plane

Z 0.333D 가
(u'v') . X=-0.667D,
Y=2.000D, Z=-0.167D

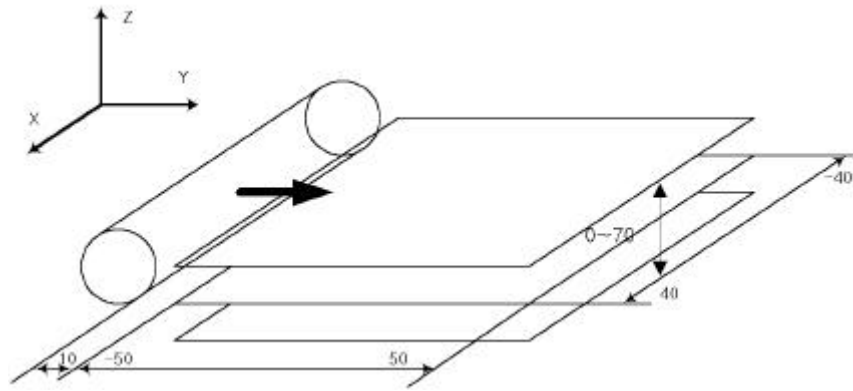
sweeping(
) ejection() ,
vortex filament

Fig. 5.21

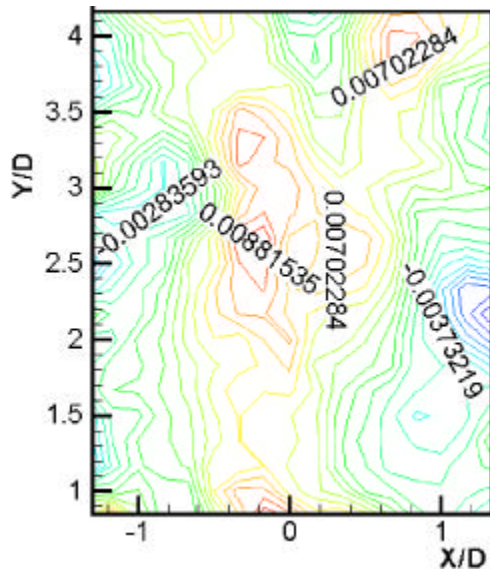
Y-Z (u'v')
3

Fig. 5.22 X-Z plane

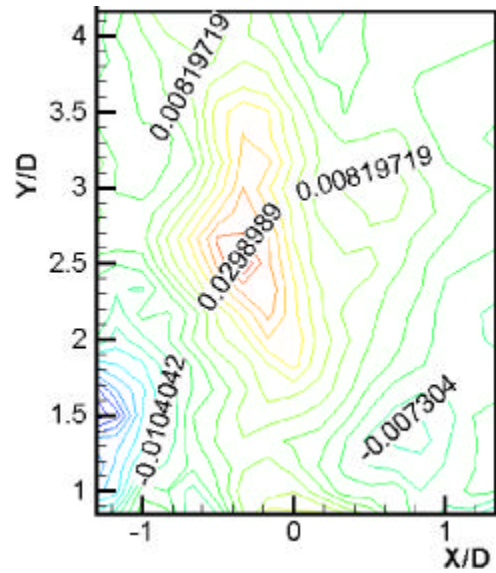
Y 0.333D 가
(u'v') .
vortex가 3 가 vortex filament ,



(a) Measuring region

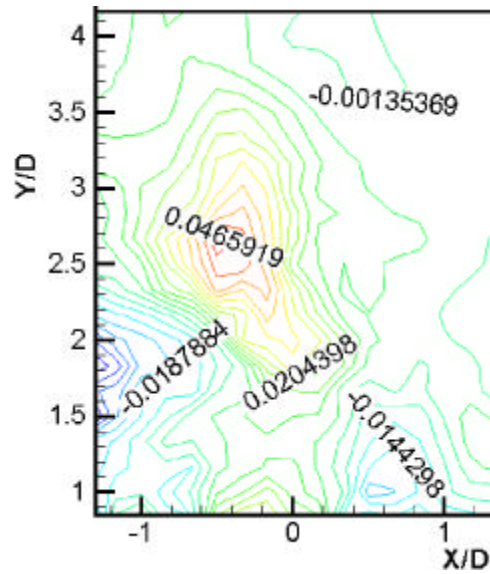


(b) $Z = -1.167D$

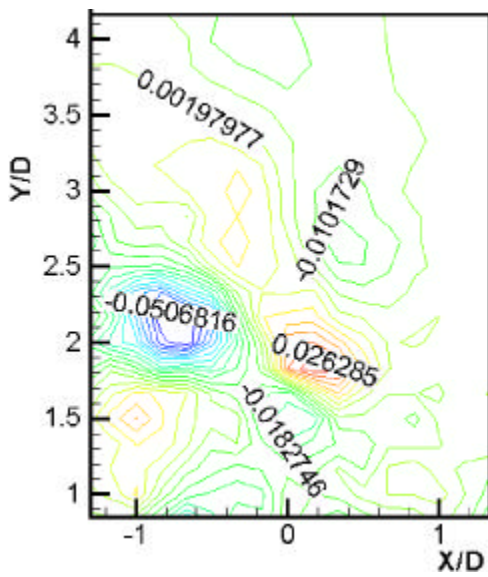


(c) $Z = -0.833D$

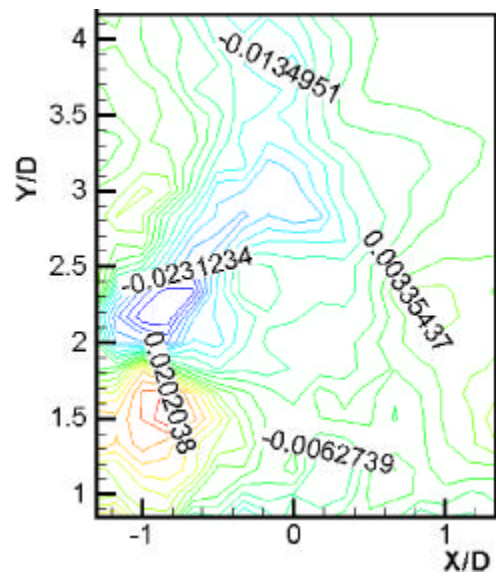
Fig. 5.20 Reynolds shear stress distribution $(-\overline{u'v'} / U_0^2)$ (continued)



(d) $Z = -0.500D$

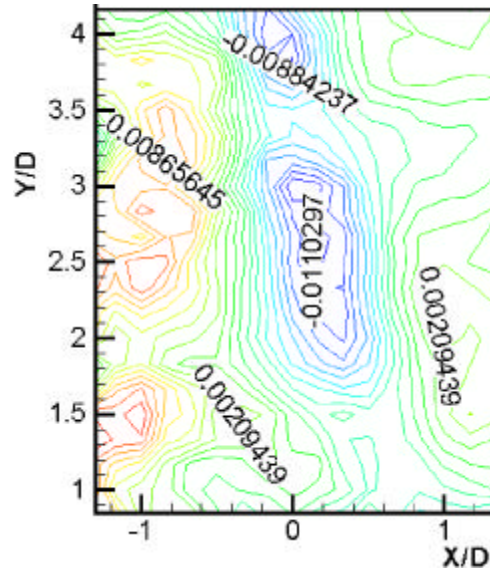


(e) $Z = -0.167D$

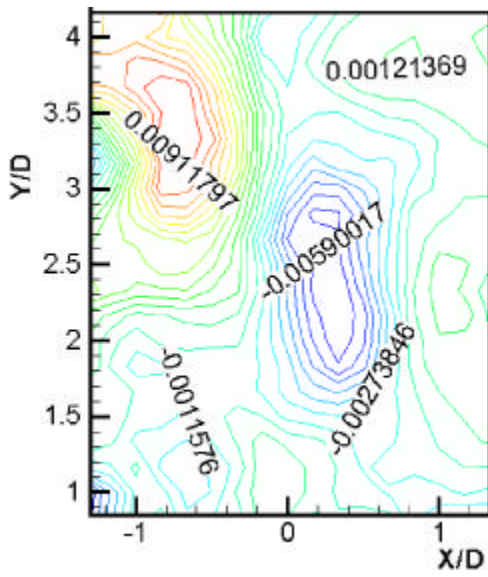


(f) $Z = 0.167D$

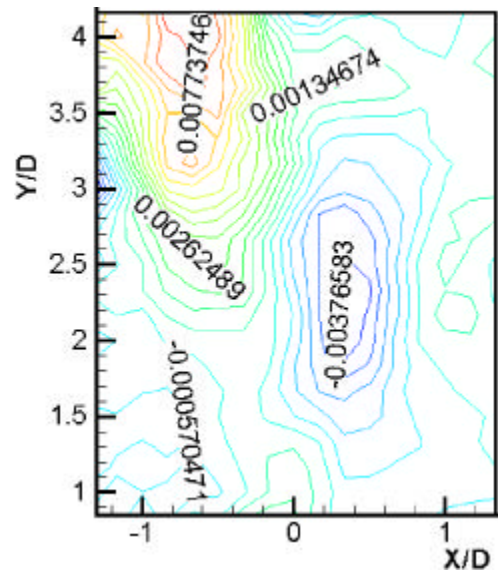
Fig. 5.20 Reynolds shear stress distribution $(-\overline{u'v'} / U_0^2)$ (continued)



(g) $Z = 0.500D$

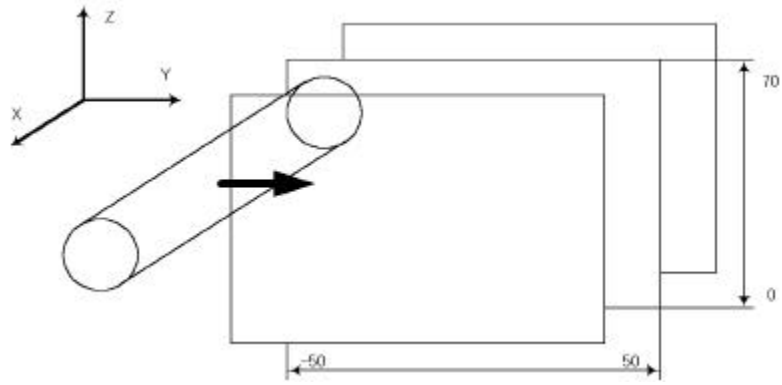


(h) $Z = 0.833D$

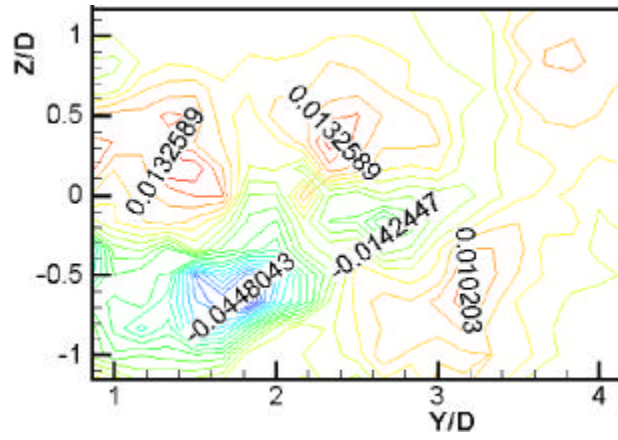


(i) $Z = 1.167D$

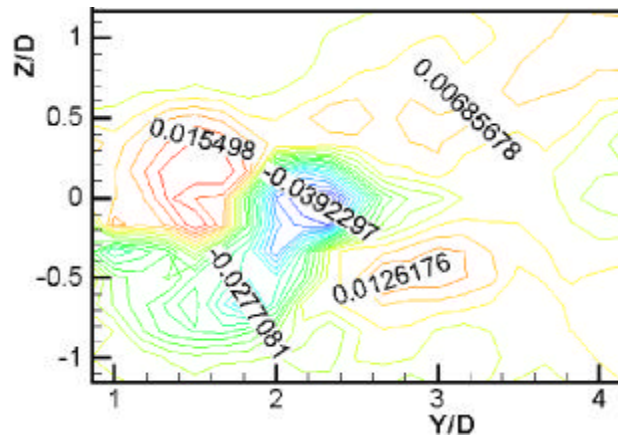
Fig. 5.20 Reynolds shear stress distribution $(-\overline{u'v'} / U_0^2)$ (continued)



(a) Measuring region

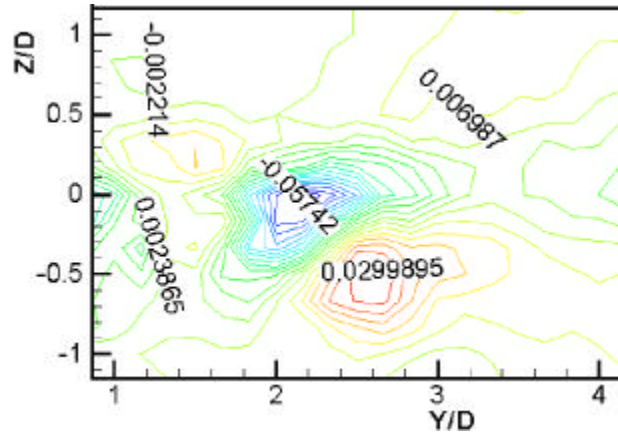


(b) $X = -1.333D$

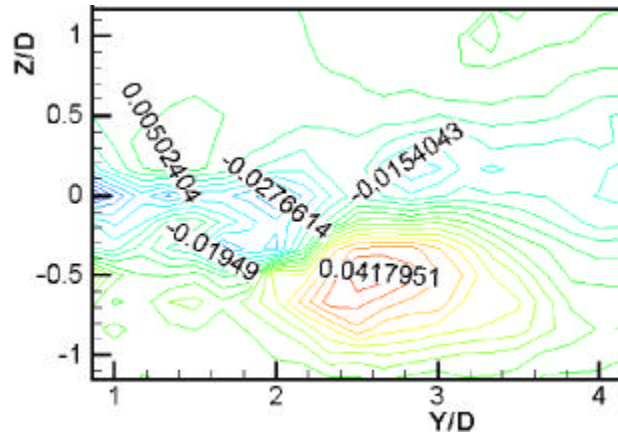


(c) $X = -1.000D$

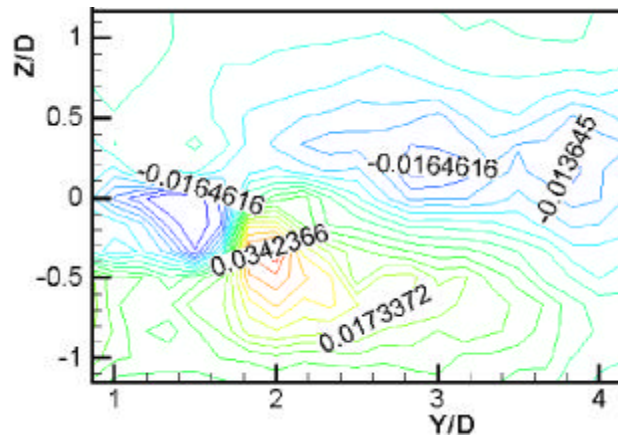
Fig. 5.21 Reynolds shear stress distribution $(- \overline{u'v'} / U_0^2)$ (continued)



(d) $X = -0.667D$

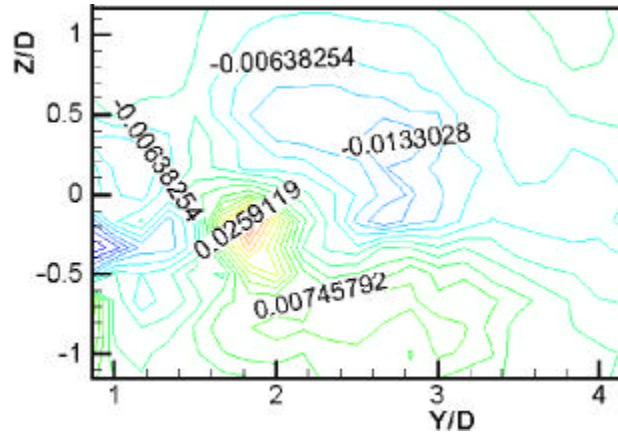


(e) $X = -0.333D$

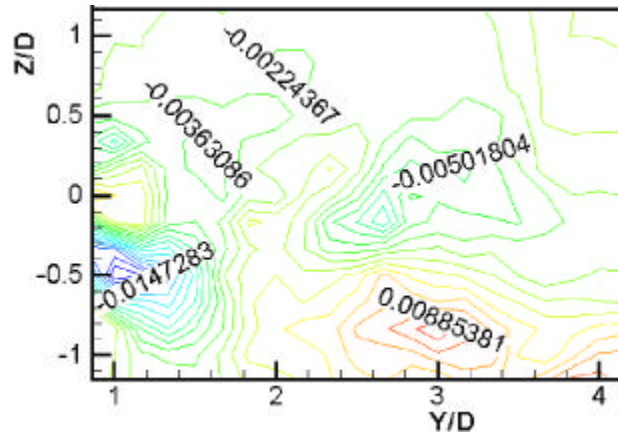


(f) $X = 0.000D$

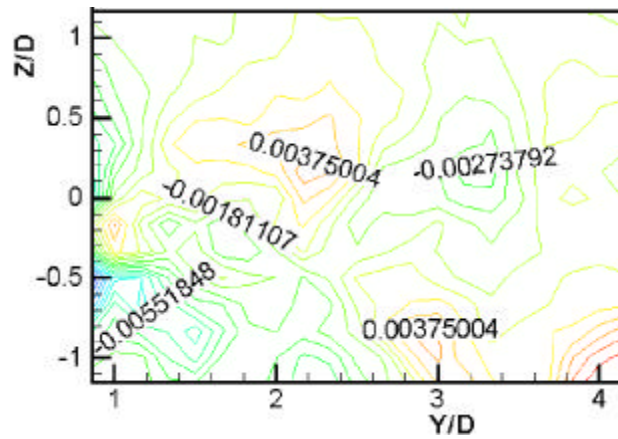
Fig. 5.21 Reynolds shear stress distribution ($-\overline{u'v'} / U_0^2$) (continued)



(g) $X = 0.333D$

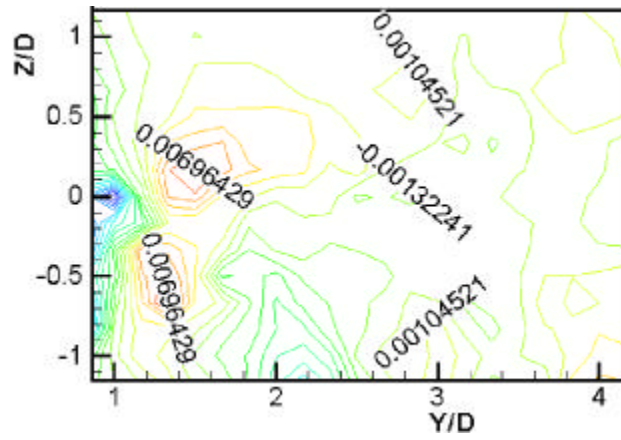


(h) $X = 0.667D$



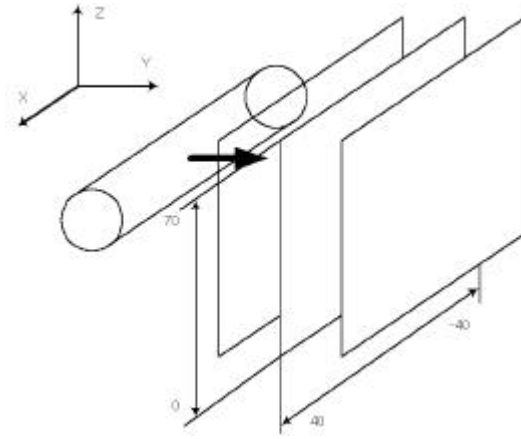
(i) $X = 1.000D$

Fig. 5.21 Reynolds shear stress distribution ($- \overline{u'v'} / U_0^2$) (continued)

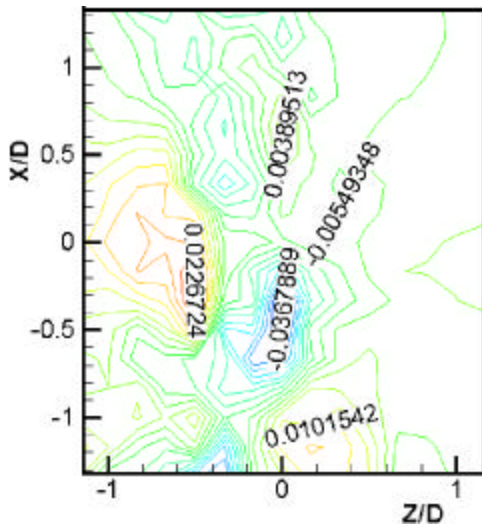


(j) $X = 1.333D$

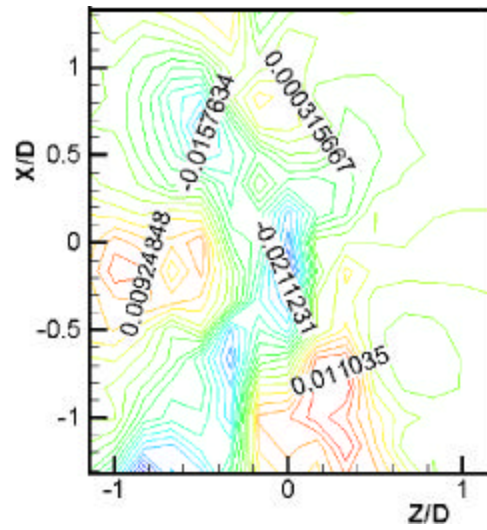
Fig. 5.21 Reynolds shear stress distribution $(-\overline{u'v'} / U_0^2)$ (continued)



(a) Measuring region

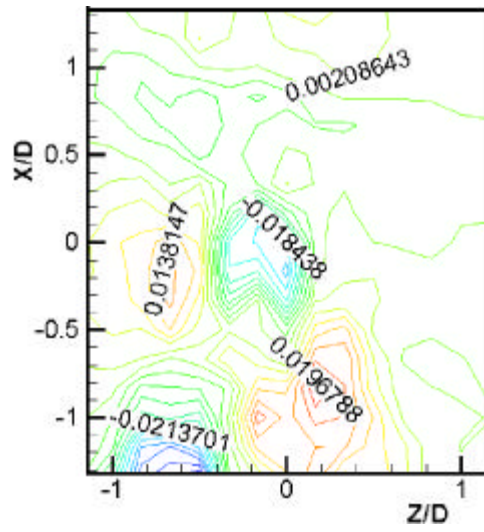


(b) $Y = 0.833D$

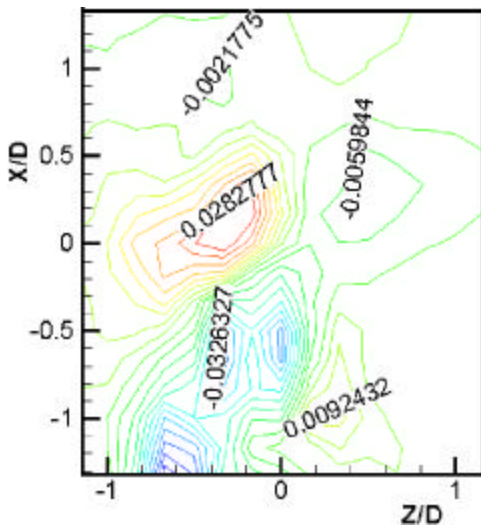


(c) $Y = 1.167D$

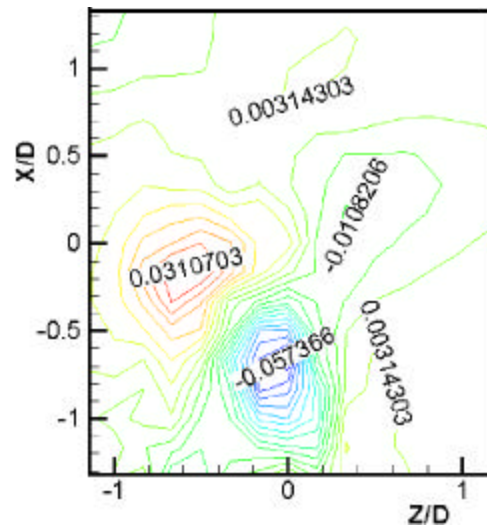
Fig. 5.22 Reynolds shear stress distribution $(-\overline{u'v'} / U_0^2)$ (continued)



(d) $Y = 1.500D$

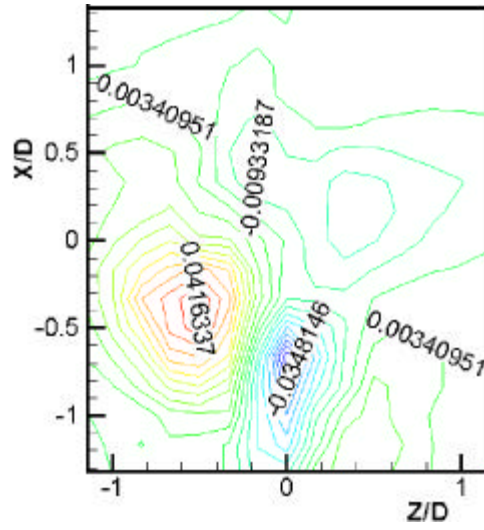


(e) $Y = 1.833D$

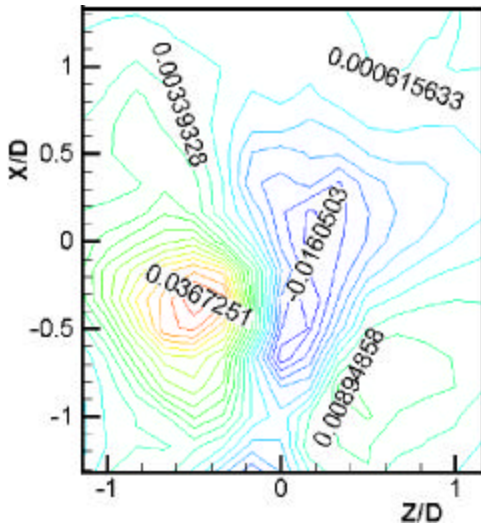


(f) $Y = 2.167D$

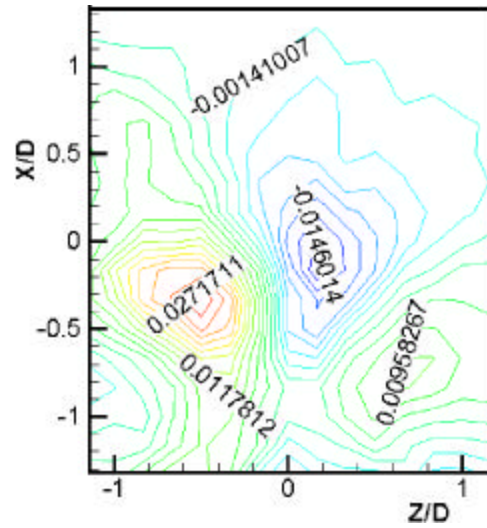
Fig. 5.22 Reynolds shear stress distribution ($-\overline{u'v'}/U_0^2$) (continued)



(g) $Y = 2.500D$

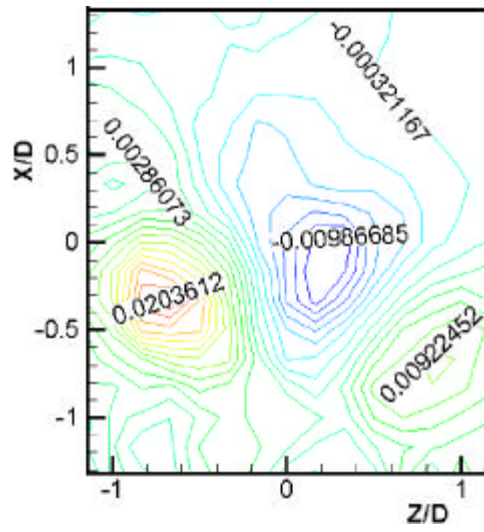


(h) $Y = 2.833D$

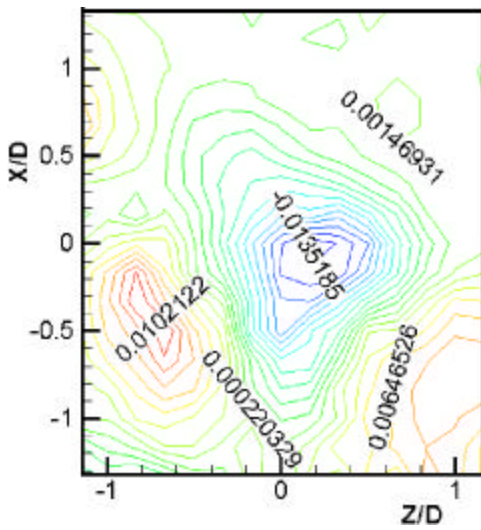


(i) $Y = 3.167D$

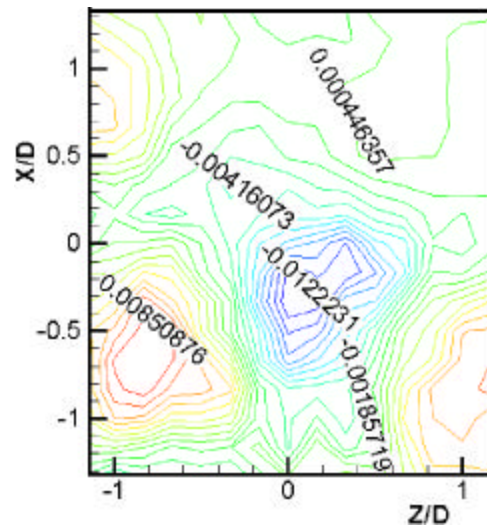
Fig. 5.22 Reynolds shear stress distribution $(-\overline{u'v'} / U_0^2)$ (continued)



(j) $Y = 3.500D$



(k) $Y = 3.833D$



(l) $Y = 4.167D$

Fig. 5.22 Reynolds shear stress distribution ($-\overline{u'v'}/U_0^2$)

Fig. 5.23 (a)

(v'w')

Fig. 5.23 (b) (i) X- Y plane

Z 0.333D 가

(v'w') . X=- 0.500D,

Y=2.500D, Z=- 0.500D

. Z=0.167D

secondary vortex가

3

Fig. 5.24

Y-Z

(v'w')

. X=0.000D 가

,

가

가 Z=0.000D

. , X

X=0.000D

가

spanwise

Fig. 3.25 X-Z plane

Y

0.333D 가

(v'w')

. X=- 0.500 & X=0.500D,

Y=2.833D, Z=- 0.500D & Z=0.167D

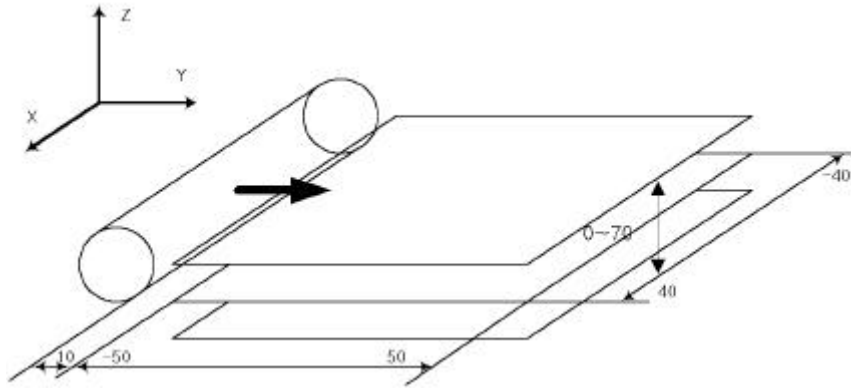
secondary vortex가

D

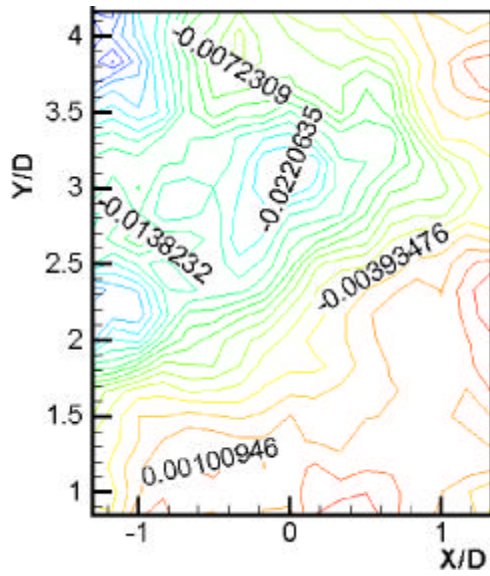
30

.

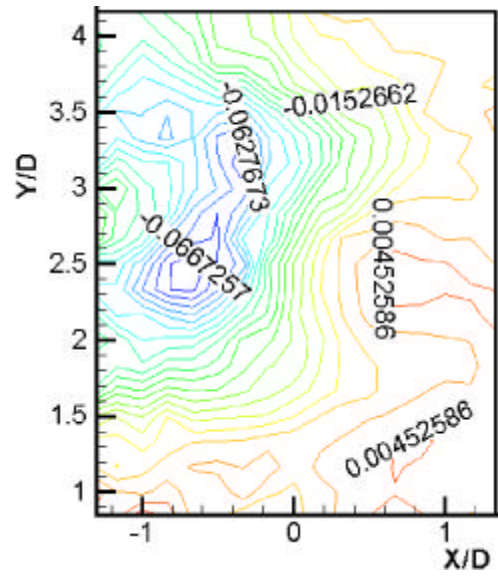
Brede



(a) Measuring region

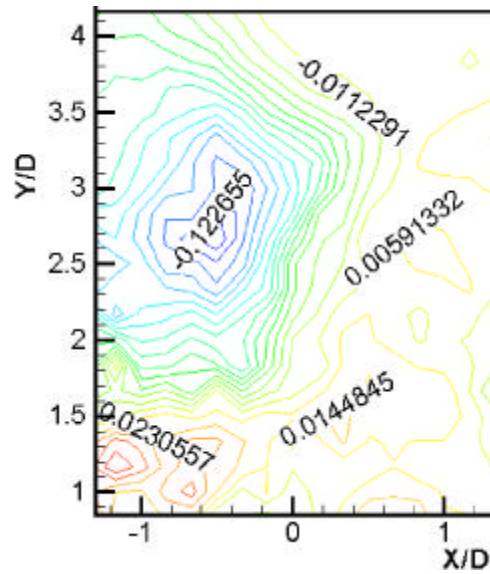


(b) $Z = -1.167D$

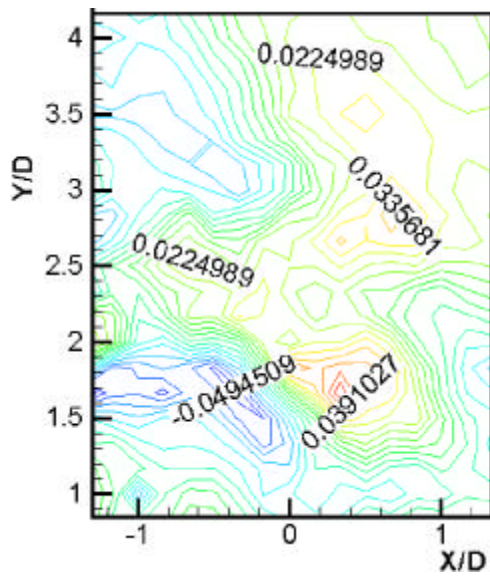


(c) $Z = -0.833D$

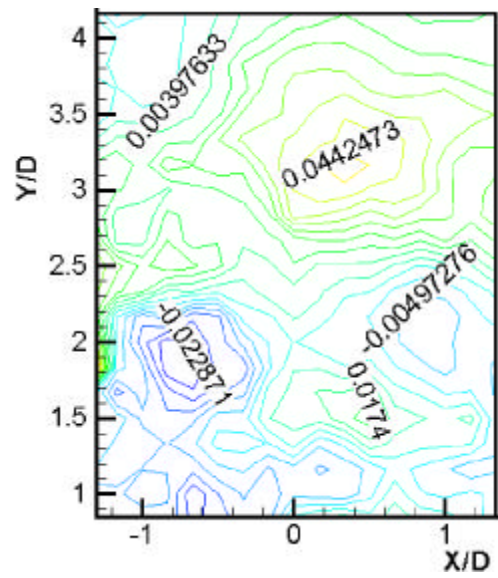
Fig. 5.23 Reynolds shear stress distribution $(-\overline{v'w'} / U_0^2)$ (continued)



(d) $Z = -0.500D$

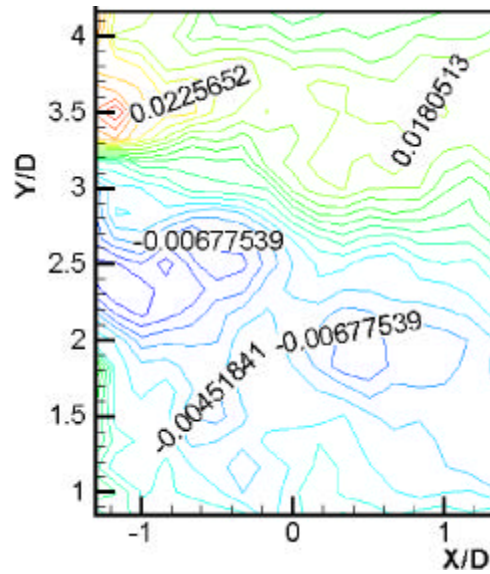


(e) $Z = -0.167D$

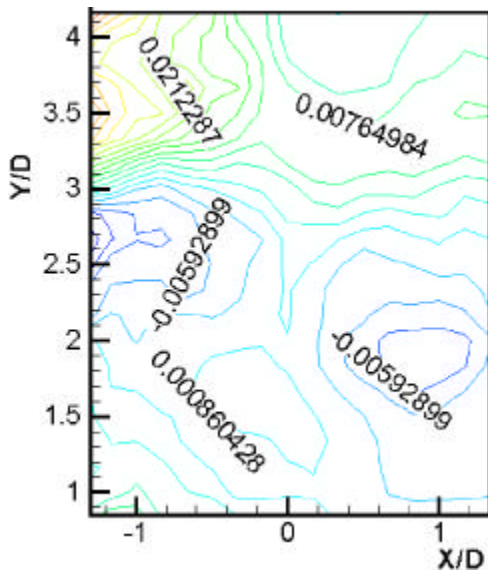


(f) $Z = 0.167D$

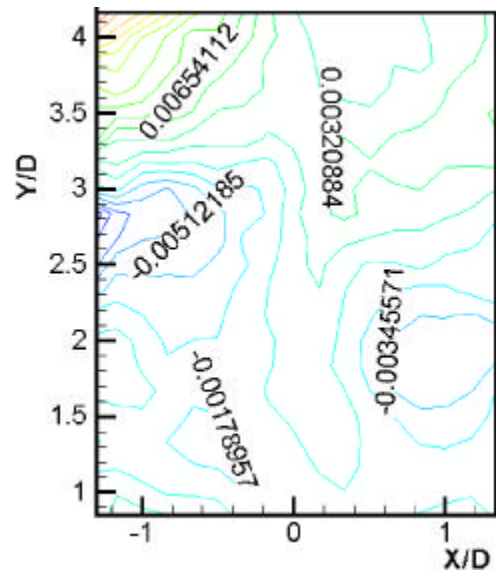
Fig. 5.23 Reynolds shear stress distribution $(-\overline{v'w'} / U_0^2)$ (continued)



(g) $z = 0.500D$

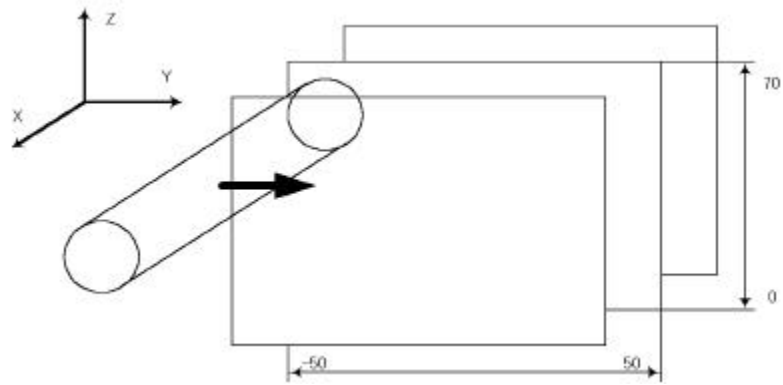


(h) $Z = 0.833D$

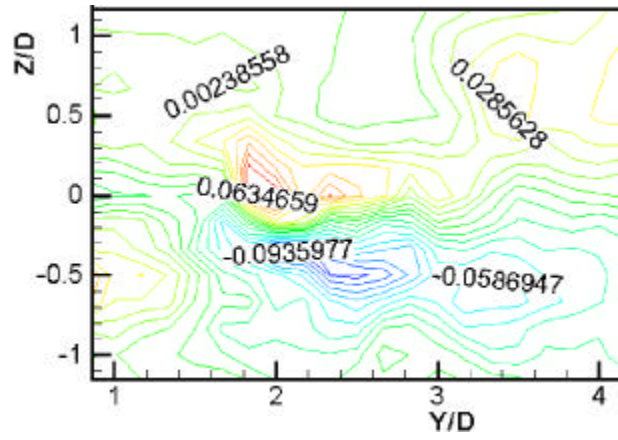


(i) $Z = 1.167D$

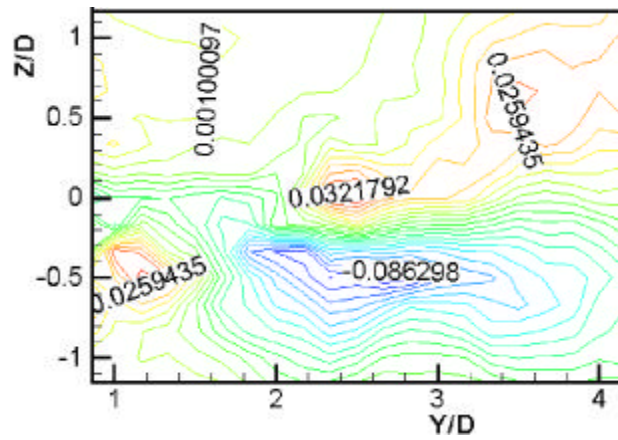
Fig. 5.23 Reynolds shear stress distribution $(-\overline{v'w'} / U_0^2)$ (continued)



(a) Measuring region

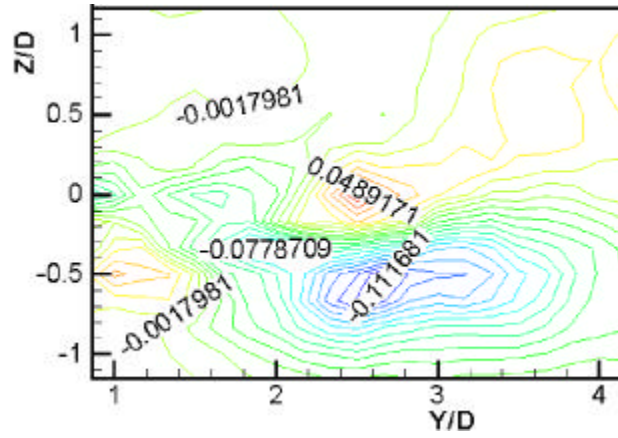


(b) $X = -1.333D$

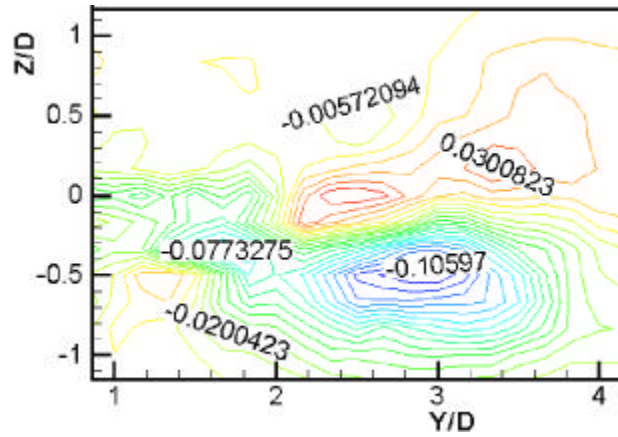


(c) $X = -1.000D$

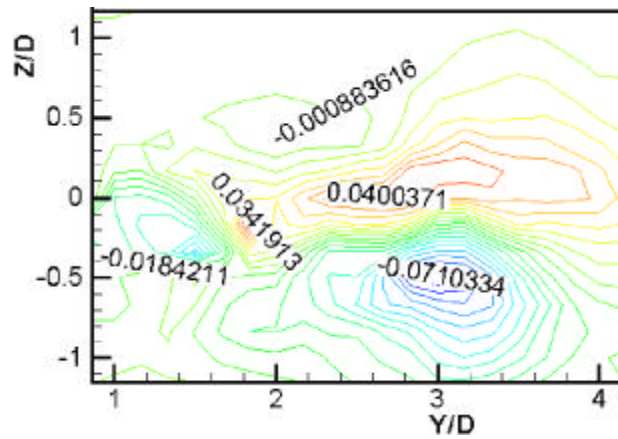
Fig. 5.24 Reynolds shear stress distribution ($- \overline{v'w'} / U_0^2$) (continued)



(d) $X = -0.667D$

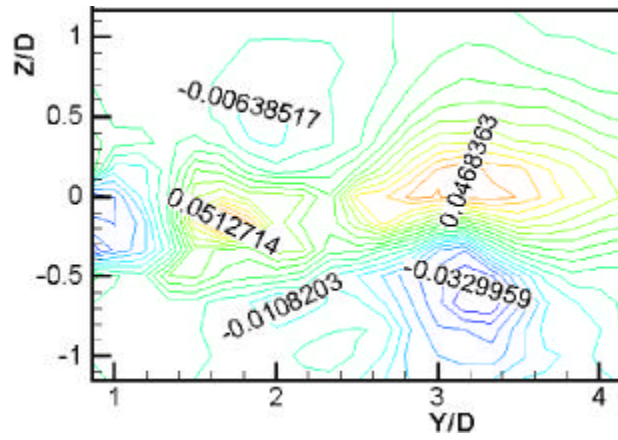


(e) $X = -0.333D$

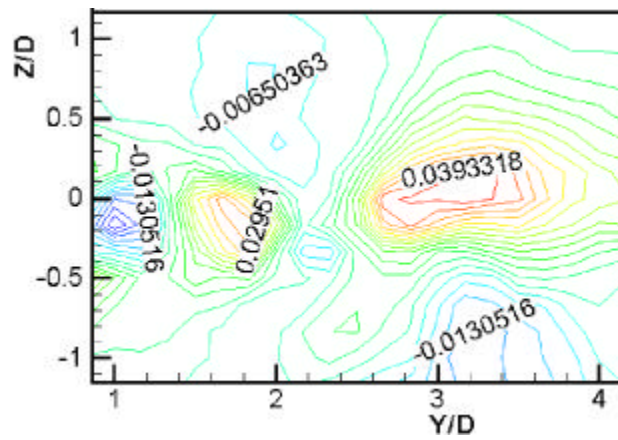


(f) $X = 0.000D$

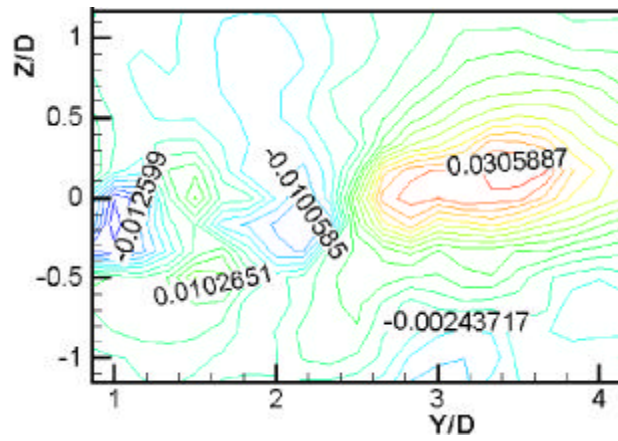
Fig. 5.24 Reynolds shear stress distribution $(-\overline{v'w'} / U_0^2)$ (continued)



(g) $X = 0.333D$

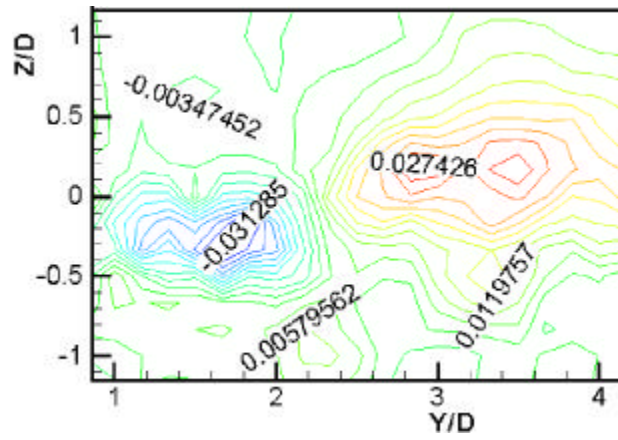


(h) $X = 0.667D$



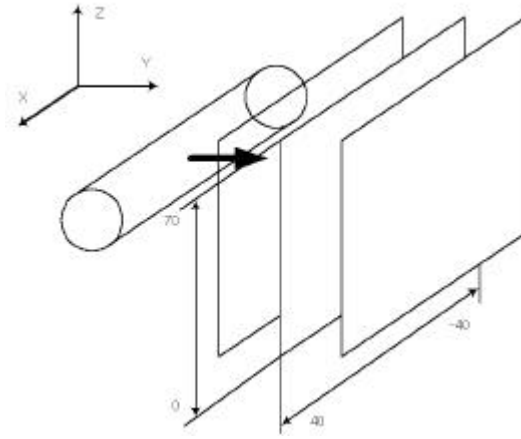
(i) $X = 1.000D$

Fig. 5.24 Reynolds shear stress distribution $(-\overline{v'w'} / U_0^2)$ (continued)

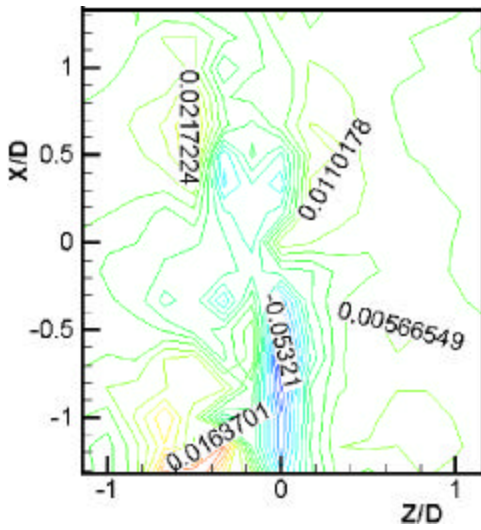


(j) $X = 1.333D$

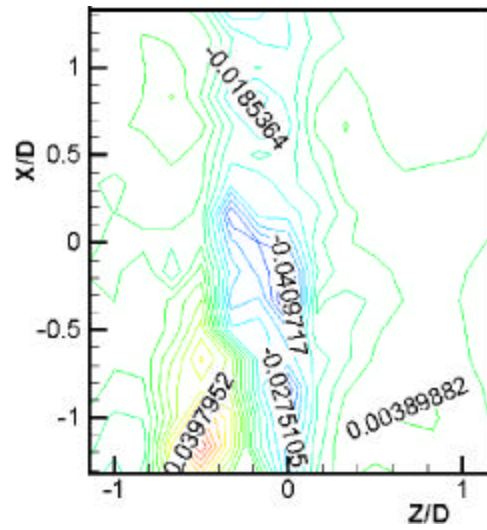
Fig. 5.24 Reynolds shear stress distribution $(-\overline{v'w'}) / U_0^2$ (continued)



(a) Measuring region

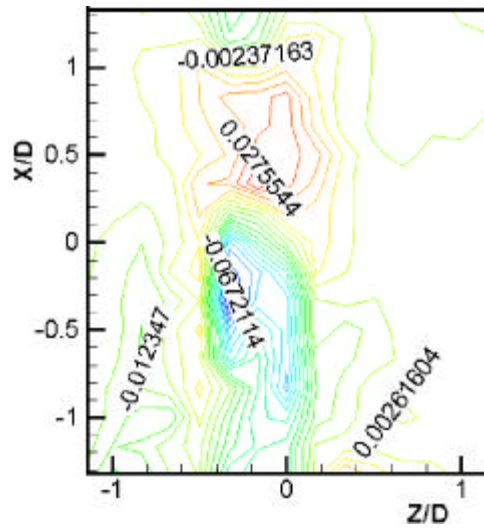


(b) $Y = 0.833D$

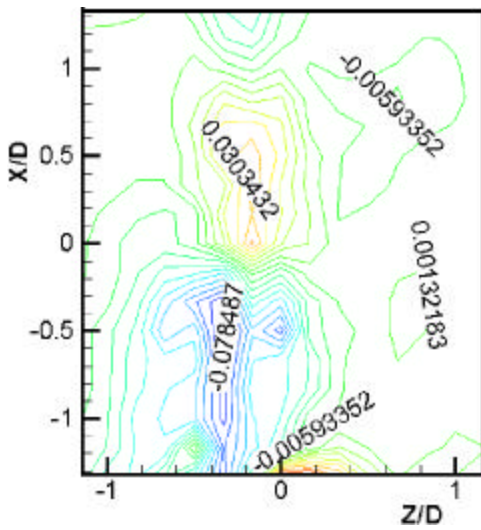


(c) $Y = 1.167D$

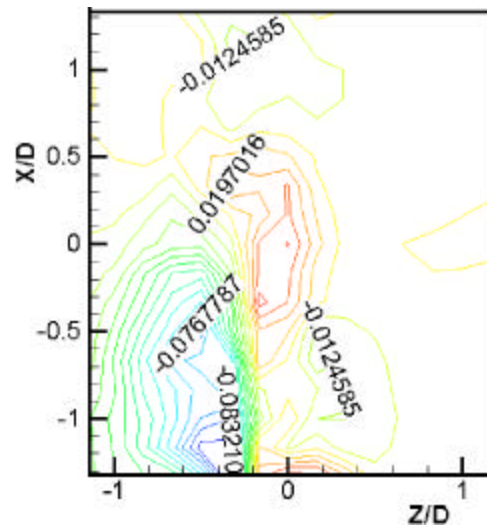
Fig. 5.25 Reynolds shear stress distribution $(-\overline{v'w'}/U_0^2)$ (continued)



(d) $Y = 1.500D$

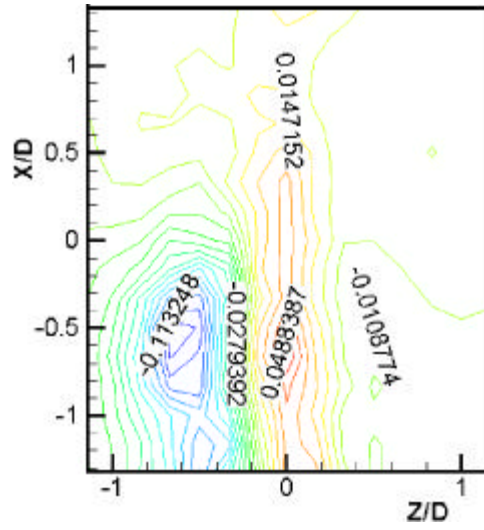


(e) $Y = 1.833D$

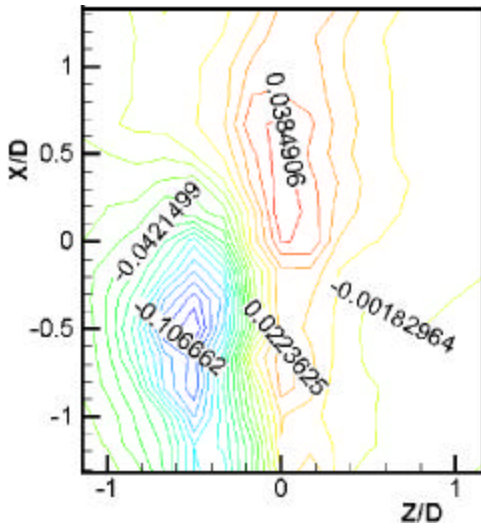


(f) $Y = 2.167D$

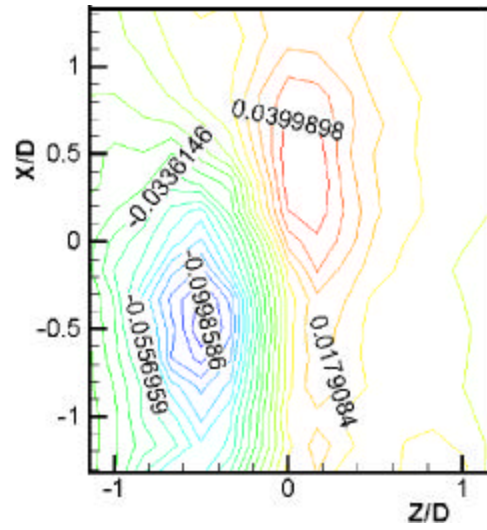
Fig. 5.25 Reynolds shear stress distribution $(-\overline{v'w'}) / U_0^2)$ (continued)



(g) $Y = 2.500D$

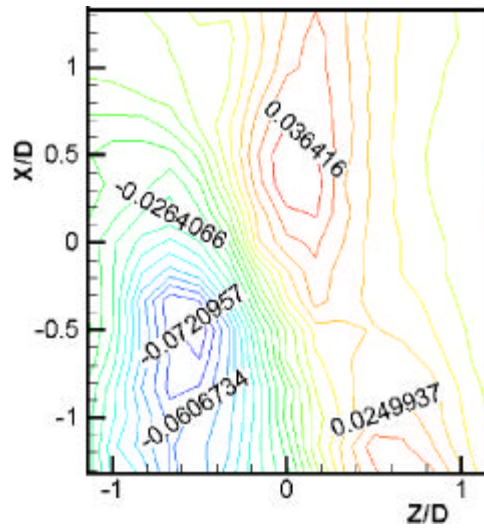


(h) $Y = 2.833D$

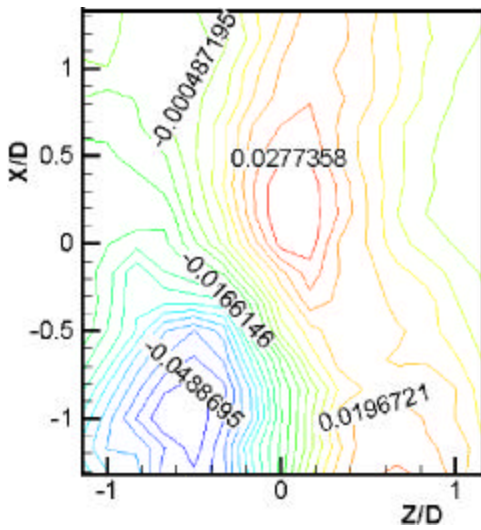


(i) $Y = 3.167D$

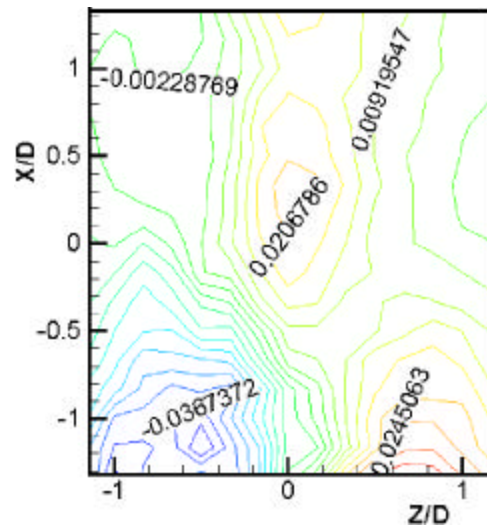
Fig. 5.25 Reynolds shear stress distribution $(-\overline{v'w'}) / U_0^2)$ (continued)



(j) $Y = 3.500D$



(k) $Y = 3.833D$



(l) $Y = 4.167D$

Fig. 5.25 Reynolds shear stress distribution ($-\overline{v'w'}/U_0^2$)

Fig. 5.26 (a)

(w'u')

Fig. 5.26 (b) (i) X- Y plane Z 0.333D 가

(w'u') . X=- 0.333D,

Y=2.800D, Z=- 0.167D X=- 0.333D

Y 3 가 .

Fig. 5.27

Y- Z (w'u')

. X=- 0.667D X=0.333D , X=- 0.333D,

Y=3.000D (w'u') 가

secondary vortex가 X

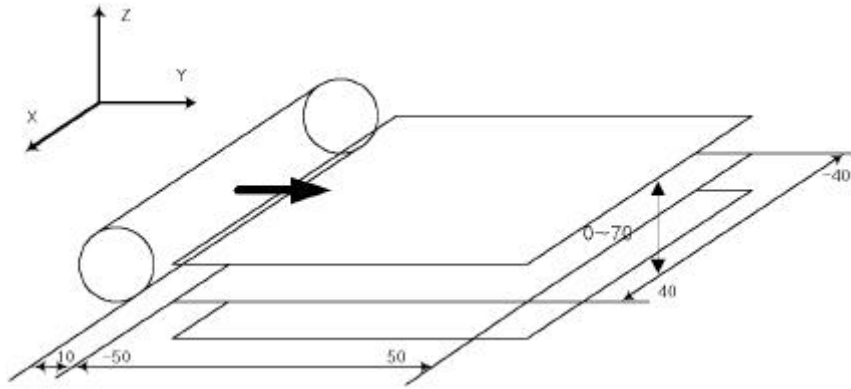
Fig. 5.28 X- Z plane Y 0.333D 가

(w'u') .

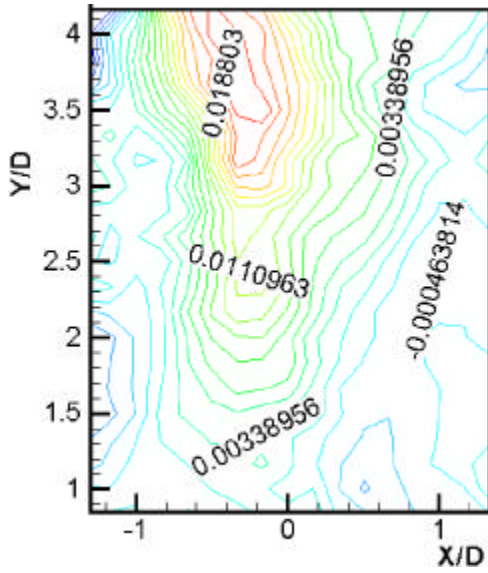
가 가 가 Y=2.500D

merging 가 가

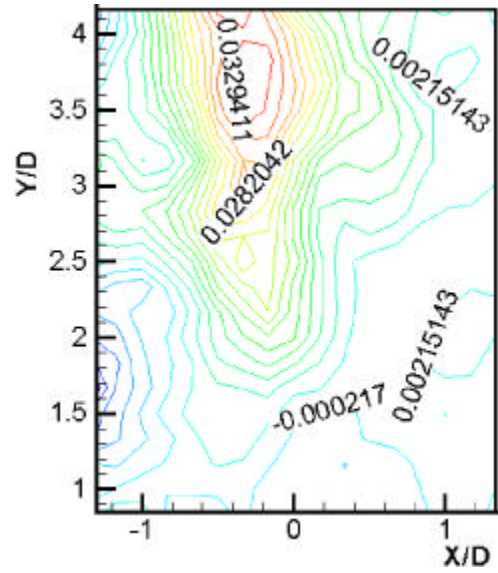
.



(a) Measuring region

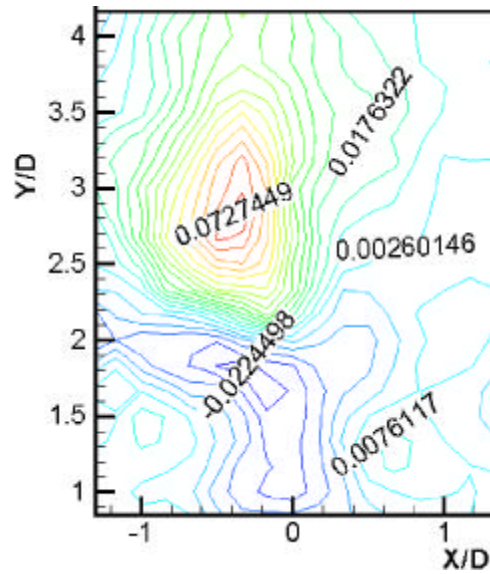


(b) $Z = -1.167D$

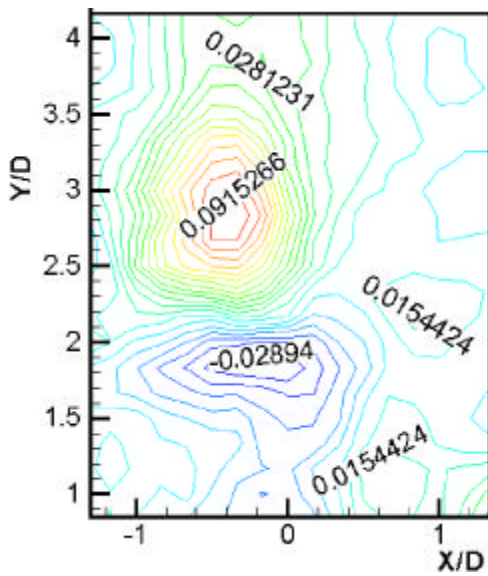


(c) $Z = -0.833D$

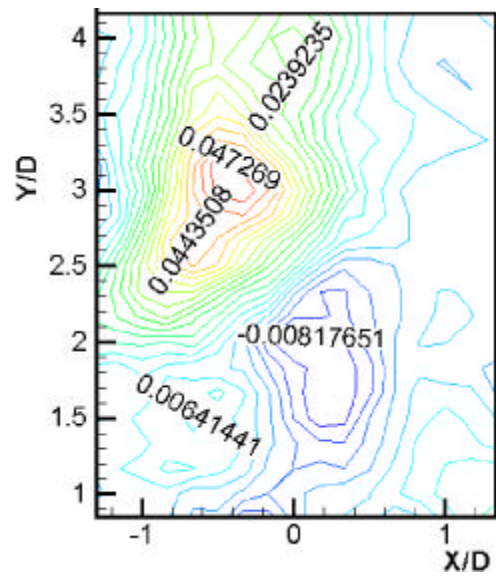
Fig. 5.26 Reynolds shear stress distribution $(-\overline{w'u'}) / U_0^2)$ (continued)



(d) $Z = -0.500D$

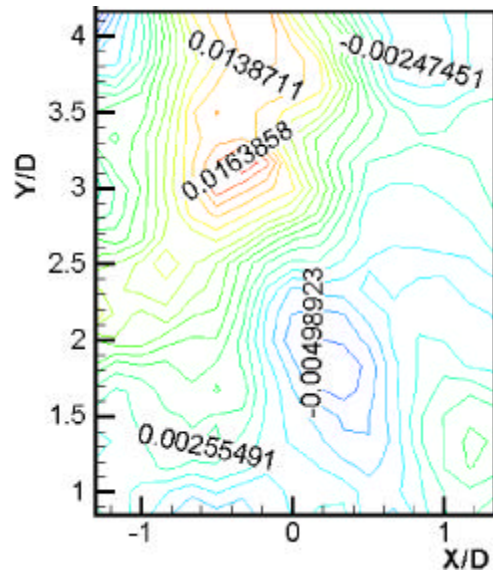


(e) $Z = -0.167D$

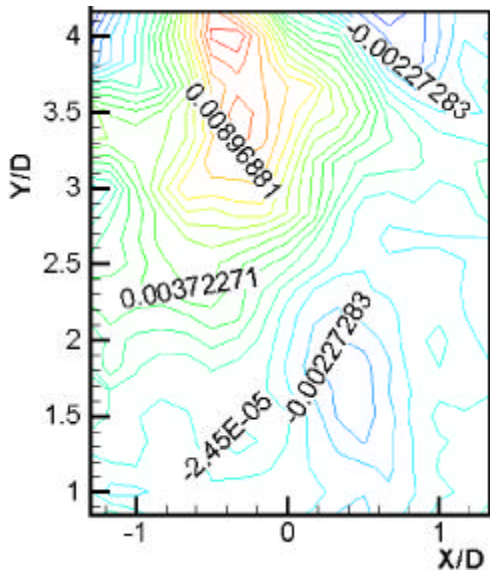


(f) $Z = 0.167D$

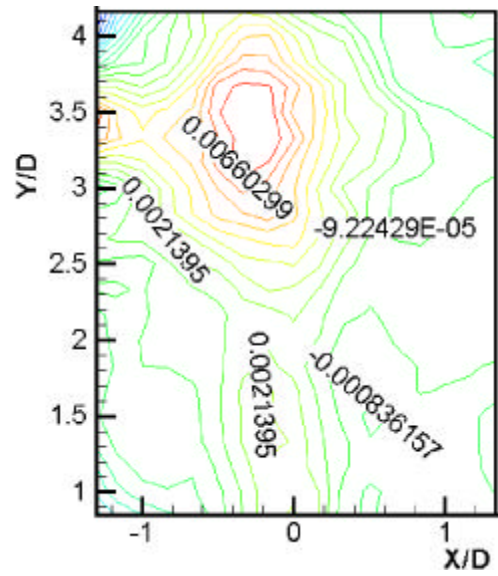
Fig. 5.26 Reynolds shear stress distribution $(-\overline{w'u'} / U_0^2)$ (continued)



(g) $Z = 0.500D$

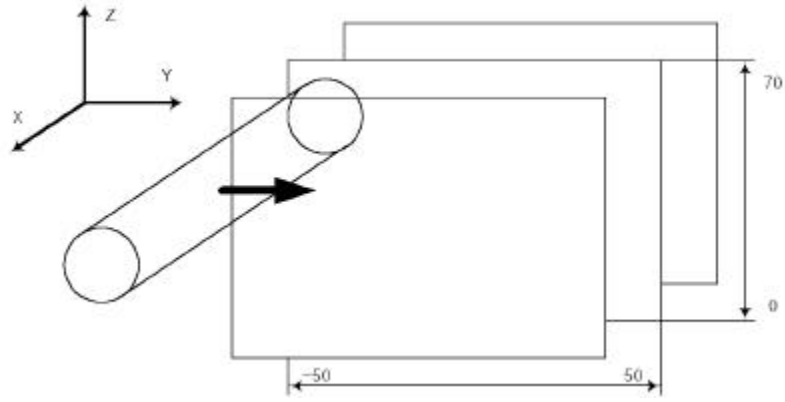


(h) $Z = 0.833D$

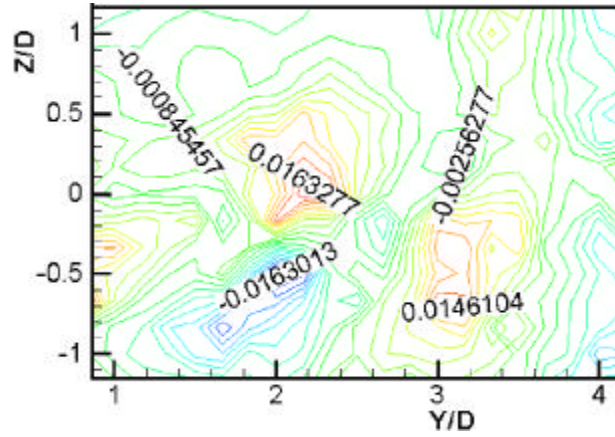


(i) $Z = 1.167D$

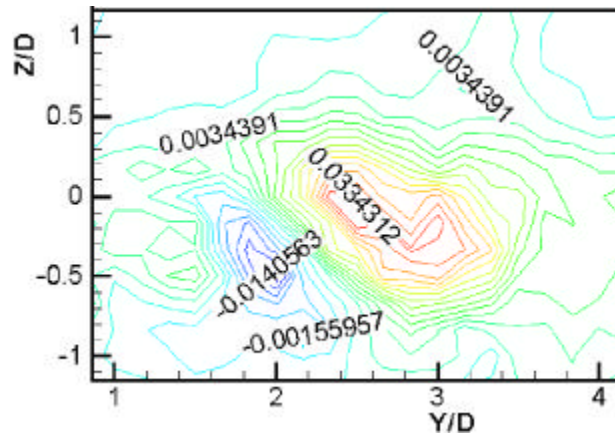
Fig. 5.26 Reynolds shear stress distribution $(-\overline{w'u'}) / U_0^2$ (continued)



(a) Measuring region

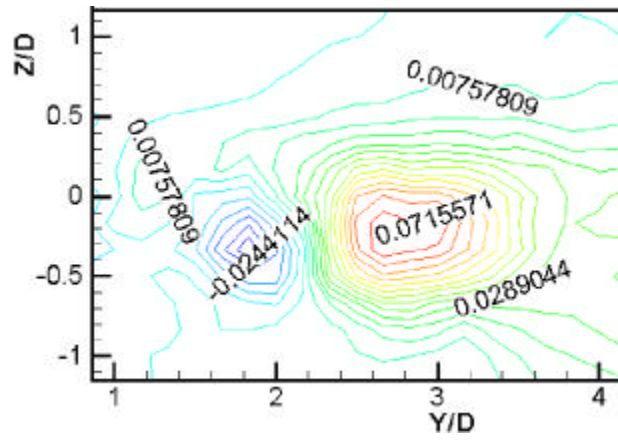


(b) $X = -1.333D$

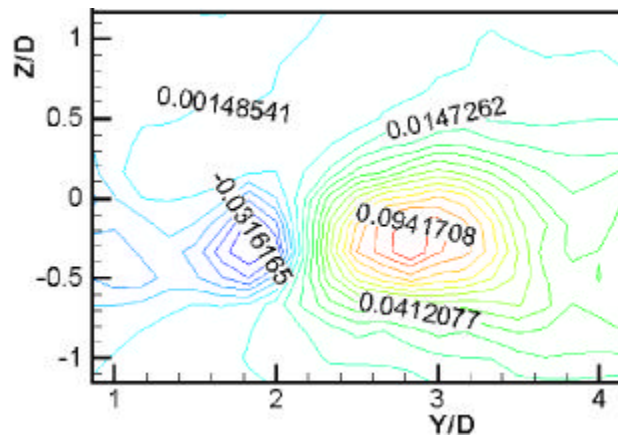


(c) $X = -1.000D$

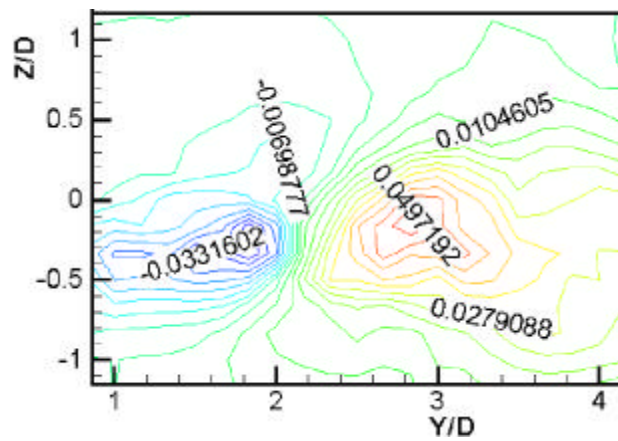
Fig. 5.27 Reynolds shear stress distribution ($- \overline{w'u'} / U_0^2$) (continued)



(d) $X = -0.667D$

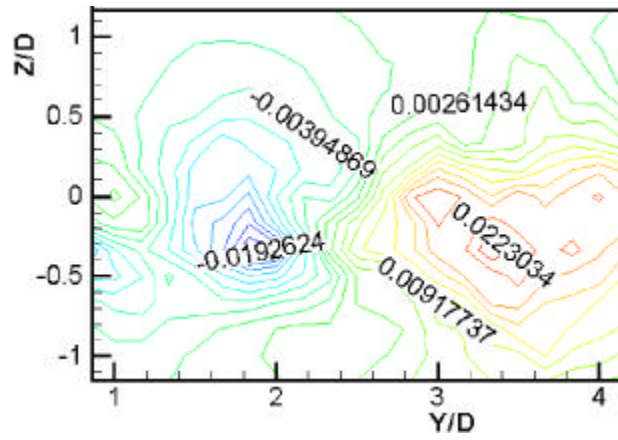


(e) $X = -0.333D$

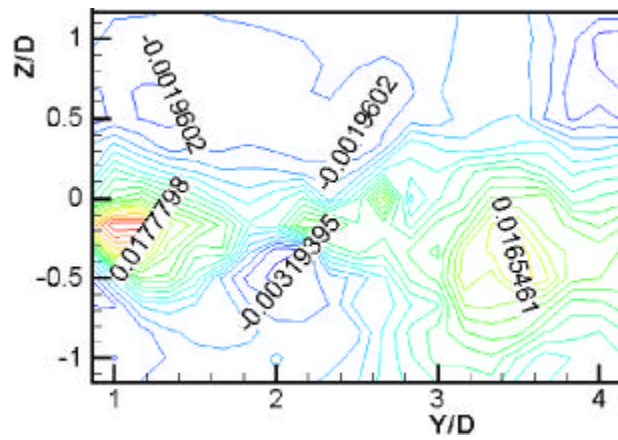


(f) $X = 0.000D$

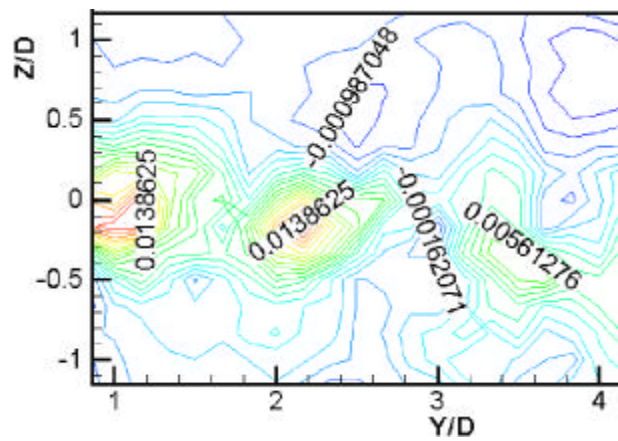
Fig. 5.27 Reynolds shear stress distribution $(-\overline{w'u'} / U_0^2)$ (continued)



(g) $X = 0.333D$

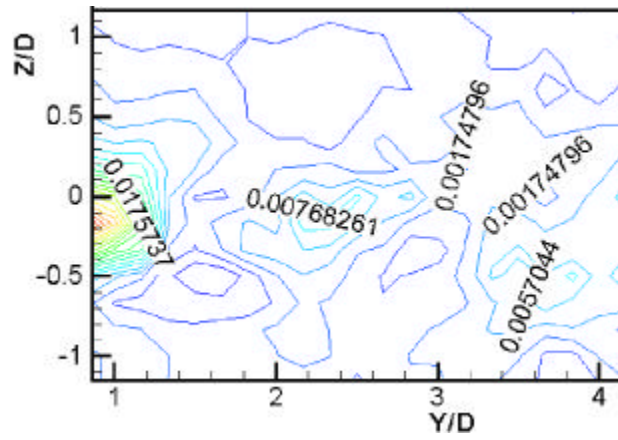


(h) $X = 0.667D$



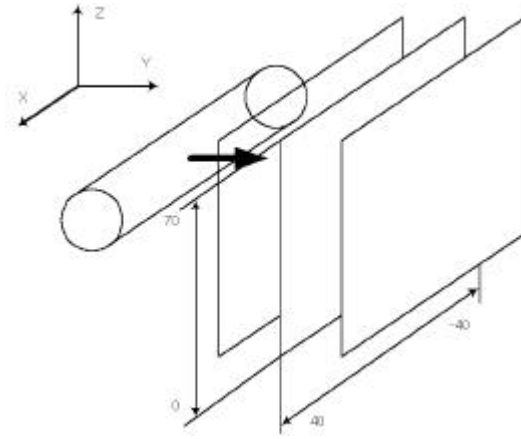
(i) $X = 1.000D$

Fig. 5.27 Reynolds shear stress distribution ($-\overline{w'u'}/U_0^2$) (continued)

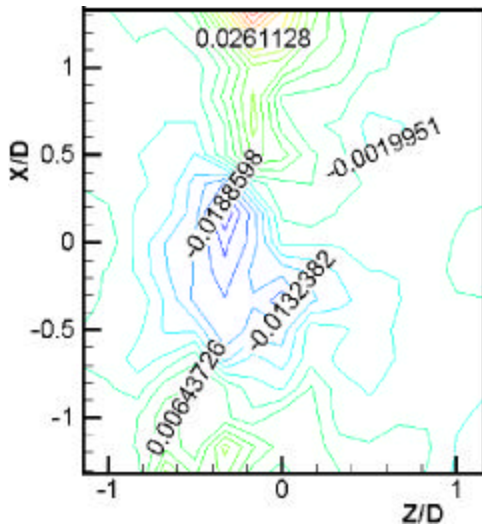


(j) $X = 1.333D$

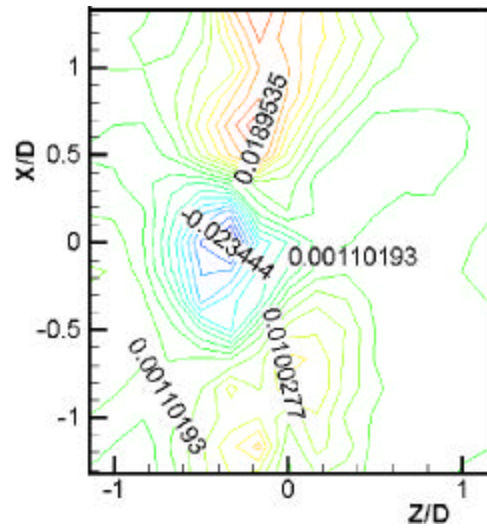
Fig. 5.27 Reynolds shear stress distribution ($- \overline{w'u'} / U_0^2$) (continued)



(a) Measuring region

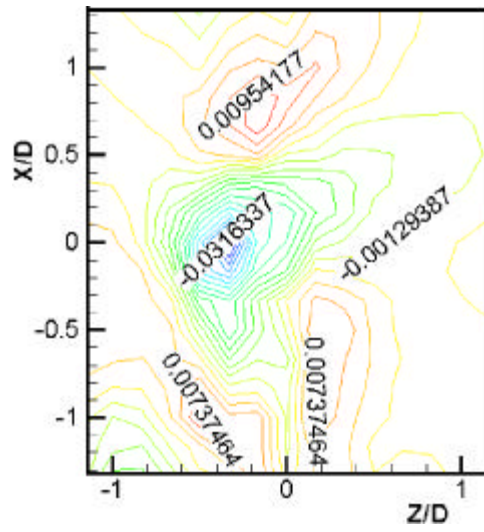


(b) $Y = 0.833D$

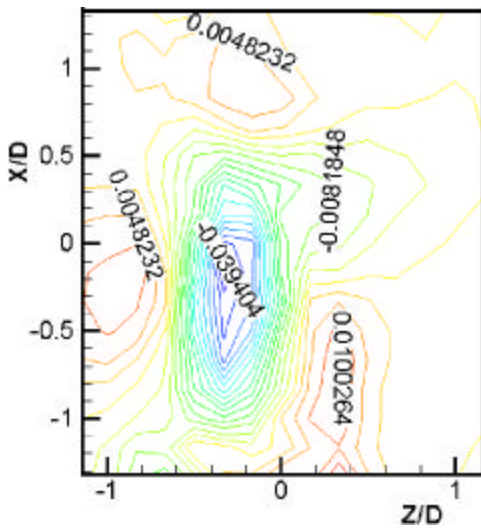


(c) $Y = 1.167D$

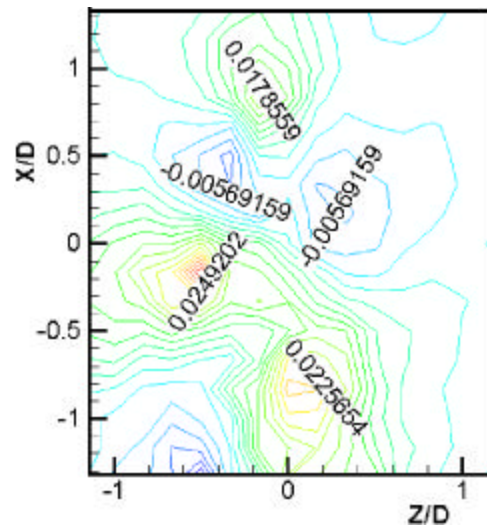
Fig. 5.28 Reynolds shear stress distribution $(-\overline{w'u'} / U_0^2)$ (continued)



(d) $Y = 1.500D$

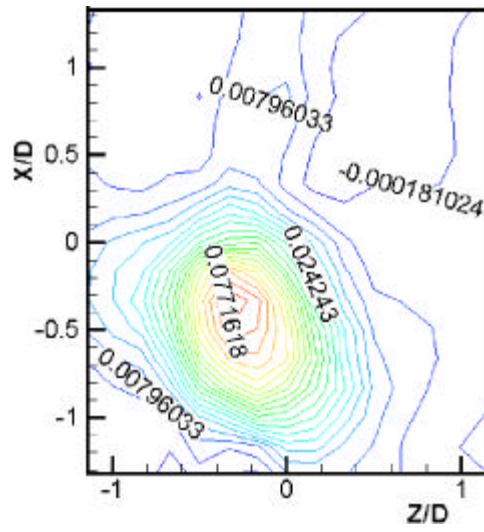


(e) $Y = 1.833D$

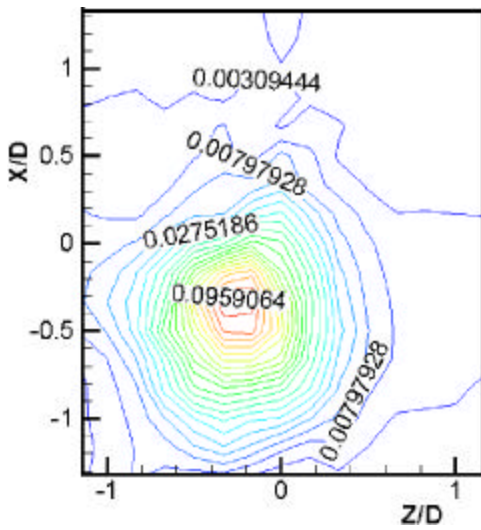


(f) $Y = 2.167D$

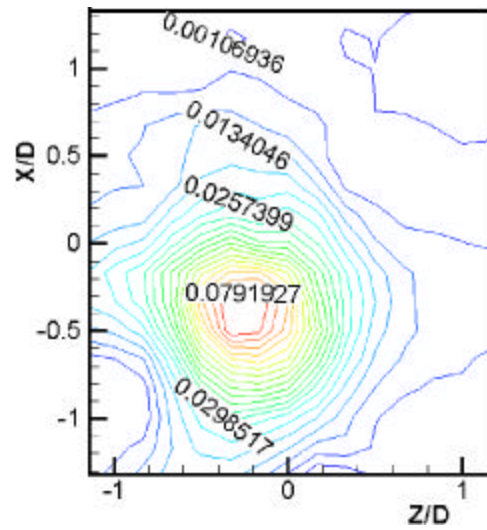
Fig. 5.28 Reynolds shear stress distribution $(-\overline{w'u'} / U_0^2)$ (continued)



(g) $Y = 2.500D$

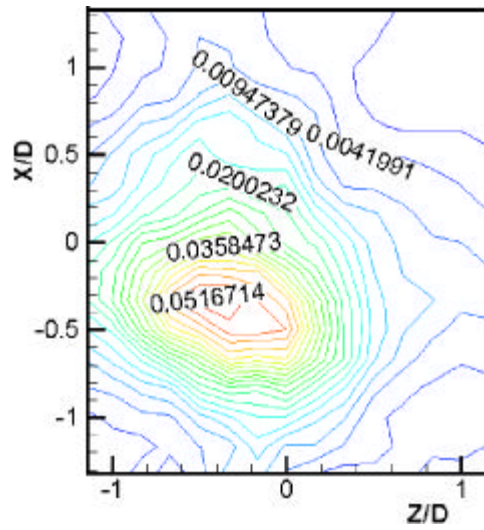


(h) $Y = 2.833D$

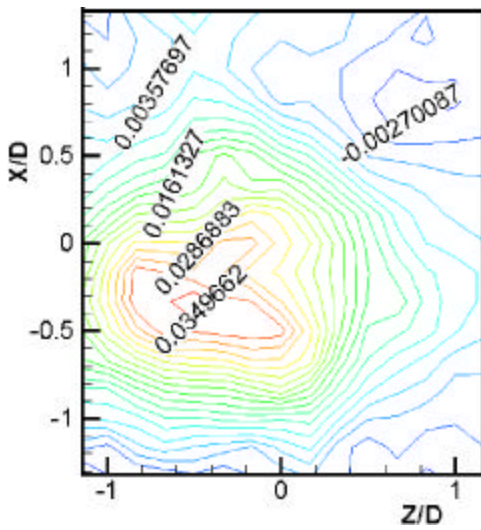


(i) $Y = 3.167D$

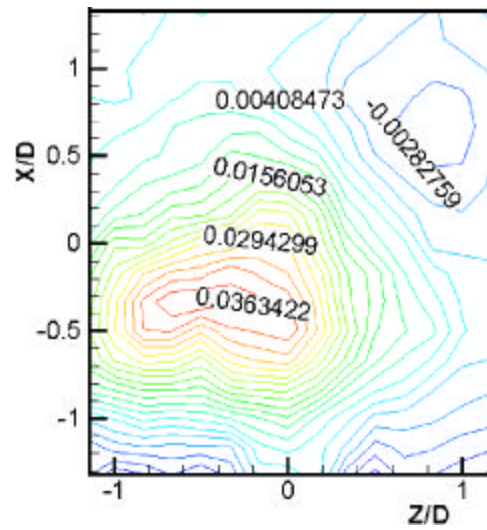
Fig. 5.28 Reynolds shear stress distribution $(-\overline{w'u'}) / U_0^2$ (continued)



(j) $Y = 3.500D$



(k) $Y = 3.833D$



(l) $Y = 4.167D$

Fig. 5.28 Reynolds shear stress distribution ($-\overline{w'u'}/U_0^2$)

6

3 PTV

3 PTV
 . Visualization Society of Japan LES
 가 3 ,
 가 2,000 65% Single-Frame 3
 PTV .

3 PTV (3D-GA-PTV)
 , , (, ,)
 . 2 1.5D 2.0D ,
 2 45mm
 60mm .

2
 1D , 30mm
 1D . , ⁷⁾ 2 1
 X/D=0.3

CFD 가

Nihino 가 1,100 700
 가
 .
 , ,
 가 . 3
 가 .

- 1) Roshko A., "On the development of turbulent wakes from vortex streets",
NACA 1191, 1954.
- 2) Mansy, H., Yang, P. M. and Williams, D. R., "Quantitative measurement of
three-dimensional structure in the wake of a circular cylinder", *J. Fluid
Mech.*, Vol. 270, 1994, pp. 277-296.
- 3) Williamson, C. H. K., "Three-dimensional wake transition," *J. Fluid Mech.*,
Vol. 328, 1996, pp. 345-407.
- 4) Chyu, C. and Rockwell, D., "Envolution of patterns of streamwise vorticity
in the turbulent near wake of a circular cylinder," *J. Fluid Mech.*,
Vol. 320, 1996, pp. 117-137.
- 5) Wu, J., Sheridan, J., Welsh, M. C., Hourigan, K. and Thompson, M.,
"Longitudinal vortex structures in a cylinder wake," *Phys. Fluids*.
Vol.6, 1994, pp. 2883-2885.
- 6) Lourenco, L., Subramanian, S. and Ding, Z., "Time series velocity field
reconstruction from PIV data," *Meas. Sci. Technol.*, Vol. 8, 1997,
pp. 1533-1538.
- 7) , , , " PIV
." 1999 , 1999,
pp. 55-60.
- 8) , , , "Cinematic PIV 3
", 2000 (B), 2000, pp. 661-666.
- 9) Chang, T. P., Wilcox, N. A., Tatterson, G. B., "Application of image
processing to the analysis of three-dimensional flow fields", *Opt. Eng.*
Vol. 23(3), 1984, pp. 283-287

- 10) Chang, T. P., Tatterson, G. B., "An automated analysis method for complex three dimensional mean flow fields", Proc. Third Int. Symp. Flow Visualization, 1983, pp. 266-273
- 11) Yamakawa, M., Iwashige, K., "On-line velocity distribution measuring system applying image processing", J. Flow Visualization Soc. Jpn., Vol. 6(20) 1986, pp. 50-58.
- 12) Racca, RG., Dewey, JM., "A method for automatic particle tracking in a three-dimensional flow field", Exp. in Fluids, Vol. 6 .1988, pp. 25-32.
- 13) Adamczyk, A. A., Rimai, L., "Reconstruction of a three-dimensional flow field from orthogonal views of seed track video images". Exp. in Fluids, Vol. 6, 1988, pp. 380-386
- 14) Kobayashi, T., Saga, T., Sekimoto, K., "Velocity measurement of three-dimensional flow around rotating parallel disks by digital image processing", ASME FED Vol. 85, 1989, pp. 29-36
- 15) Kasagi, N., Hirata, M., Nishino, K., Ninomiya, N., Koizumi, N., "Three-dimensional velocity measurement via digital image processing technique", J flow Visualization Soc. Jpn., Vol. 7(26), 1987 , pp. 283-288.
- 16) Nishino, K. Kasagi, N., Hirata, M., "Three-dimensional particle tracking velocimetry based on automated digital image processing", ASME J. Fluids Eng. Vol.111 No. 4, 1989, pp. 384-391.
- 17) Panantoniou, D., Dracos, T., "Analyzing 3-D turbulent motions in open channel flow by use of stereoscopy and particle tracking", Advances in Turbulence 2 (Ed. Fernholz HH; Fiedler HE). 1989, pp. 278-285. Berlin: Springer-Verlag.
- 18) Kent, JC., Trigui, N., Choi, WC., Guezennec, YG., Brodkey, RS., "Photogrammetric calibration for improved three-dimensional particle tracking velocimetry", Proc. SPIE Int. Symp. on Optical Diagnostic in Fluid and Thermal Flows, San Diego, July. 1993,

- 19) Kasagi, N., Nishino, K., "Probing turbulence with three dimensional particle tracking velocimetry". Exp. Thermal and Fluid Sci. Vol. 4, 1991, pp. 601-612
- 20) Mass, H. G., Gruen, A., Papantoniou, D. A., "Particle tracking velocimetry in three-dimensional flows". Part 1 photogrammetric determination of particle coordinates, Exp. In Fluids. Vol. 15 1993, pp. 133- 146
- 21) Malik, N. A., Dracos, Th., Papantoniou, D. A., "Particle tracking velocimetry in three-dimensional flows", Part 2. Particle tracking. Exp. In Fluids. Vol. 15, 1993, pp. 279-294
- 22) Doh, D. H., D. H. Kim, Choi, S. H., Hong, S. D., Kobayashi, T., Saga, T., "Single-frame 3D-PTV for high speed flows", Exp. in Fluid (to be published in 2000)
- 23) , "3 PIV 3 ", 99 , 1999, 5, 14, pp. 41-49.
- 24) Ballard, D. H., Brown, C. M., "computer vision". New Jersey: Prentice-Hall, 1982, pp. 195-225.
- 25) Kobayashi, T., Saga, T., Haeno, T., Tsuda, N., "Development of a real-time velocity measurement system for high Reynolds fluid flow using a digital image processing design", In: Experimental and Numerical Flow Visualization (Ed Khalighia B et al.). ASME FED Vol. 128, 1991, pp. 9-14
- 26) Okamoto, K., "Three-dimensional particle tracking algorithm Velocity Vector Histogram and Spring Model", Proc. of 3rd PIV Workshop, Fukui, Japan. 1995.
- 27) Yamada, H., Yamane, K., "Particle image velocimetry using a genetic algorithm", 可視化情報, Vol. 15 Suppl. No. 1, 1995, pp. 165-168.

- 28) Ohyama, R., Takagi, T., Tsukiji, T., Nakanishi, S., Kaneko, K., "Particle tracking technique and velocity measurement of visualized flow fields by means of genetic algorithms", 可視化情報, Vol. 13 Suppl. No. 1, 1993, pp. 22-25.
- 29) Kimura, I., Hattori, A., and Ueda, M., "Particle pairing using genetic algorithms for PIV", Proceedings of VSJ-SPIE98 December 6-9, 1998, Yokohama, JAPAN AB093
- 30) , , , " PIV ", (B), , 2000, pp. 650-654.
- 31) Murai, S., Nakamura, H., Suzuki, Y., "Analytical orientation for non-metric camera in the application of terrestrial photogrammetry", In Architecture Photogrammetry . Commision V. 1980, pp.516-524.
- 32) 北條, 高島, "PIVにおける異常ベクトルの検出",可視化情報, Vol.15, Suppl. No.2, 1995, pp.177- 180.
- 33) Masagi, N., "An introduction to measurement uncertainty analysis", J. Visualization. Visualization Society of Japan. Vol. 9(31), 1998, pp. 29-35
- 34) Agui, J. C., Jimenez, J., "On the performance of particle tracking", J. Fluid Mech. No1. 185, 1987, pp. 447-468.
- 35) Willert, C. E., and Gharib, M., "Digital particle image velocimetry", Exp. in Fluids, Vol.10, No. 4, 1991, pp.181- 193.
- 36) Okamoto, K., "Evaluation of the 3D-PIV standard images(PIV-STD project Proc. The third international workshop on PIV'99-Santa Barbara (Ed. Adrian R. J.)". 1999, pp. 31-36
- 37) Brede, M., Eckelmann, H. and Rockwell, D., "On secondary vortices in the cylinder wake," *Phys. Fluids*, Vol. 8, 1996, pp. 2117-2124.

“

.”

5

.

,

가

,

가

,

, 가

1

,

,

.

,

가

,

,

,

,

, ,

,

.

,

.

가

.

,

.

.

,

,

가

,

,

.

- 155 -